FOG

Freiberg Online Geoscience

FOG is an electronic journal registered under **ISSN 1434-7512**

2015, Volume 42

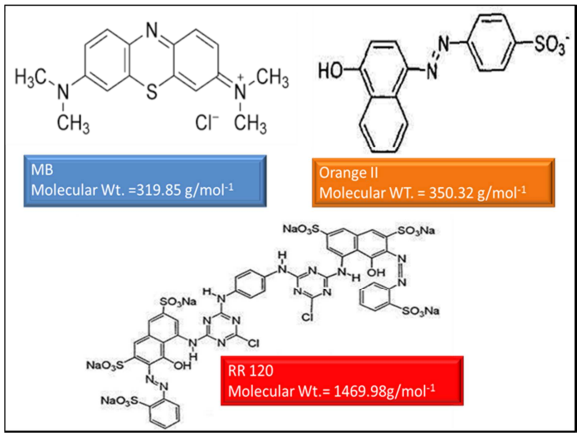

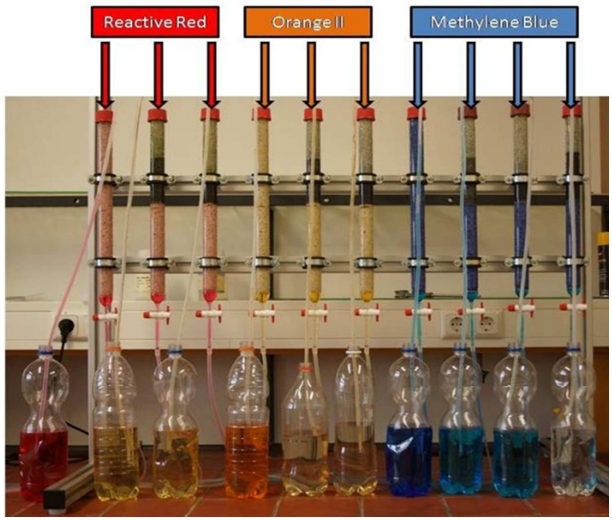

Meghalim Phukan

Characterizing the ion-selective nature of Fe^0-based systems using azo dyes: batch and column experiments

60 pages, 23 figures, 9 tables, 140 references

Acknowledgement

I would like to express my gratitude to my supervisor PD. Dr. Chicgoua Noubactep for understanding my interest in the field of water treatment and providing me with technical support that added considerably to my graduate experience. Due to his understanding and patience, he became more of a mentor and a friend than a supervisor.

I would further like to express my appreciation to my second supervisor PD. Dr. Tobias Licha for his assistance and giving me the opportunity to work in the laboratory.

I also express my warm thanks to Dr. Azizur Rahman for his immense guidance and support during my thesis.

I would like to acknowledge my friends, Apoorv Jyoti, Nura Abadat for their excellent technical assistance and the useful discussions during the entire course of my thesis.

Mr. Lothar Laake and Mr. Gehard Hundrmark from the Centre for Geoscience (University of Göttingen) are thanked for technical support. The International Büro of the University of Göttingen is thanked for financial support (scholarship). The equipment used in this work was funded by German Ministry for Environment (BMU) within the project “Reactherm” under Grant No.0325417

Finally I thank and appreciate my parents and family for their material and spiritual support in all aspects of my life. Without their love, encouragement and assistance, this thesis would not have been a success.

Abstract

Elemental iron (Fe^0) has been successfully tested and used for water treatment for decades due to its worldwide availability and inexpensiveness. Fe^0-based filtration technology has been used for (i) environmental remediation (e.g. subsurface permeable reactive barriers) (ii) wastewater treatment and (iii) safe drinking provision. The evidence that Fe^0 oxidative dissolution and subsequent precipitation at pH > 4.0 is a volumetric expansive process ($V_{oxide} > V_{iron}$) implies that Fe^0 should be amended with non-expansive aggregates such as activated carbon, manganese oxides, pumice or sand. Only such hybrid systems are likely to be sustainable.

The present work focuses on the characterization of the ion selective nature of Fe^0-based filters using three azo dyes: methylene blue (cationic), Orange II and Reactive Red 120 (anionic). The dyes are used as indicators for the reactivity of Fe^0/H_2O system in both batch and column experiments. The idea is to demonstrate that downwards from a Fe^0/sand system; available aggregates are in-situ coated with iron oxide, such that in the medium to long term, the whole system is ion-selective. The selectivity being fixed by positively charged iron oxides.

The characterization of the Fe^0/H_2O system is realized herein by amending (i) Fe^0 with sand and MnO_2 in batch experiments and (ii) Fe^0 with sand in column experiments. Sand is a pure adsorbent with a negatively charged surface while MnO_2 is reactive in nature. MnO_2 addition enables the control of the availability of in-situ generated iron corrosion products and thus the role of corrosion product in the process of contaminant removal. The investigated systems in batch mode are (i) pure sand, (ii) pure MnO_2, (iii) pure Fe^0, (iv) Fe^0/sand mixture, (v) Fe^0/MnO_2 mixture and (vi) Fe^0/sand/MnO_2 mixtures with various amounts of sand and MnO_2 loadings. Column experiments were performed with the following systems: (i) pure sand (0 % Fe^0), (ii) pure Fe^0 (100 % Fe^0), and (iii) Fe^0/sand (50 % Fe^0- vol/vol).

Results of batch experiment showed that sand is a good adsorbent for MB and has negligible effect on anionic dyes. MnO_2 also favors MB discoloration. Pure Fe^0 favors discoloration of both cationic and anionic dyes but shows best discoloration efficiency for Orange II. Among the Fe^0 amended systems, the Fe^0/sand system is most efficient for dye discoloration. The discoloration efficiency in Fe^0-based systems is 75 % for MB and > 95 % for Orange II and RR120. Results confirmed quantitative adsorptive MB discoloration and negligible adsorption of anionic dyes on negatively charged sand. Quantitative discoloration of the anionic dyes (Orange II and RR120) in Fe^0-based systems was attributed to high affinities of both species to positively charged iron corrosion products. The ion selective nature of the Fe^0/H_2O system is elegantly demonstrated.

Keywords: Dye discoloration, Fe^0-based filters, Iron corrosion, Iron metal, Water treatment.

Table of Contents

Acknowledgement ..... **II**

Abstract ..... **III**

List of Figures ..... **VI**

List of Tables ..... **VIII**

List of Acronyms ..... **VIIIX**

1. Introduction **1**
1.1 Motivation **1**
1.2 Fe^0-based filtration systems **2**
1.2.1 Sustainable Fe^0-based filters 2
1.2.2 The selectivity of Fe^0-based filters 2
1.3 Objective of the thesis **3**
1.4 Methodology **3**
1.5 Outline of the thesis **3**

2. Theory **4**
2.1 Aqueous iron corrosion **4**
2.2 The electrochemical cell **5**
2.3 Oxide scale and mass transport **5**
2.4 Diffusion and advection **6**
2.5 Contaminant removal in Fe^0/H_2O system **7**
2.5.1 Adsorption 8
2.5.2 Co-precipitation 9
.2.5.3 Adsorptive size-exclusion 9
2.6 Packed bed design (Fe^0 amended sand filter) **10**

3. Materials and Methods **11**
3.1 Solutions **11**
3.1.1 Dyes 11
3.1.2 Iron solution 13
3.2 Solid Materials **14**
3.2.1 Metallic Iron (Fe^0) 14
3.2.2 Sand 14
3.2.3 MnO_2 14
3.3 Analytical methods **15**
3.3.1 UV-Vis Spectra method 15
3.3.2 Further analytical methods 15

4. Experimental Procedure **16**
4.1 Performed experiments **16**
4.2 Dye Discoloration **16**
4.2.1 Batch Experiment 16
4.2.2 Column experiments 19

4.3 Analytical Methods **21**
4.3.1 Calibration of the spectrophotometer 21
4.3.2 Determination of dye concentration 22
4.3.3 Determination of Fe concentration 23
4.4 Characterizing the compaction of the column material **24**
4.5 Pore volume determination **24**
4.6 Presentation of the experimental results **24**
5. Results and Discussion **27**
5.1 Batch Experiment **27**
5.1.1 Reproducibility of the experimental results 27
5.1.2 Single material systems 28
5.1.3 Fe^0 amended systems 30
5.1.4 Discoloration efficiency of dyes by sand loadings 32
5.1.5 Discoloration Efficiency of dyes by MnO_2 loadings 33
5.1.6 pH values of discolored dyes 34
5.2 Column Experiment **35**
5.2.1 Visual observation 35
5.2.2 Pure sand systems 36
5.2.3 Fe^0-based systems 36
5.2.4 Evidence of dye retention 38
5.2.5 Evidence of chemical reactions 41
5.2.6 pH values of the column effluent 43
5.2.7 Total iron concentration of the effluent 44
5.2.8 Hydraulic conductivity or permeability loss 45
5.2.9 Cementation of the column materials 45
5.3 Summary of the results **46**
6. Concluding Remarks **47**
7. Epilogue **49**
REFERENCES **51**
Appendix **61**
APPENDIX 1: Batch Experiments **62**
APPENDIX 2: Column Experiments **80**

List of Figures

Fig 1: Schematic diagram showing migration of (i) contaminants-X, (ii) dissolved oxygen (DO) (iii) electron(e^-) (iv) ferrous iron(Fe^{2+}) (v) hydrogen in the vicinity of immersed metallic iron **6**

Fig 2: Chemical Structure and molecular weights of the azo dyes (a) methylene Blue (b) Orange II (c) reactive red 120(RR 120) **12**

Fig 3: Preparation process for measurement of Fe concentration in solution..... **13**

Fig 4: Preparation of the Dye sample with reactive material in the batch experiment (a) methylene blue (MB) (b) Orange II (c) reactive red 120(RR 120). **17**

Fig 5: Schematic diagram of the column experiment **19**

Fig 6: Experimental set-up of column experiment on day 1..... **20**

Fig 7: Calibration graphs of light absorbance at various concentration of dyes and its linear regression (a) MB (b) Orange II(c) RR 120..... **21**

Fig 8: Calibration graphs of light absorbance at various concentration of Fe^0 and its linear regression **22**

Fig 9: Volume dependent electrical conductivity of NaCl solution. **23**

Fig 10: Discoloration extent in pure Fe^0 (a) under non-shaken experimental conditions for 6 weeks and (b) under non-shaken conditions for 2 weeks..... **26**

Fig 11: Dye discoloration by single material systems under non- shaken condition for 6 weeks **28**

Fig 12: Dye discoloration by mixed system under non- shaken conditions for 6 weeks. The used the used mass loadings are: Fe^0 is 4.55 g L^{-1}, sand and MnO_2 is 22 g L^{-1}. **29**

Fig 13: Dye discoloration by Fe^0/Sand system under shaken conditions for 2 weeks..... **31**

Fig 14: Dye discoloration by Fe^0/MnO_2 system (a) under non shaken conditions for 6 weeks (b) shaken conditions for 2 weeks..... **32**

Fig 15: pH values of the discolored dyes by sand and MnO_2 loadings under shaken conditions for 2 weeks. The Fe^0 mass is fixed..... **33**

Fig 16a: Photograph of the experimental set–up of column experiment on 22nd day..... **34**

Fig 16b: Photograph of the experimental set–up of column experiment on 93rd day **35**

Fig 17: Time dependent evolution of the cummulative dye breakthrough: (a) pure sand system (b) 50 % Fe^0 system (c) pure Fe^0 system **36**

Fig 18: Time evolution of dye breakthrough: (a) pure sand system (b) 50 % Fe^0 system (c) pure Fe^0 system **37**

Fig 19: The working solution of MB, Orange II and RR 120 (31 μM) were diluted by a factor 2 and 20 in order to observe the nature of maximum diluted contaminants that could be analysed succesfully. **40**

Fig 20: UV-Vis Spectra of dyes after 90 days . For RR 120 and Orange II , the peak of the sand system corresponds to that of the working solution..... **41**

Fig 21: Time dependent evolution of pH of the column experiment..... **42**

Fig 22: (a) Preparation of samples from the effuent of the columns for measurement of Fe^0 concentration (b) Concentration of dissolved Fe^0 in the effleunt of columns with Fe^0 loading **43**

Fig 23: Time dependent evolution of the flow velocity in the 10 test columns **44**

List of Tables

Table 1: Some relevant chemical reactions characterizing aqueous iron corrosion **4**

Table 2: The possible reaction pathways in the removal of contaminants from the aqueous solution is shown in table **8**

Table 3: Some relevant physio-chemical characteristics of tested dyes. The dye molar concentration was 31.5 M. The corresponding weight concentrations (mg L^{-1}) of individual dyes are specified **11**

Table 4: Empty bed contact time in the Fe^0-based systems of the column experiment **20**

Table 5: Standard solutions used for the calibration of the Cary 50 UV-VIS –Spectrophotometer for the determination of dye concentrations **21**

Table 6: Standard solutions used for the calibration of the Cary 50 UV-VIS –Spectrophotometer for iron determination **22**

Table 7: Summary of the results of dye discoloration (%) in individual Fe, sand and MnO_2 systems under 6 weeks quiescent and 2 weeks shaken condition **27**

Table 8: Comparison of the extent of dye discoloration in the H_{sand1} layer (180 g of sand) of Fe^0-based systems **38**

Table 9: Summary of the results of the column experiments after 93 days **39**

List of Acronyms

Å	Angstrom
BT	breakthrough
cmd^{-1}	centimeter per day
DO	Dissolved oxygen
LF	electrical conductivity
Fe^{2+}	Ferrous ion
Fe^{3+}	Ferric ion
H_{sand2}	Height of top sand layer
H_{sand1}	Height of bottom sand layer
H_{RZ}	Height of reactive zone
MnO_2	Manganese dioxide
MB	Methylene Blue
µmol	micromole
pzc	point of zero charge
PRB	Permeable Reactive Barriers
RR120	Reactive Red 120
rpm	revolution per minute
NaCl	Sodium chloride
UNICEF	United Nations Children's Fund
λ	wavelength(nm)
WHO	World Health Organization
ZVI/Fe^0	Zero-valent iron/Metallic iron

1. Introduction

1.1 Motivation

Safe clean water is essential for the live but contamination of water sources is currently observed in several regions of the world. Global intensified water contamination is due to urbanization and industrialization. The source of water pollution is mainly due to increase use of chemicals in many sectors including agriculture, domestic, health care, education, housing, industry, research, textile and transport (Noubactep 2010a, Ali 2012, Chiu 2013, Ali 2014).

According to the WHO/UNICEF 2014 updates, since 1990 drinking water coverage in developing nations have increased by 17 % which means that 89 % of the world population had access to safe drinking water in 2012. About 56 % (4 billion) of the global population have the privilege to enjoy piped drinking water connection. Despite of this significant progress on safe drinking water, 748 million people still lack access to safe drinking water and 173 million out of the huge number rely on untreated surface water particularly in small communities in the rural areas where centralized drinking water systems are not available (Shannon et al. 2008, Noubactep 2010a, Nitzsche et al. 2015, Noubactep 2011a, Ali 2014, Tepong-Tsindé et al. 2015a). The world has achieved the Millennium Development Goal for drinking water in 2010, but still 45 countries mostly in the Sub-Saharan Africa will fail to meet this target by 2015.

Around the world, there is availability of different efficient methods of treating drinking water such as adsorptive filtration, coagulation, electrocoagulation, membrane filtration, reverse osmosis. However, most of these methods are expensive and consume a great amount of energy. Adsorptive filtration using activated carbon, alumina, titania, porous titania aerogels (Abramian et al. 2009) are proven sustainable water treatment technologies but its drawbacks are (i) requires extensive pretreatment (ii) it attracts not only contaminant but also dissolved organic matter which may be harmless (iii) constant monitoring is required to ensure the reactive doses are high enough to adsorb all contaminants and (iv) can be used for short-termed treatment responses of poor water condition such as taste and colour deficiencies.

There is urgency for an affordable but efficient approach to treat water for safe drinking purpose (Bhaumik et al. 2015). Sand filters amended with up to 50 % (vol/vol) metallic iron (Fe^0) have been discussed in the literature as a powerful tool for water treatment at decentralized level (Noubactep et al. 2009a, Noubactep et al. 2009a, Noubactep 2014a, Noubactep 2014b, Noubactep 2015a, Noubactep 2015b, Tepong-Tsindé et al. 2015a). Such a technology would be ideal for rural areas of the developing world. Fe^0/sand filters have the ability to quantitatively remove (i) wide range of chemical contaminants (organic and inorganic in nature) (Henderson and Demond 2007, Noubactep 2009a, Guan et al.2015) and (ii) pathogens (bacteria and viruses) (Bojic et al. 2001, Bojic et al. 2004, You et al. 2005, Noubactep 2011b). Additionally, the Fe^0/sand filter system is (i) cost effective, (ii) easy to maintain, (iii) could de designed to be gravity driven (no power requirement) and (iv) Fe^0 and sand are potentially abundantly available and affordable. Fe^0/sand filters can be easily

designed to deserve household and small communities with safe drinking water (Noubactep et al. 2012, Rahman et al. 2013, Nitzsche et al. 2015, Tepong-Tsindé et al. 2015a).

1.2 Fe^0-based filtration systems

Fe^0/sand filters (e.g. amended with sand) have been successfully used in the permeable reactive barriers (PRBs) for groundwater remediation (O'Hannesin and Gilham 1998 Henderson and Demond 2007, Comba et al. 2011, Gheju 2011). Here, Fe^0 is mainly regarded as reducing agent for contaminant degradation or reductive immobilization. However, documented results disproved the view that contaminant reductive transformation is the cathodic reaction accompanying Fe^0 oxidative dissolution. (Noubactep 2007, Jiao et al. 2009, Noubactep 2008, Ghauch et al. 2010, Noubactep 2010a, Ghauch et al. 2011, Gheju and Balcu 2011, Noubactep 2011b, Noubactep et al. 2011, Scott et al. 2011, Crane and Noubactep 2012, Noubactep 2012a, Noubactep 2012b, Togue-Kamga et al. 2012, Btatkeu-K et al. 2013, Gatcha-Bandjun and Noubactep 2013, Kobbe-Dama et al. 2013, Noubactep 2013b, Noubactep 2013b, Noubactep 2013c, Noubactep 2013d, Gatcha-Bandjun et al. 2014, Noubactep 2015a, Noubactep 2015b, Noubactep 2015c). Fe^0/sand filters are also used for on-site water treatment and household filters (Hussam and Munir 2007, Ngai et al. 2007, Aviles et al. 2013, Kowalski and Sogard 2014, Wenk et al. 2014). In this context Fe^0 is used both as reducing agent and generator of iron oxides to improve contaminant removal in sand filters. But more systematic research is required to optimize the technology as a whole.

1.2.1 Sustainable Fe^0-based filters

Recent works (Caré et al. 2013, Domga et al. 2015 and ref. cited therein) have established/recalled that Fe^0 undergoes volumetric expansion (Pilling and Bedworth 1923), making pure Fe^0 systems non-sustainable. Fe^0 requires free space to quantitatively undergo corrosion. In the absence of space, clogging occurs and corrosion stops (Caré et al. 2013). When corrosion stops, the filter is no longer useful. In order to render a Fe^0 filter more sustainable, the Fe^0 amount is minimized by admixture with non-expansive materials (Noubactep 2013d, Noubactep 2015c). An alternative approach is to manufacture porous Fe^0 materials (Hussam and Munir 2007, Rahman et al. 2013, Allred and Trost 2014). Sand has been tested and used as the most suitable admixture (Kaplan and Gilmore 2003, Westerhoff and James 2003). Sand is comparatively cheap, non-reactive and porous. The volumetric proportion of Fe^0 should not exceed 50 to 60 % according to calculation by Caré et al. (2013). Theoretical and experimental works have demonstrated that the optimal volumetric Fe^0 : sand ratio is 25:75 (Miyajima 2012, Bilardi et al. 2013, Noubactep 2012a, Noubactep 2013a, Noubactep 2013b, Noubactep 2013c, Noubactep 2013d, Btatkeu-K et al 2014a, Btatkeu-K et al 2014b, Tepong-Tsindé et al. 2015a).

1.2.2 The selectivity of Fe^0-based filters

The evidence that there is no Fe^0/H_2O stability domain in natural water (Pourbaix diagram) recalls that there are at least two interfaces in a Fe^0/H_2O system: (i) the Fe^0/Fe oxide and (ii)

the Fe oxide/H_2O interfaces (Sato 2001). This implies that a dissolve contaminant must first adsorb onto Fe oxides (corrosion products) before it migrates to the Fe^0 surface. Theoretically this is possible but practically it has been observed that even oxygen reduction under environmental conditions is not the cathodic reaction coupled to Fe^0 dissolution (Stratmann and Müller 1994). In other words, Fe^0 is oxidized by water (producing Fe^{2+} and H/H_2) and O_2 is reduced by Fe^{2+}. Thus reductive transformations in Fe^0/H_2O systems mainly occur in the oxide scale on Fe^0 (Fe oxide). This observation is well-documented in the corrosion literature (Sato 2001) but has been mostly overseen in the Fe^0 remediation community. Since the seminal work of Matheson and Tratnyek (1994), the selectivity is considered to be governed by the redox reactivity of dissolved species (including contaminants).

1.3 Objective of the thesis

The aim of the current study is to characterize the ion selective nature of Fe^0-based systems for water treatment and environmental remediation. Three dyes are used in batch and column experiments: methylene blue (MB), Orange II and reactive red 120 (RR 120). MB is cationic in nature whereas Orange II and RR 120 are anionic. Orange II and RR 120 largely differ in size, thus beside the ion selectivity (anionic vs. cationic) this study aims at characterizing steric effects as well.

1.4 Methodology

The extent of dye discoloration was used to assess the impact of sand and manganese oxide (MnO_2) addition on the reactivity of Fe^0 in quiescent and shaken in batch experiments. Sand is an inert additive. MnO_2 is a reactive additive controlling the availability of 'free' corrosion products. Observations from batch experiments are fine-tuned in column experiments, limited at investigating the impact of sand addition on the efficiency of Fe^0. The efficiency of individual columns was characterized by the time-dependent evolution of: (i) the pH value, (ii) the iron breakthrough, (iii) the dye breakthrough and (iv) the hydraulic conductivity (permeability). The results are comparatively discussed.

1.5 Outline of the thesis

The present work is a part of on-going research activities on designing sustainable Fe^0-based filters. The preliminary part of the work was reviewing of the theoretical background of the process of contaminant removal by Fe^0/H_2O systems including the mechanisms of iron corrosion which are presented in Chapter 2. Chapter 3 presents used materials and rationalized their use. Chapter 4 elaborates the experimental procedure for batch and column experiments. The results are discussed in the Chapter 5. Finally, Chapter 6 gives an overview on achieved results and their significance of the scientific community. Here some tools for the continuation of the work presented herein are given. Finally, Chapter 7 ends the work with a short epilogue.

2. Theory

2.1 Aqueous iron corrosion

Iron corrosion under environmental conditions is the process of oxidative iron dissolution (Fe^0 to Fe^{2+}) followed by the formation of layers of mixed iron oxides (iron corrosion products) around the parent material (Fe^0). Involved chemical processes include: (i) partial or total oxidation of Fe^{II} to Fe^{III}, (ii) formation of Fe^{II}/Fe^{III} hydroxides, (iii) polymerization of Fe^{II}/Fe^{III} hydroxides and precipitation and crystallization of Fe^{II}/Fe^{III} hydroxides/oxides. In this chain Fe^0 is first transformed to nebulous hydroxides and then to more or less crystalline oxides (Nesic 2007). The volume of each oxide is at least 2.02 times larger than that of the parent Fe^0 (Noubactep 2010a, Noubactep 2011a, Rahman et al. 2013, Domga et al. 2015). In another phrase, a volumetric expansion of the iron metal in aqueous solutions occurs, leading to the development of an oxide scale around the parent material.

$$Fe^0 \rightarrow Fe^{2+}/Fe^{3+}\ (H_2O)_6 \rightarrow Fe^{2+}/\ Fe^{3+}(OH)_n \rightarrow FeOOH \rightarrow Fe_2O_3 \rightarrow Fe_3O_4 \quad [2.1]$$

Or in case of insoluble species (Noubactep 2010a, Noubactep 2011b)

$$Fe^0 \rightarrow Fe(OH)_2/Fe(OH)_3 \rightarrow\ FeOOH \rightarrow Fe_2O_3 \rightarrow Fe_3O_4 \quad [2.2]$$

Table 1: Some relevant chemical reactions characterizing aqueous iron corrosion.

Reactions	Eq.
$Fe^0 \leftrightarrow Fe^{2+} + 2e^-$	[2.3]
$Fe^{2+} + 2H_2O \leftrightarrow Fe(OH)_2 + 2H^+$	[2.4]
$4\,Fe^{2+} +\ O_{\ 2}\ +\ 4\,H^+ \rightarrow\ 4\,Fe^{3+}\ +\ 2\,H_2O$	[2.5]
$Fe^0 + 2H^+ \leftrightarrow Fe^{2+} + H_2$	[2.6]

In essence, iron oxidative dissolution is an anodic reaction (donation of electrons). Fe^{2+} is release into the solution (Eq. 2.3, Table. 1), the electrons left behind migrate to cathodic sites, where a coupled or simultaneous reduction occurs. The science of aqueous iron corrosion teaches that the cathodic reaction coupled to iron oxidative dissolution Eq. (2.3) is water reduction Eq. (2.4) (Stratmann and Müller 1994). In particular, even dissolved oxygen (O_2) is reduced by Fe^{II} in (Eq. 2.5) within the oxide scale on iron (Togue-Kamga et al. 2012, Gatcha-Bandjun et al. 2014). Another reducing agent resulting from iron oxidative dissolution is hydrogen (atomic H, or molecular, H_2) (Gould 1982, Gheju and Balcu 2011) (Eq. 4). In another phrase, Fe^0 is a reducing agent in which aqueous oxidative dissolution generates two other reducing agents (Fe^{II}, H_2) in Eq. (2.6). Since 2006, some scientists are arguing, in tune with the mainstream corrosion science, that the well-documented reduction of selected species in the presence of Fe^0 (Fe^0/H_2O system) (Matheson and Tratnyek 1994, Weber 1996, Roberts et al. 1996, O'Hannessin and Gillham 1998) has been confounded with reduction by Fe^0 (Noubactep 2006, Noubactep 2007 Jiao et al. 2009, Ghauch et al. 2010, Ghauch et al. 2011, Gheju and Balcu 2011, Togue-Kamga et al. 2012, Ghauch 2013, Noubactep 2014a,

Noubactep 2015b, Noubactep 2015c). This assertion is valid for nm, µm and mm Fe^0 materials.

2.2 The electrochemical cell

The zone at which corrosion occurs have four important components (i) an anodic site where metal is dissolved (Eq. 2.3) in Tab. (1), (ii) an electrolytic solution where metal ions are released and transported from the anode to the cathode in order to maintain electro neutrality, (iii) a cathodic site where electrons left behind by metal dissolution are consumed, and (iv) a path for electron conduction: the non-corroded metal. During corrosion process the corroding material does not bear or accumulate any charge and hence neutrality is maintained. In the absence of any of the component (anode, cathode, electrolyte or metal) corrosion fails to occur. In particular, the formation of the oxide scale might hinders electron transfer from the anodic to the cathodic sites if it is not (electronic) conductive. Electronic conductive corrosion layers, under environmental conditions should be made up of Fe_3O_4 only. Such a pure Fe_3O_4-layer has not been reported in the literature. In essence the oxide scale is multi-layered with an outer layer of non-conductive Fe^{III} oxides, and a Fe_3O_4-layer adjacent to the metal (Cohen 1959, Sato 1989, Noubactep 2008a, Noubactep 2012a, 2012b, Noubactep et al. 2012a, 2012b, 2012c) As a matter of fact; the scale growth decreases the rate of iron corrosion. In presence of oxidants in the bulk water the released iron (Fe^{2+}) is oxidized to Fe^{III}-species which form suspended particles due to their low solubility (Liu and Millero 1999).

2.3 Oxide scale and mass transport

Based on historical reports (Larson 1957, Herro and Port 1993, Sarin et al., 2001) scale structure around the Fe^0 surface due to iron corrosion have significant four characteristic layers of oxide films as (i) corroded floor, (ii) porous core where both fluid and solid coexist, (iii) shell-like structure, relatively denser covering the porous core serving as structural integrity of the shell and (iv) top surface layer, located at the shell-water interface and loosely attached to the shell surface shown in Fig. 1. The corroded floor is the source of iron corrosion products. After the formation of the typical scale the further corrosion of the corrosion floor proceeds at a slow and constant rate (approximately 0.5mm y^{-1}) causing continuous growth of the scale (Herro and Port 1993). The porous core consists of agglomerate of small particles of different morphologies According to Sarin et al. (2001, 2004a, 2004b), the composition of the porous core are α-FeOOH, Fe_3O_4, α-Fe_2O_3 and $FeCO_3$ and high concentration of Fe^{2+} in the form of solid or dissolved iron (Sarin et al., 2004b). The presence of green rust, ferrihydrite and ferric hydroxides might be expected inside the core. The shell like structure is comparatively thicker than core and top layer and the thickness was found to vary from fractions of millimeters to a few millimeters (Clement et al. 2002). The composition of the shell structure is Fe_3O_4 and α-FeOOH (Sarin et al. 2001) and this layer separates the bulk water from readily oxidizable Fe^{2+} ions and solid matter present in the tubercle. There is a possibility of occurrence of multiple shell layers due to successive fractures in the single shell layer. These fractures are results of expansions and contractions caused due to change in the temperature (Herro and Port 1993). The top layer exists in the

scale water interface and it is influenced by the water quality. This layer might comprise of lepidocrocite and amorphous $Fe(OH)_3$ in addition to precipitates of the unwanted ions.

Typically there is a tendency of the solution to migrate towards the surface of the Fe^0 in an aqueous solution. This phenomenon is known as "mass transport".

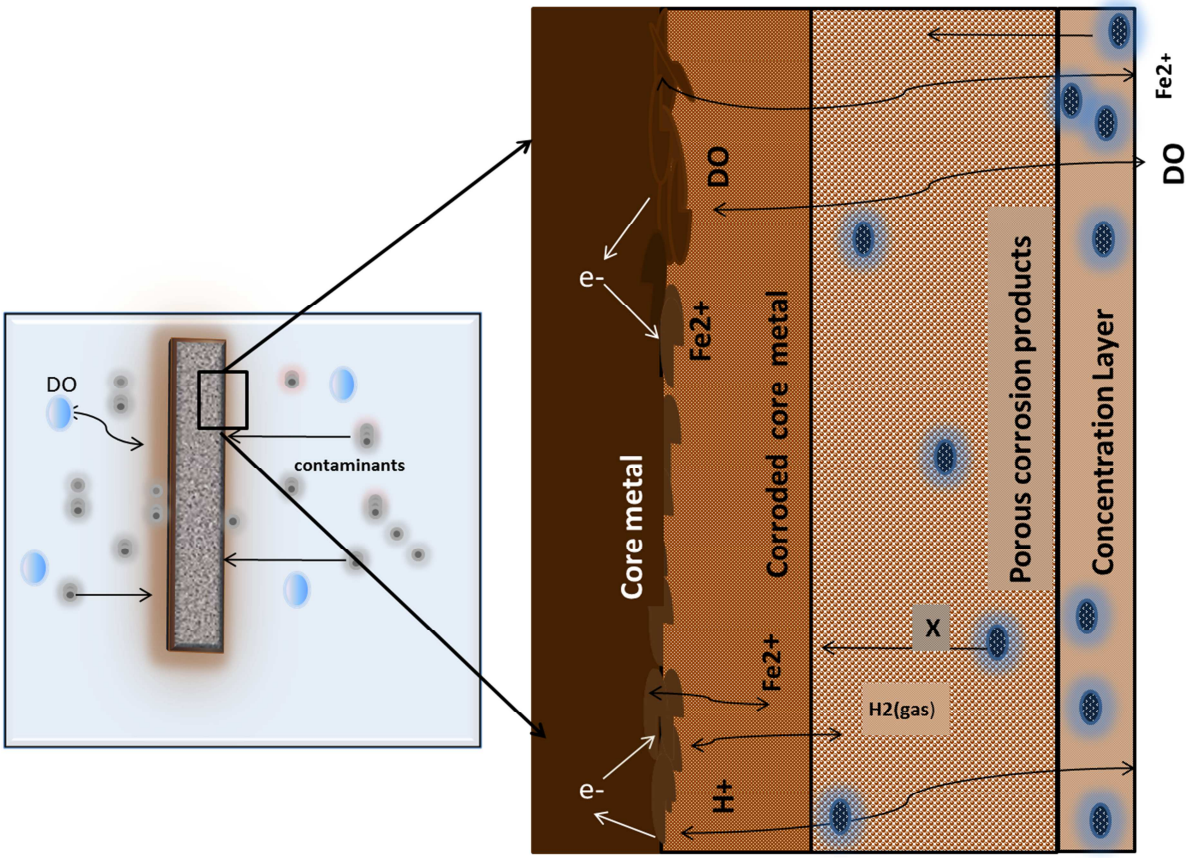

Fig 1: Schematic diagram showing migration of (i) contaminants-X, (ii) dissolved oxygen (DO) (iii) electron(e^-) (iv) ferrous iron(Fe^{2+}) (v) hydrogen in the vicinity of immersed metallic iron (adapted and modified after Sarin et al. 2004b).

2.4 Diffusion and advection

Mass transport occurs in two distinctive modes under environmental conditions namely diffusion and advection. Diffusion is the mass transport due to random fluctuations of molecules or in other words it is the movement of molecules due to concentration gradients (Karmanova et al. 2002). On the contrary advection is caused by mean velocity field or due to fluid flow (Honrath et al. 1995). In the present experiment diffusion is caused in the non-shaken batch experiment in which the contaminant molecules are fluctuating randomly and being transported towards the surface of the reactive material from the bulk solution. The contaminant molecules are treated in the vicinity of the reactive material and hence it builds a concentration gradient driving the remaining contaminant molecules to plunge on to the surface of the reactive system. The availability of the contaminants in the system after the reactive period depends on its concentration amount or the saturation of the reactive material.

Advection acts a major role in the shaken batch experiment and the contaminant molecules move towards the reactive substance in a faster mode than by diffusion (Kurth 2008).

Under groundwater flow condition, advection is dominant near the oxide film layer but large flow scale is restricted near the Fe^0 surface due to presence of tubercle. Tubercle are mounds of rust formation due to corrosion (Sarin et al. 2004a) and thereby turbulence is absent in the vicinity of Fe^0 surface (Noubactep 2009b, Noubactep et al 2009b, Noubactep et al 2009c, Noubactep 2010b, Noubactep 2012b). The migration of the contaminants across the oxide film is mainly due to molecular diffusion and electro-migration depending on the pore structure and tortuosity (film permeability) (van der Kamp et al. 1996, Nordsveen et al. 2003). The electrochemical reactions in aqueous iron corrosion process produces Fe^{2+} ions and simultaneously deplete O_2, H^+ ions and contaminants in the purlieu of Fe^0. This process develops concentration gradients of the species and contaminants across the oxide film and hence they tend to move towards or away from the surface of the Fe^0, in other words there is occurrence of molecular diffusion (Noubactep 2008b, Gunawardana et al. 2011). The molecular diffusion separates the charges by short range but there is a presence of strong attractive forces between oppositely charged species and hence this separation cause movement of electrons, i.e. there is transfer of electrons from Fe^0 surface to the bulk solution and contaminants across the oxide film. Hence, the oxide film is potentially an electron conductor, but only if it is conductive (e.g. made of Fe_3O_4).

2.5 Contaminant removal in Fe^0/H_2O system

According to historical studies a broad array of species of contaminants such as organic, inorganic, ionic, non-ionic, and neutral and even living species (microorganisms) can be efficiently reduced or removed in Fe^0/H_2O systems. So this draws to a sensible conclusion that mechanism of contaminant removal depends on the iron corrosion process rather than specific properties of the contaminant itself (Noubactep 2007, Noubactep 2008a, Miyajima 2012, Noubactep 2012a, Noubactep 2012b, Noubactep 2013a, 2013b, 2013c). As stated earlier (§ 2.1), the cycles of volumetric expansion/contraction characterizing aqueous iron corrosion lead to the entrapment of contaminants in the matrix of corrosion products. There are two paths for ending the cycles of volumetric expansion/contraction: (i) Fe^0 is exhausted, and (ii) the pore space is filled (clogging) (Noubactep et al. 2010b).

Adsorption, co-precipitation and adsorptive size exclusion are the three mechanisms that explain the removal of contaminants by aid of iron corrosion in the Fe^0/H_2O system (Noubactep 2007, Noubactep 2008a, Ghauch et al. 2011, Gheju and Balcu 2011).

Fe^0 is oxidized to Fe^{II} species when it is immersed into solution when $pH \geq 4.5$ releasing part of it into the bulk solution and the remaining gets converted to Fe (III) and hence precipitates as it reacts with the contaminants present in the solution. Along with precipitation, occurrence of co-precipitation is viable as the contaminant might get adsorbed in the oxide film and entrapped in the emergent matrix of the corrosion products or even on the mature corrosion product surface bearing high adsorption capacity. So it is observed that adsorption, precipitation and co-precipitation are tough to distinguish since it is related to each other

(Miyajima 2012). But then again these mechanisms have been argued over the differences of their geometry of the adsorbents surface, where co-precipitation is believed to be three-dimensional process and more effective than plain adsorption (Crawford et al. 1993). Further the adsorbed or co-precipitated contaminants are directly reduced by (Fe^0) or indirectly reduced by Fe^{II}. However, reduction by indirect process is more favorable than direct process. In history, reduction was considered the excellent method or way of removing contaminants from the solution but recent researches support adsorption and co-precipitation over reduction. The cause for accepting adsorption and co-precipitation as fundamental process for the contaminant removal is due to the requirement of sheer chemical reductions for the class of quantitatively removed contaminants without redox properties. So the removal of contaminants can be well explained by the adsorption and co-precipitation process by their dynamic mechanism (Noubactep 2011a) and hence these two mechanisms are considered the primary processes in the removal of contaminants in the company of adsorptive size exclusion (Table 2).

Table 2: The possible reaction pathways in the removal of contaminants from the aqueous solution is shown in table (cited from Noubactep, 2009a)

Mechanism	**Reaction**	**Eq.**
Precipitation	$\mathrm{Ox(aq) + nOH^- \leftrightarrow Ox(OH)_{n(s)}}$	[2.7]
Adsorption	$S_{(\text{sorption site})} + \mathrm{Ox \leftrightarrow S - Ox}$	[2.8]
Co-precipitation	$\mathrm{Ox + nFe_x(OH)_y}^{(3x-y)} \leftrightarrow \mathrm{Ox - \left[Fe_x(OH)_y}^{(3x-y)}\right]_n$	[2.9]

2.5.1 Adsorption

The role of adsorption is stated earlier in this thesis in which an adsorbate and adsorbent plays the fundamental role at an interface between two phases such as liquid-liquid, gas-liquid, gas-solid, liquid solid interfaces. But in the Fe^0/H_2O system interface between liquid and solid is of prime importance. The mechanism of adsorption helps the contaminants to adhere to the surface of the oxide film due to chemisorption or physical sorption. Chemical sorption occurs due to the reaction between the adsorbate and adsorbent which forms a covalent bond and requires high energy to break the bond. Physical sorption is due to electrostatic forces or weaker Van der Waal forces and hence low energy is sufficient to break the bonds (Miyajima 2012). In functional barriers both adsorption into aged corrosion products and co-precipitation with nascent iron oxides occur (Noubactep 2007) controlling the concentration of contaminants in the aqueous solution.

The adsorption capacity depends on the structural, physical and chemical properties of the adsorbent and adsorbate and the liquid phase conditions (Ghosemi et al. 2007) and one of the important structural characteristics of the adsorbent is its specific area (Smith et al. 1983).

The specific surface area is given by

$$S = Y.N.A[m^2g^{-1}] \qquad [2.10]$$

S= specific surface area ($m^2 g^{-1}$)

Y= adsorbed dye (mol g^{-1})

N= Avogadro's number ($6.023*10^{23}$ molecules mol^{-1})

A= area covered by each molecule (m^2molecule $^{-1}$)

Depending on the adsorption process, kinetics of adsorption might be described based on Langmuir or Freundlich isotherms which are valid only in equilibrium. Adsorbate might form a monolayer on adsorbent e.g. MB on granular activated carbon or might form aggregated on the surface of the adsorbent depending on the physical properties of the adsorbent (Richards et al. 1996). In some of the adsorbents depending on the nature of the adsorbate, desorption might occurs (Imamura et al. 2002). Desorption of MB occurs from a pure sand system (Phukan et al. 2015)

2.5.2 Co-precipitation

There is yet no clear distinction between co-precipitation and adsorption. According to Crawford et al. (1993) co-precipitation ameliorates the removal process of the contaminants from the solutions than direct adsorption. It can only be effective until the availability of free corrosion products during the aging of Fe^0 (Noubactep 2008a). Co-precipitation is a mechanism in which soluble species or impurities (which include living bacteria, viruses) are removed from the solution leading to settling of the impurities. Moreover, these impurities gets deposited or entrapped in the matrix of the continuously formed corrosion products (Crawford et al. 1993). The precipitation of the corrosion products continues by nucleation, growth, aggregation or stabilization and ageing of the corrosion products. The nucleation process is heterogeneous and incorporation of the contaminants leads to its growth (Kurth 2008). In Fe^0/H_2O systems, the foreign bodies lead to co-precipitation in presence of iron oxide film and the contaminants undergone co-precipitation and are released when iron oxide gets dissolved but the new layer formation of iron oxide again entraps the impurities and hence refrains it from getting mixed with the solution (Miyajima 2012).

2.5.3 Adsorptive size-exclusion

This mechanism in simple words is known as 'straining' and is relevant to the particle size of the impurities and the pore of the filter. When the particle size is bigger than the filter pore than it gets strained in the outer layer of the filtration system and cleaner water or solution is passed through. When the particles get accumulated continuously than there is a development of a cake layer whose void size is smaller than the void size of the filter itself and hence it aids in straining even more infinitesimal particles (Miyajima 2012).

In Fe^0/H_2O systems, the targeted contaminant is continuously adsorbed onto the in-situ generated adsorptive corrosion product and it is observed as a trickledown effect (Keeney-Kennicutt and Morse 1985) and layer of oxide formation in the Fe^0 surface is of prime

importance. The working of the system of Fe^0/H_2O has also been investigated by mixing process to facilitate the contaminant from the bulk to the Fe^0 surface. But the mixing process inevitably transports the corrosion products (including Fe^{II} species) away from the Fe^0 surface which either delays the formation of oxide layer or in some cases avoidance of oxide layer formation is observed (Noubactep et al. 2009a, Noubactep 2015c).

2.6 Packed bed design (Fe^0 amended sand filter)

As it was discussed in the earlier section the corrosion process in Fe^0/H_2O system was dependent on number of factors (DO, pH) of the solution. Water treatment using Fe^0-amended filtration system might be not sustainable (durable) due to porosity loss (clogging). Clogging is caused due to (i) adsorption of fouling material, (ii) bio-corrosion, (iii) particle cementation or cake formation, and (iv) volumetric expansion of iron corrosion (Noubactep 2010d).

The volumetric expansion of the iron corrosion has been a major factor which leads to clogging of the system within a short duration. In order to resolve this problem Fe^0 filter can be amended with a porous and chemically inert material like sand. Sand increases the void volume and allows the iron corrosion species to reside on its intra particles space and thus increasing the life of the filter system. But the main positive aspect of sand admixture is that it does not contribute to porosity loss as it is inert and not expansive.

Contaminant removal mechanisms are adsorption, co-precipitation and size exclusion. Removal of relevant contaminants occurs mainly in the reactive zone (Fe^0/sand layer). In the Fe^0 containing zone adsorptive size exclusion is a major removal mechanism due to expansion and contraction of the iron corrosion cycle and entraps the contaminants in the relatively less porous matrix of the iron corrosion mainly termed as ultrafiltration (Noubactep 2010d). Therefore it is necessary to keep the void space in Fe^0 amended system wide enough for the expansion and contraction process.

The design of the column has been proposed as to be sandwich like structure in which the reactive mixture is located in between two layers of pure sand material. In order to have a homogeneous mixture of Fe and sand in the column experiment the height of the sand have to be at least 5 cm (i.e $h_{RZ} > 5$ cm) (Noubactep and Caré 2011). The volumes and masses of the iron material were already calculated (Miyajima and Noubactep 2013). The necessity of the pure sand layers is to (i) characterize the interaction between sand and dyes and (ii) as an inexpensive filling material for the column.

3. Materials and Methods

3.1 Solutions

The aqueous solutions used in the present work are (i) three dyes solutions (ii) an iron standard solution (1000 mg L^{-1}).

3.1.1 Dyes

The dyes used are methylene blue (MB), Orange II and reactive red 120 (RR 120) purchased from Merk Acros Organics and Sigma Aldrich respectively. These dyes are used as received. The molar concentration of the working solution is 31.5 µm corresponding to initial weight concentrations of 10 mg L^{-1}, 11 mg L^{-1} and 46.3 mg L^{-1} of MB, Orange II and RR 120 respectively. The selected dyes are of analytical grade, are dissimilar in sizes and have different affinity to iron oxides (Table 3). RR 120 is larger in size, whereas other two are of comparable sizes (Fig 2).

The working solution was prepared by diluting a 100 fold concentrated solution with tap water of Göttingen whose pH is 8.2 and its average composition was in mg L^{-1} (Cl^-: 12.9; NO_3: 7.5; SO_4^{2-} : 35.5; Na^+: 9.7; K^+: 0.9; Mg^{2+}: 8.2; Ca^{2+}: 37.3). The concentration of dye used here is selected to approach the concentration range of micro-pollutants in natural waters (dyes as model micro pollutants, concentrations non representative for industrial wastewater).

Table 3: Some relevant physico-chemical characteristics of tested dyes. The dye molar concentration was 31.5 M. The corresponding weight concentrations (mg L^{-1}) of individual dyes are specified.

Dye	Symbol	Nature	M	λ_{max}	[Dye]
		(pH 8.2)	(g mol^{-1})	(nm)	(mg L^{-1})
Methylene blue	MB	cationic	319.85	664.50	10.10
Orange II	-	anionic	350.32	485.00	11.00
Reactive Red 120	RR 120	anionic	1469.98	515.00	46.30

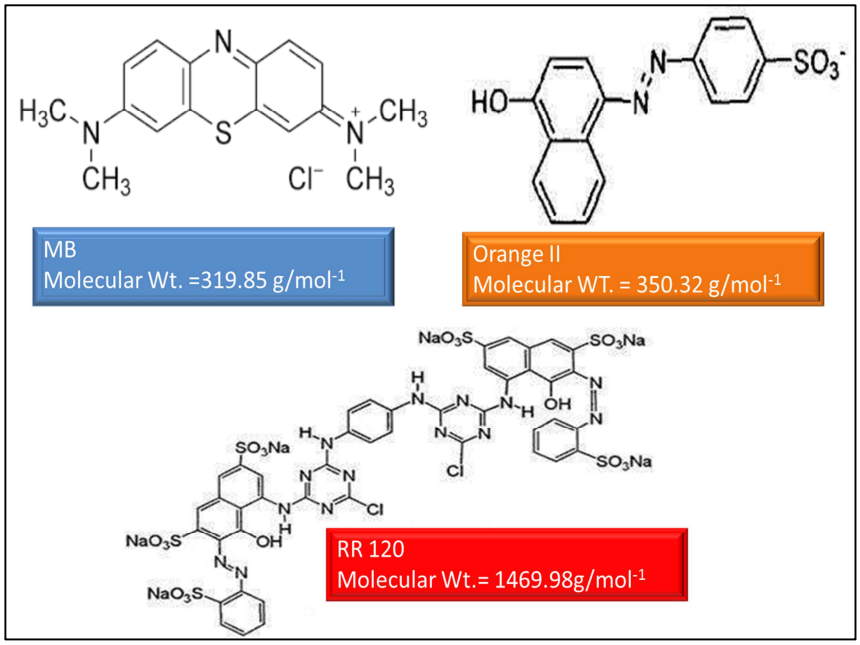

Fig 2: Chemical Structure and molecular weights of the used azo dyes (a) methylene blue (MB) (b) Orange II (c) reactive Red 120(RR 120).

3.1.1.1 Methylene Blue (MB) - $C_{16}H_{18}ClN_3S$

Methylene Blue is a heterocyclic aromatic compound and is a cationic dye. In its original state at room temperature it is solid, odorless, dark green powder. The molecular dimension of MB is 16.0 Å length, 8.4 Å breath and minimum thickness of 4.7 Å (Kipling and Wilson 1960). It has a pKa value of 3.8. MB has a high adsorption affinity for solid surface (Imamura et al. 2002) especially for oppositely charged surfaces (Janos et al. 2005). In its oxidized form the colour changes from dark green to deep blue colour and in its reduced form it changes to colorless also called as leukomethylene blue LMB. The wavelength of MB is 664.5 nm bearing molar mass of 319.85 g mol^{-1}.

3.1.1.2 Orange II- $C_{16}H_{11}N_2NaO_4S$

Orange II is a one of the form of Orange 7 which is an acid dye and it also comes under azo-group (mono-azo). Its length, breath and thickness is 15 Å, 10 Å and 5 Å. Orange II has two pKa values (10.6 and 1.0) and thus three different form of azo dye could exist in the aqueous solution depending on the pH of the medium(Abramian et al. 2009). It is water soluble mostly in the form of sodium salts of carboxylic and sulfonic acids. Solubility in water is 116 g L^{-1} at 30^0 C. Its wavelength is approximately 485 nm. It is an anionic dye and strongly gets attach to the cationic groups of solid surfaces. The molar mass of Orange II is 350.32 g mol^{-1} (Ramavandi et al. 2013).

3.1.1.3 Reactive Red 120 - $C_{44}H_{24}Cl_2N_{14}O_{20}S_6Na_6$

RR 120 is a form of azo-group chromophores which when combined with different classes of reactive groups form covalent bonds with textiles like cotton. The pKa value of this dye is 12.5. It generally exists in hydrazine form due to the intra-molecular H-bonding (Jhimli et al. 2011). It is bright colored and consumes low energy. These dyes are stable to light, heat and oxidizing agent. They are non-degradable by biological activity. RR 120 is majorly used in textile industries (Dafale et al. 2008).

Figure 2 summarizes the chemical structures and the molecular weight of the dyes is presented and it is observed that the size of RR 120 is comparatively larger than the other two dyes.

3.1.2 Iron solution

In the column experiment, additional Fe concentration is measured which is dissolved in the outflow solutions. The iron determination followed the 1,10 Orthophenanthroline method (Fortune and Mellon 1938) commonly used for colorimetric analysis of Fe in solution. The Fe(III) species in the solution is reduced to Fe(II) by ascorbic acid and further Fe(II) under goes complexation process with the aid of Orthophenanthroline. The Fe solution to measure dissolved Fe concentration in the effluent dye solution is prepared as follows

10 mL probe/sample +1 mL Ascorbic acid + 2*4 mL H_2O + 1 mL Orthophenanthroline

Fig 3: Preparation process for measurement of Fe concentration in solution

After vigorous shaking the samples are allowed to react in an undisturbed condition for 15 minutes before the spectrophotometric concentration measurement.

3.1.1.4 Other Solutions

In order to measure pore volume in the pure sand column in the column experiment, a concentrated solution of NaCl (278 µS cm^{-1}) solution was passed through the pure sand column. The electrical conductivity of the effluent solution was measured for each collected volume of the effluent. The electrical conductivity of the effluent solution is initially that of tap water and increases as water is progressively replaced from the pore volume (inter-granular porosity). The electrical conductivity of the effluent remains constant when all water is flushed from the column. The point for NaCl breakthrough corresponds to the pore volume (PV) of the column. It is considered herein, that the Fe^0-containing columns depict the same value of PV.

3.2 Solid Materials

The investigated systems include single aggregates (Fe^0, MnO_2, sand) or selected mixtures thereof (Fe^0/sand, Fe^0/MnO_2, and Fe^0/sand/MnO_2).

3.2.1 Metallic Iron (Fe^0)

Fe^0 is the main material to be characterized in this study. The used commercial sample is obtained from iPutechGmbh (Rheinfelden, Germany). The size of the Fe^0 particles varies from 0.30 mm and 2.0 mm in the form of fillings and was used without any further pretreatment. The composition of the elemental iron was C: 3.52%, Si: 2.21%, Mn: 0.93%, Cr: 0.66% and Fe: 92.68%. The discoloring effect for MB by Fe^0 is proven by Noubactep (2009b). A second type of Fe^0 is used in the batch experiment which is referred as "ZVI2". The composition of ZVI2 was C: 3.13%. Si: 2.17%. Mn: 0.36%. Cr: 0.077% Ni: 0.056% and Fe: 96.7%.

3.2.2 Sand

Sand used in the experiment is commercial aviculture product known also as "Papageiensand" (RUT – Lehrte/Germany). The size of the sand particle varies from 0.5 mm to 2.0 mm. "Papageiensand" is used as a pure adsorbent without any pretreatment. Due to its natural abundance, sand is commonly used in the Fe^0/H_2O system as an admixture (O'Hannesin and Gilham et al. 1988).

3.2.3 MnO_2

Manganite is a natural MnO_2-bearing mineral. The sample used herein was obtained from Ilfeld/Harz (Thüringen, Germany). The minerals were crushed and fractioned by sieving. MnO_2 is a known adsorbent for MB; it is also reductively dissolved by Fe^{2+} which inhibits MB discoloration by co-precipitation, due to accumulation of iron corrosion products on MnO_2 surface. MnO_2 is used in this study as admixing agent to Fe^0 to control the availability of insitu 'free' corrosion products. MnO_2 draws the corrosion products that are generated in situ with Fe^0 and layers on its surface whereas the surface of the Fe^0 gets free from 'passivating' iron oxides (Noubactep et al. 2005, Noubactep 2009a, Ghauch et al. 2011, and Noubactep 2011a, Noubactep 2011b). The corrosion product is main sole for adsorption and co-precipitation of the dyes. In some past experimental works use of MnO_2 did not improve the discoloration of MB due to delay in the availability of free corrosion products (Noubactep et al. 2005, Miyajima and Noubactep 2015). The discoloration of MB has failed (or was delayed) due to the reductive dissolution of MnO_2. The MB discoloration can only be quantitative when the oxidation capacity for Fe^{II} of the present MnO_2 is exhausted. Thus "excess" corrosion products are available to entrap MB (Noubactep 2008a, 2009a, 2009b). Orange II and RR 120 are anionic in nature and have more adsorption affinity for iron corrosion products (Kosmulski 2009). But in the presence of MnO_2, there is lack of corrosion products for the anionic dyes to be adsorbed and co-precipitate.

3.3 Analytical methods

Methods used in this present study are (i) UV-Vis Spectra Method (ii) pH measurement (iii) EC measurement

3.3.1 UV-Vis Spectra method

The Cary 50 Varian spectrophotometer was calibrated initially by using standard solutions (diluted and original working dye solutions) $\leq 31.5\mu M$. Then the concentration of the samples of batch experiment and column experiment was determined using a Cary 50 Varian -UV-Vis spectrophotometer in which cuvettes of 1cm light path was used. The wavelength set for MB, Orange II and RR120 were 664.5 nm, 485 nm and 515 nm respectively (Table 3). Additionally, dissolved iron concentration of the effluent solution was measured for (column experiment). The wavelength for Fe concentration measurement was set to 510 nm.

3.3.2 Further analytical methods

The pH value of the solution was measured using combined glass electrode (WTW Co. Germany). During the pH measurements, a magnetic stirrer was used to homogenize the solution and to avoid statistical errors. In batch experiments, 3 consecutive samples (each triplicate) were mixed and the pH value measured for at least 3 min. (A2.2-A2.10)

The electrical conductivity was measured using a calibrated WTW instrument. The aim was to measure the pore volume of the columns. (A2.II)

4. Experimental Procedure

4.1 Performed experiments

In order to investigate the dye discoloration by the tested granular materials and thus to characterize the impact of the ionic nature of the dye on its discoloration in Fe^0/H_2O systems, batch and column experiment were designed. The reactive system in the batch experiment comprises of Fe^0, sand and MnO_2 and mixtures thereof. The reactive systems in the column experiment are pure sand, pure Fe^0 and Fe^0/sand (50 % of Fe^0-vol/vol).

For batch experiments, accurately weighted amounts of granular materials (Fe^0, MnO_2, sand and related combinations) are introduced in graduated test tubes of 20 mL. In total 30 samples were assigned for each dye per batch (10 samples, each in triplicates). 22 mL of each dye working solution was filled in the tubes and sealed with caps. Filling with 22 mL of the working solution aimed at reducing the free space above the solution and also to reduce the availability of molecular oxygen (Vidic et al. 1991). The sealed test tubes were allowed to equilibrate under quiescent or shaken conditions for 2 to 6 weeks.

For column experiments, glass columns with 26 mm internal diameter and 400 mm height were used. Columns were mostly filled with sand and 100 g Fe^0. For each dye, three columns were tested: (i) pure sand (0 % Fe^0), (ii) a 1:1 (vol/vol) Fe^0: sand layer sandwiched between two layers of sand, and (iii) a pure Fe^0 layer (100 % Fe^0) sandwiched between two layers of sand. For MB an additional column with a pure Fe^0 layer, but 200 g of Fe^0 was investigated. For each column, dye effluent was collected periodically (twice a week) and the volume is recorded as a function of elapsed time for the assessment of flow velocity or hydraulic conductivity. Additionally, the pH value, the iron breakthrough and the dye concentration were monitored for 93 days.

The initial concentration of MB, Orange II and RR 120 are 10, 11, 46.3 mg L^{-1} respectively. The pH of the initial solution is 8.2. The concentration of dyes is selected as 31.5 µM to compare the concentration range of natural water in which all three dyes acts as micro-pollutants

4.2 Dye discoloration

4.2.1 Batch experiments

The investigation systems for the batch experiment were single pure sand, MnO_2, Fe^0 and segregates of its mixtures. The single pure systems consist of only 4.55 g L^{-1} mass loadings of individual material. In total 3 triplicates were assigned for each material for each dye. Additionally another Fe^0 is used referred as “ZVI2” in Fig. 9. The pure systems were monitored in order to observe its individual capability to adsorb different ions under same experimental condition (temperature, pH and time). The mixture batch experiments consist of 30 samples (3 triplicates) which make 10 samples in total and of that 1 sample are blank (only

supernatant solution). Only mixture Fe^0/sand/MnO_2 consists of 1 sample for each material for each dye. Here, the Fe^0 mass loading is constant of 4.55 g L^{-1} and only sand and MnO_2 loadings vary from 4.55 g L^{-1} to 22.0 g L^{-1}. But Fe is the main scope of discussion in this study and thereby it is mixed with other material to characterize the behavior of the reactive system when subjected to different kinds of ions under same or different experimental conditions. The investigation were carried out under same experimental conditions but only difference is that mixtures Fe^0/sand/MnO_2 and Fe^0/MnO_2 were carried under 6 weeks non shaken period whereas mixtures of Fe^0/sand, Fe^0/MnO_2 and pure MnO_2 under shaken conditions for 2 weeks. Fig.4 represents the dye sample preparation for each reactive material and its mixtures.

Fig 4: Preparation of the dye sample with reactive material in the batch experiment (a) methylene blue (MB); (b) Orange II and (c) reactive red 120 (RR 120). The experiment was performed at room temperature (22 ± 3^0C) and the initial pH was 8.2.

The amount of sand and MnO_2 loadings varies from 0.05 to 0.5 g (4.55 g L^{-1} to 22 g L^{-1}) with fixed amount of 0.1 g (4.55 g L^{-1}) of Fe^0 and combination of mixtures. The experimental duration of the batch experiments were 6 weeks under quiescent condition and 2 weeks under shaken conditions at a rate of 75 rpm. The investigation systems were (i) pure sand (ii) pure MnO_2 (iii) pure Fe^0 (iv) Fe^0/sand (v) Fe^0/MnO_2 and (vi) Fe^0/sand/MnO_2 mixtures.

Hence all the measured samples are loaded into test tubes and filled with the working solutions (MB, Orange II and RR120) up to full volume of 22.0 mL and then sealed with caps. Therefore the test-tubes are made ready with the reactive material and working solutions to place into a shaker for 2 weeks at a moderate speed (75 rpm) and 6 weeks in a non-shaken

condition. After the equilibrium time, 3.0 mL of the supernatant solution are retrieved and its concentration is measured. Each experiment was performed in triplicates from measured samples to measured concentration and its averaged values are exhibited.

4.2.1.1 Shaking

Rotational shaking has been a major aiding factor for adsorption and co-precipitation (Kurth 2008). Therefore shaking helps in transporting contaminant from the aqueous solution to the Fe^0 surface much faster and equilibrium is attained at an early stage. Shaking certainly accelerates processes leading to dye discoloration by adsorption and co-precipitation. In earlier experimental works the critical shaking intensity enabling an undisturbed formation of an oxide-scale on Fe^0 was found to be 50 rpm (Kurth 2008, Noubactep 2008a, 2008b, Noubactep et al. 2009b, Noubactep et al. 2009c). Herein a shaking intensity of 75 rpm is used as it was demonstrated to yield reproducible results (Miyajima 2012).

4.2.1.2 Discoloration effect of the dyes due change in sand loadings

Two different batch experiments with fixed amount of Fe^0 and varying sand loadings were carried out under (i) Fe^0/sand under shaken conditions for 2 weeks at 75 rpm and (ii) Fe^0/sand/MnO_2 under quiescent conditions (non-shaken) for 6 weeks. For shaken condition, 10 different samples for each dye can be presented as sand (0.0 to 0.5) g + Fe^0 (0.0*2, 0.1*8) g (A1.2). For quiescent conditions, 10 batch samples are presented for each dye as sand (0.0 to 0.5) g + MnO_2 (0.0 to 0.5) g + Fe^0 (0.0*4, 0.1*6) g (A1.1) in order to determine the effect of the adsorption of the dyes by the sand in presence of MnO_2.

In each set 30 samples were measured for each dyes with different configuration of the reactive materials. Every three consecutive sample configuration were same making in total 10 samples with different configuration of the reactive material including the first blank samples (consecutive 3 samples) used as a reference system. In both the cases amount of Fe^0 remains unchanged.

4.2.1.3 Discoloration effect of the dyes due change in MnO_2 loadings

Three different batch experiments with MnO_2 loadings were carried out under (i) Fe^0/MnO_2 under quiescent conditions for 6 weeks (non-shaken) and (ii) Fe^0/MnO_2 and MnO_2 under shaken conditions at 75 rpm for 2 weeks.

For shaken condition, 10 different samples for each dyes were presented as MnO_2 (0.0 to 0.5) g + Fe^0 (0.0*2, 0.1*8) g. (A1.3). In order to investigate the behavior of the Fe^0-based system, and to understand the correspondence of the system with the different ions, reaction was carried out only with MnO_2 loadings (A1.5) and the trend of the dye discoloration was studied. This particular shaken batch was only used for MB and Orange II. The amount of MnO_2 loading as 10 different samples was (0.0 to 0.50 g). In order to figure out the discoloration efficiency of the dyes kept under longer time period and to compare with the efficiency of the shaken batch system, quiescent batch was studied for Fe^0/MnO_2. The

configuration of 10 different samples for each dyes are as MnO_2 (0.0 to 0.5) g + Fe^0 (0.0*2, 0.1*8) g (A1.4).

4.2.2 Column experiments

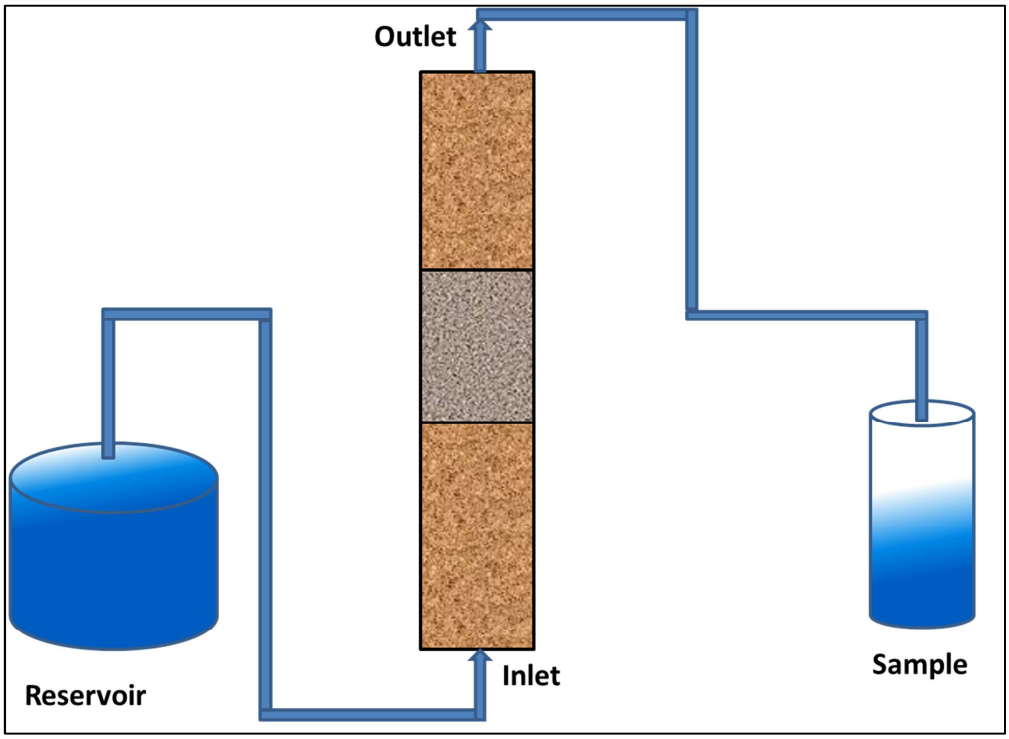

Fig 5: Schematic diagram of the column experiment

The experiment was carried out in saturated, continuous upflow mode with a constant flow rate of 0.1 mL^{-1}/min regulated by a peristaltic pump (Ismatec, ICP 24) at a temperature of (22 ± 3°C). The experimental set-up of column experiments consists of 10 columns with cross-section area of 5.31 cm^2. The empty bed contact time (EBCT) in Fe^0-based systems is shown in (Table 4). EBCT is the amount of time the dyes were in contact with the reactive media in the respective columns. In Tab. 4, H_{sand1} represents sand layer before reactive zone (Fe^0/sand mixture) and H_{sand2} represents sand layer after the reactive zone. Tygon tubes were used for connecting inlet reservoir, pump, column and outlet. The samples in the outlet are collected in PE bottles. The materials in the 10 columns are packed in dual manner. Sand (H_{sand1} and H_{sand2}) and pure Fe^0 layers (column 3, 6, 9, 10) were wet packed. Dry homogenized Fe^0/sand mixture were introduced in the columns in small lofts (about 2 cm each), later wet packed with manual tapping for all other reactive zones ($0 < Fe^0$ (%) < 100) (Table A2.1). The experimental set-up is presented in Fig. 6. Each column was gently tapped with PET flacon containing water in order to warrant optimal compaction. The reactive zone was built while using the volume occupied by 100 g Fe^0 (32 mL - apparent volume) as unity. The same volume of sand was took (mass: 48 g - weight ratio 32.5 %) and homogeneously mixed to Fe^0 (32 mL). The concentration of the dye solutions pumped into the columns is 32.5 µM. The

effluent is collected periodically and the volume is recorded as a function of elapsed time for the assessment of flow velocity or hydraulic conductivity.

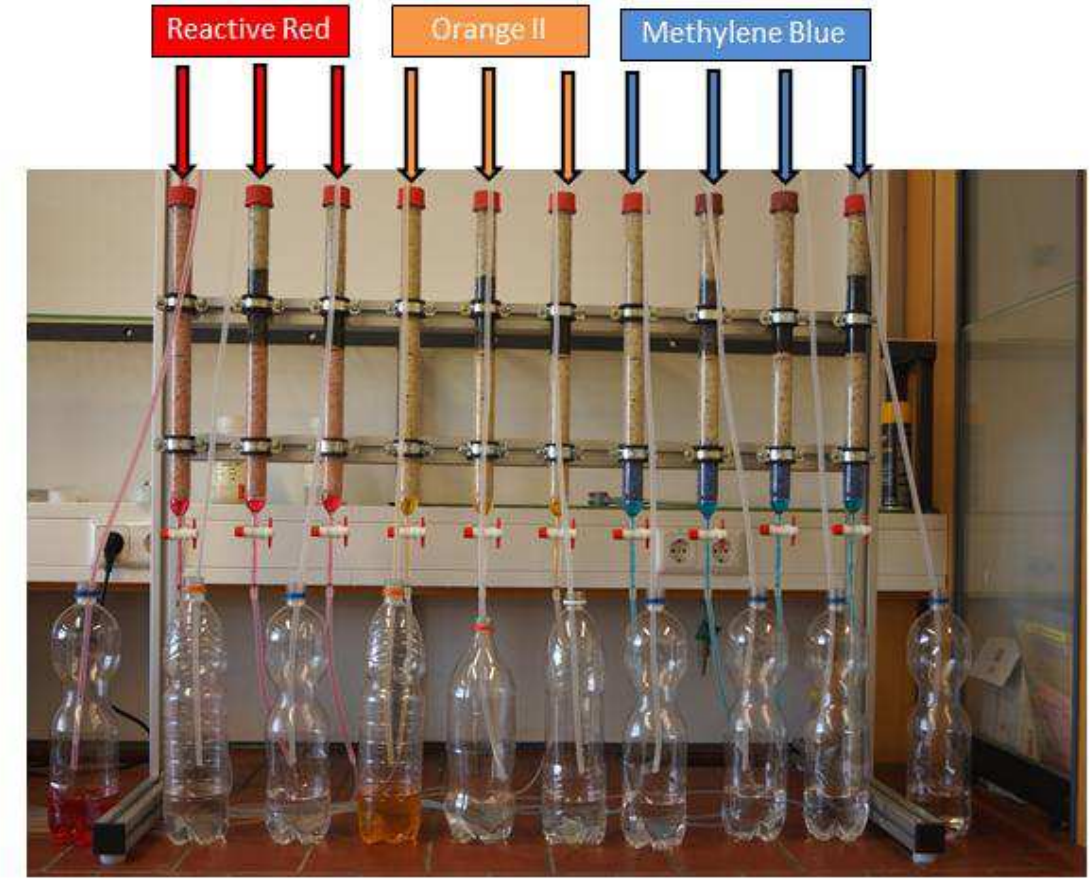

Fig 6: Experimental set-up of column experiment on day 1

Table 4: Empty Bed Contact Time in the Fe^0-based systems of the column experiment. The columns were made up from the bottom to the top of: bottom sand layer ($H_{sand,1}$), the reactive zone (H_{RZ}) and top sand layer ($H_{sand,2}$).

Fe^0 (%)	$H_{sand,1}$(cm)	H_{RZ} (cm)	$H_{sand,2}$ (cm)	V_{HRZ}(cm^3)	EBCT (hrs.)
50	20.0	14.0	6.0	74.3	6.46
100	20.0	6.0	14.0	28.2	2.45
100(200g) MB	20.0	10.0	10.0	53.1	4.61

4.3 Analytical Methods

The analytical methods include (i) calibrating the standard solution of dyes and Fe, (ii) determining the residual dye concentration and (iii) determining the iron concentration in the effluents (column experiments).

4.3.1 Calibration of the Spectrophotometer

The spectrophotometer was initially calibrated by 5 standards solutions of each dye (Table 5) in order to determine the unknown concentration of the sample dyes (Fig. 7). The standard solutions are prepared by diluting by parts with tap water of Gottingen with 1000 mg L^{-1} dye stock solution. The calibration standard solutions are measured at the beginning of the experiment at the respective wavelength of the dyes. (Table 2)

Table 5: Standard solutions used for the calibration of the Cary 50 UV-VIS – Spectrophotometer for the determination of dye concentrations.

Std	Vo	RR120	Orange II	MB
	(mL)	(mg L^{-1})	(mg L^{-1})	(mg L^{-1})
1	0	0.0	0.0	0.0
2	1	11.6	2.8	2.5
3	2	23.2	5.5	5.0
4	3	34.7	8.3	7.5
5	4	46.3	11.0	10.0

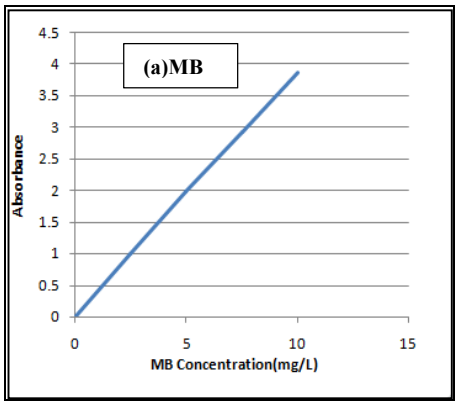

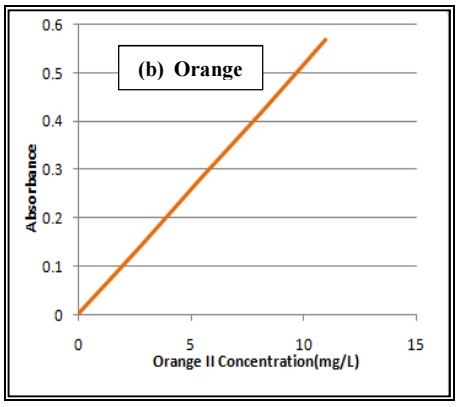

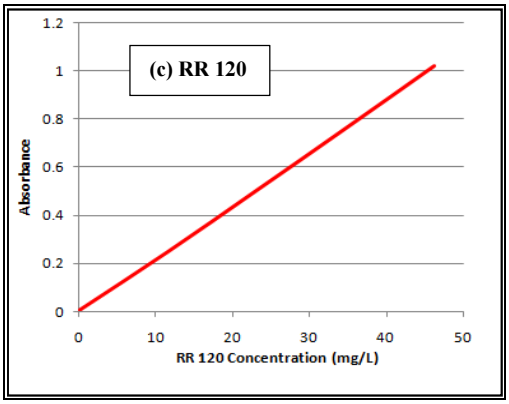

Fig 7: Calibration graphs of light absorbance at various concentration of dyes and its linear regression (a) MB (b) Orange II (c) RR 120

The calibration of the spectrophotometer (Fig. 8) was done also for iron concentrations ≤ 10.0 mg L^{-1}. For the concentration of the dissolved iron, calibration was performed using ten variable concentrations (0.0, 0.25, 0.50, 0.75, 1.0, 2.0, 4.0, 6.0, 8.0, and 10.0) mg L^{-1}. The standards were prepared from a commercial stock solution (1000 mg L^{-1}) and tap water with total volume of 10 mL each (Table. 6). The calibration procedure were same as the dyes, but at a wavelength of 510 nm.

4.3.2 Determination of dye concentration

The initial dye concentrations are 10 mg L^{-1}, 11 mg L^{-1} and 46.3 mg L^{-1} for MB, Orange II and RR 120 respectively. The dye concentrations at the end of the batch experiments or in the effluents from columns are measured using the calibrated UV-Vis Spectrophotometer. For the batch experiments, the concentration of each sample was determined by the average value of each triplicate used. For column experiment, effluents were sampled in test tubes twice a week and the dye concentration determined once a month.

Table 6: Standard solutions used for the calibration of the Cary 50 UV-VIS – Spectrophotometer for iron determination.

Standard	**[Fe]**	**V_0**	**VH_2O**	**V_1H_2O**	**V_2H_2O**
		(mL)	(mL)	(mL)	(mL)
1	0.00	0.00	10.00	10.00	0.00
2	0.25	0.25	9.75	7.50	2.25
3	0.50	0.50	9.50	7.50	2.00
4	0.75	0.75	9.25	7.50	1.75
5	1.00	1.00	9.00	7.50	1.50
6	2.00	2.00	8.00	7.50	0.50
7	4.00	4.00	6.00	6.00	0.00
8	6.00	6.00	4.00	4.00	0.00
9	8.00	8.00	2.00	2.00	0.00
10	10.00	10.00	0.00	0.00	0.00

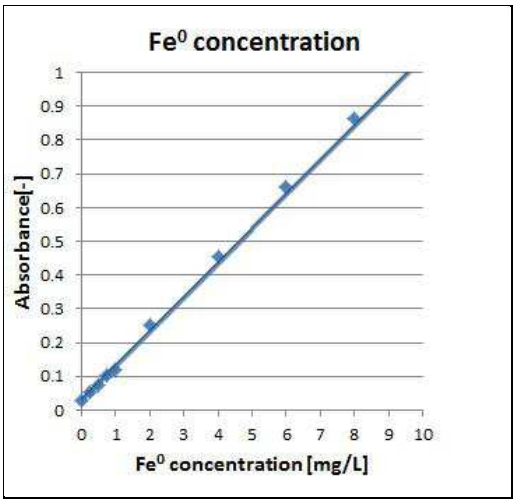

Fig 8: Calibration graph of light absorbance at various concentration of Fe^0.

4.3.3 Determination of Fe concentration

The iron concentrations in the effluents from columns are determined using the calibrated UV-Vis Spectrophotometer. 10 mL of the effluent from each column were sampled in test tubes twice a week. The iron concentration was determined one time every two months (twice for the whole thesis) at a wavelength of 510 nm.

4.4 Characterizing the compaction of the column material

After the end of the desorption experiments (Phukan et al. 2015), the columns were characterized by visual observations and the extent of the compaction of material within the reactive zone (Westerhoff and James 2003). As the columns had been operated in an upflow mode with a completely blue in colored $H_{sand,1}$, the challenge was reduced to observe the reactive zone and $H_{sand,2}$. In particular, the ease with which the reactive zone was removed from the column was described.

4.5 Pore volume determination

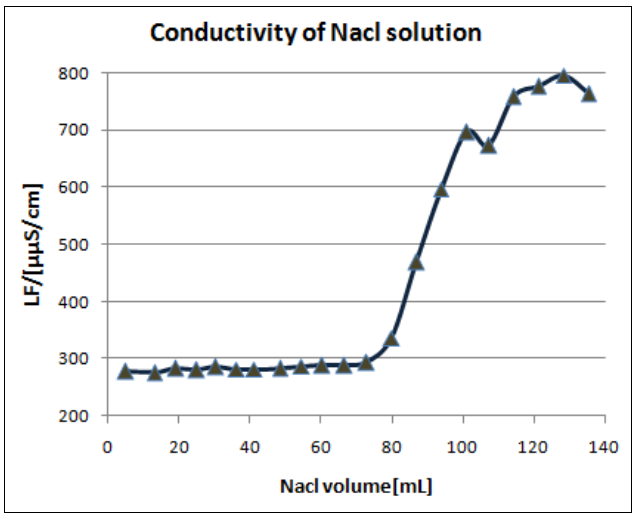

Fig 9: Volume dependent electrical conductivity of NaCl solution.

Fig. 9 depicts the variation of the electrical conductivity of a NaCl (table salt) solution as tap water is progressively fed into the pure sand column. The electrical conductivity increases as the NaCl volume reaches 80 mL and from 120 mL it becomes more or less stable. This indicated that increase in NaCl volume from 120 mL and beyond shows the same result as the system is saturated with only NaCl solution. Based on this result, the pore volume of the column was determined as 95 mL.

4.6 Presentation of the experimental results

The change in magnitude of the tested system for dye discoloration was presented in the form of discoloration efficiency of each dye for each sample containing different configuration of the reactive material. The residual or final concentrations of the dyes are determined and the corresponding dyes discoloration percentage is calculated by the following expression [Eq. 4.1]:

$$E = \left[1 - \left(\frac{Ci}{C_o}\right)\right] * 100\% \quad [4.1]$$

In case of column experiment the dye breakthrough curves in terms of normalized concentration similar to batch experiment which is defined as the ratio of the effluent dye concentration to inlet dye concentration as a function of time. The extent of discoloration for individual column set up at each time is calculated according to the following expression:

$$E = \left[\frac{\sum Vi * C_0 - \sum Vi * Ci}{\sum Vi * C_0}\right] * 100\% \quad [4.2]$$

$$BT\ (\%) = 100\text{-}E \quad [4.3]$$

Where,

C_0 = initial concentration of the dye
C_i = final concentration of each dye after the reactive period.
E = discoloration efficiency in percentage
V_i = Volume of individual collected sample
BT = dye breakthrough

In order to confront experimental errors during dilution of stock solutions, corrections were made due to adsorption of dyes on PE bottles and possible biodegradation. Mainly adsorption of MB by the glass test tubes and glass column which is a product of sand and negatively charged. Corrections were made through the assimilation of the operational initial concentration in triplicates under controlled experiment in the absence of any reactive material (blank system) or reference systems. In case of batch experiment blank systems are filled only with dyes but in column experiment the reference system is filled with sand.

In case of column experiment the dye concentration of the reference system (100 % sand) was set to 100 % and the correction of the effluent from other systems was corrected accordingly. The extent of MB discoloration (m_{MB} in mg) within the reactive zone of column 8 to 10 was calculated from H_{sand1} using rule of proportion. In this circumstance, column 7 was used as reference (40 cm of sand for 44.8 mg MB). The breakthrough value in this work was calculated in the following order:

Below only the calculation for column 7 for MB is described in detailed and for Orange II and RR 120 directly the results are presented.

BT value 44.8 mg = $\sum V_i C_0$ (difference in the cumulative influent and the cumulative effluent of the dyes)

Cumulative influent = Amount of volume in x concentration
= 216.42 mg

Cumulative effluent= Amount of volume out x concentration
= 261.25 mg

Hence the difference = (261.25-216.25)

= 44.8 mg

Therefore 44.83 mg of dye (mass) is retained in the reference system containing 100 % sand.

Now, in other systems Fe^0/sand (50 % and 100 %),

Height of H_{sand1} = 20 cm

Therefore (m_{MB}),

$$m_{MB} = \frac{H_{sand1}}{40} * 44.8 \quad [4.4]$$

= 22.4 mg

Subtracting 22.4 mg from the total mass of discolored MB gives the MB mass which is discolored by H_{sand1} in Fe^0-based system is 22.4 mg or 70.2 µmol.

Similarly in the reference systems in column 4 and column 1 for Orange II and RR120 respectively, the BT values are 7.5 mg and 21.68 mg. Therefore in Fe^0- based system the amount of the anionic dyes retained in the H_{sand1} layer are 10.7 µmol for Orange II and 7.4 µmol for RR 120.

5. Results and Discussion

5.1 Batch Experiment

The investigation systems for the batch experiment were: (i) pure sand, (ii) pure MnO_2 (iii) pure Fe^0, (iv) Fe^0/sand, (v) Fe^0/MnO_2, (vi) Fe^0/sand/MnO_2 mixtures.

5.1.1 Reproducibility of the experimental results

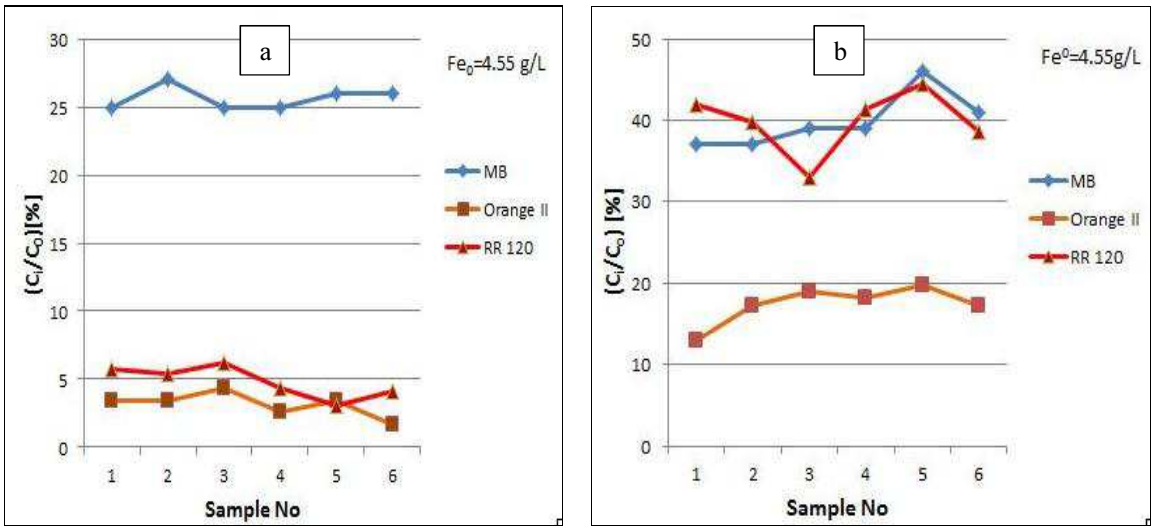

Fig 10: Discoloration extent in pure Fe^0 (a) under non-shaken conditions for 6 weeks and (b) under shaken conditions for 2 weeks. The lines are not fitting functions; they simply connect points to facilitate visualization.

*C_0: initial concentration; C_i: final concentration of the dyes

In Fig. 10 the experimental results are presented in the form of residual dye concentration in the pure Fe^0 systems. The amount of Fe^0 loading is constant which is 4.55 g L^{-1}, and volume of the filled solution is 22 mL. The initial concentration of MB, Orange II and reactive red 120 are 10, 11 and 46.3 mg L^{-1}respectively and the initial pH of the solutions are 8.3.

It is observed that the pure Fe^0 system shows a quantitative discoloration of all tested dyes, irrespective from the shaking conditions. Under non shaken conditions, the discoloration for MB is 25 % and for Orange II and RR 120 is almost below 5 %. In other words, the amount of dye retained in the filter system for MB is 75 % and for the anionic dyes around 95 %. Under shaken conditions for 2 weeks the discoloration are 40, 20 and 38 % for MB, Orange II and RR 120 respectively. In spite of both RR 120 and Orange II being anionic in nature, the discoloration effect was less for RR 120 compared to Orange II might be due to higher molecular weight of RR 120 and thus steric effects. Similar results (Tab. 7) were obtained for pure sand and pure MnO_2 systems under same experimental conditions. The discoloration % for MB in the sand system is 65 % and 75 % under non-shaken and shaken conditions respectively i.e. dye retained % in the system are 35 % and 25 % respectively whereas for the anionic dyes the discoloration % values approaches 100 % under both experimental

circumstances. In other words, anionic dyes retained by the pure sand system are 0 % and has shown no effect. Dye discoloration % for MB, Orange II and RR 120 are around 5 %, 100 % and 85 % respectively under both experimental conditions.

Table 7: Summary of the results of dye discoloration (%) in individual Fe^0, sand and MnO_2 systems under 6 weeks quiescent and 2 weeks shaken condition.

Dyes	**Experimental conditions(weeks)**	**Extent of dye Discoloration (E) (%)**		
		Fe	Sand	MnO_2
MB	6-quiescent	75 ± 5	35 ± 5	100 ± 5
	2-shaken	60 ± 5	25 ± 5	95 ± 5
Orange II	6 quiescent	100 ± 0	5 ± 2	0 ± 5
	2-shaken	80 ± 5	5 ± 2	0 ± 0
Reactive Red 120	6–quiescent	90 ± 5	4 ± 2	4 ± 2
	2-shaken	65 ± 5	4 ± 2	5 ± 5

Results clearly demonstrated better reproducibility under non-shaken conditions compared to shaken conditions. This trend is justified by the fact that the non-shaken system was more likely near to a steady state than the shaken system. However, while considering both the ionic nature (charge) and the size (steric effects) of the dyes, shaken batch experiments still give satisfactory results and will be favorably used in this study. The main reason for this is the duration of the Master thesis and the number of opportunities to investigate. It should be delineated that the large majority of batch experiments reported in the literature are performed under more vigorous shaking speeds and for experimental durations rarely exceeding two days (Noubactep 2009a, Noubactep et al. 2009b, Noubactep et al. 2009c, Tepong-Tsindé et al. 2015a, Noubactep 2015c). For the used shaking intensity, 75 rpm, the process of oxide scale formation on Fe^0 is not significantly disturbed (conditions in nature are nearly reproduced) (Miyajima 2012).

5.1.2 Single material systems

In Fig. 11 results of the single material systems are presented under non-shaken conditions for 6 weeks for three systems namely (i) sand (ii) MnO_2 and (iii) Fe^0.

5.1.2.1 Sand system

It is observed in Fig. 11 that the MB discoloration efficiency by sand is around 30 % and that for anionic dyes the discoloration efficiency is negligible despite prolonged experimental duration (6 weeks). The used sand mass loading is 22.0 g L^{-1}. Sand has negatively charged surface and shows affinity for positively charged MB.

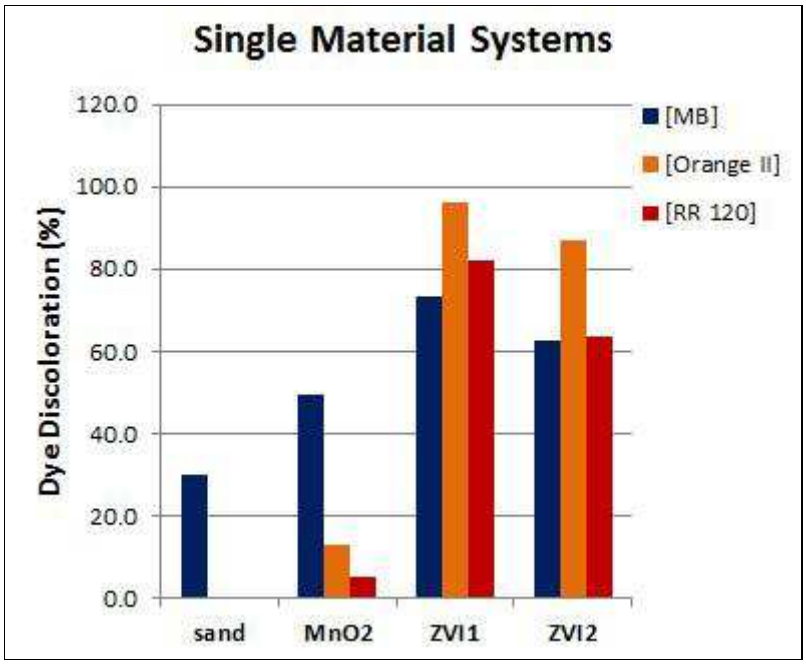

Fig 11: Dye discoloration by single material systems under non shaken conditions for 6 weeks. Experimental conditions: temperature 20 ± 3 ^{0}C; volume of solution was 22.0 mL, dye concentration was 32 µM and initial pH of the solution is 8.3.

5.1.2.2 MnO_2 system

Fig 11 shows that MnO_2 is superior to sand in its capability to remove all tested dyes. About 50 % of MB, 15 % of Orange II and 5 % of RR120 could be discolored. The order of decreasing discoloration efficiency (MB >> Orange II > RR120) suggests that the surface of MnO_2 is equally negatively charged. Again, the significance of (i) the ionic nature and (ii) the steric effects for the efficiency of Fe^0/H_2O systems for environmental remediation is delineated. Whether dye discoloration by MnO_2 is mediated by surface precipitation or chemical reduction of pure adsorption, the first step of the discoloration is adsorption which depends on electrostatic attractions/repulsions.

5.1.2.3 Fe^0-based systems

Fe^0 is the most reactive discoloring agent in the whole experiment. In order to ascertain the efficient reactivity of Fe^0 for discoloration of Orange II and RR 120, two types of materials (ZVI = Fe^0) are studied under 6 weeks non shaken experimental condition in order to compare the discoloration efficiency by both ZVI1 and ZVI2.
Fig. 11 shows that ZVI1 is a more efficient material than ZVI2. The discoloration efficiency by ZVI1 is higher for both cationic and the anionic dyes. The discoloration efficiency is shown highest for Orange II, about 96 % and 90 % respectively.

This evidence supports the premise that Fe^0 produces in-situ positively charged Fe oxides and hydroxides. Hence it preferentially adsorbs negatively charged species (anions) and thus Orange II and RR 120 are strongly adsorbed and quantitatively removed. Discoloration can be

observed for MB as well because adsorption is not only the sole mechanism. MB (cation) is weakly adsorbed onto positively charged iron-oxides and co-precipitated.

5.1.3 Fe^0 amended systems

Figure 12 shows the extent of dye discoloration by the following admixtures (i) Fe^0/sand (ii) Fe^0/MnO_2 (iii) Fe^0/sand/MnO_2 as reactive systems.

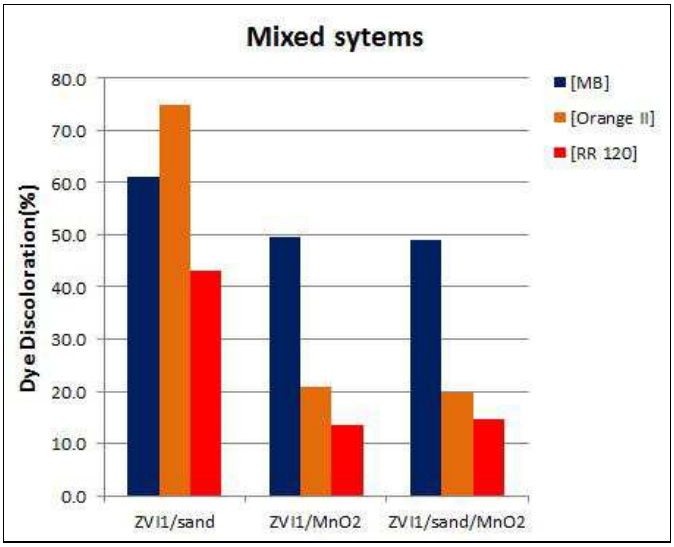

Fig 12: Dye discoloration by mixed system under non- shaken conditions for 6 weeks. The used mass loadings are: Fe^0 is 4.55 g L^{-1}, sand and MnO_2 is 22 g L^{-1}.

It is remarked that the Fe^0/sand system has shown higher discoloration efficiency for all three dyes. The discoloration efficiencies are about 60 %, 75 % and 45 % for MB, Orange II and RR 120 respectively. The highest discoloration efficiency for Orange II testifies that sand could sustain the in-situ generation of iron oxides. This assertion is supported by the higher extent of MB discoloration comparatively to the Fe^0/MnO_2 and Fe^0/sand/MnO_2 systems. There was no significant difference between the Fe^0/MnO_2 and Fe^0/sand/MnO_2 systems. This behavior is attributed to the presence of MnO_2 which consumes Fe^{II} at its surface and delays the availability of free corrosion products for dye co-precipitation (Noubactep 2009b, Miyajima 2012, Miyajima and Noubactep 2015, Tepong-Tsindé et al. 2015b). Again the lowest discoloration extent observed for RR 120 is rationalized by steric effects.

Dye discoloration in the Fe^0/sand system results from the following processes: (i) adsorption onto sand, (ii) adsorption onto iron oxide (from Fe^0 corrosion) and (iii) co-precipitation with iron corrosion products. Because of differences in density between Fe^0 and sand (and the fact that sand is larger in size), Fe^0 tends to be shielded by sand. Accordingly, dye co-precipitation is inhibited to a certain extent by the presence of sand (Miyajima and Noubactep 2015). On the other hand, as Fe^0 corrosion proceeds, there is a concurrence between dyes, Fe^{II} and Fe^{III} for adsorption at the surface of sand. At this time sand is completely coated with iron oxide and from this moment on, adsorption occurs on iron oxides, coated on sand or 'free' in the vicinity of Fe^0.

The presence of MnO_2 increases the complexity of the system as MnO_2 reductive dissolution by Fe^{II} ions (Koch, 1957) destroys adsorption site at the surface of MnO_2 and favors Fe^{III} oxide precipitation at the same site. The net result is a delay of the availability of 'free' iron corrosion products for contaminant co-precipitation. With this overview of fundamental processes in mind, the results of the three systems will be shortly discussed in the following section.

5.1.3.1 Fe^0/sand system

MB gets adsorbed on sand and co-precipitates on iron oxides. On the other hand Orange II and RR 120 get adsorbed on the positively charged corrosion products. In Fe^0/sand system, the amount of used sand is not enough to shield the Fe^0 particles; thereby it is not able to inhibit the adsorption and co-precipitation process between dyes and the Fe oxides. In other words there is availability of free iron corrosion products. An alternative justification might be that the available iron oxides do not precipitate; it rather gets adsorbed onto sand to form iron-oxide coated sand bearing weak adsorption capacity than pure sand for the cationic dye (Mitchell et al. 1955). Hence it shows more discoloration of the anionic dyes specially Orange II since it gets adsorbed on the oxide layer above pure sand. Similarly anionic RR120 has more affinity towards iron coated sand. The effect on sand amended with Fe^0 has shown great effect on dye discoloration and hence another experiment was conducted under 2 weeks shaken condition (Fig. 13).

5.1.3.2 Fe^0/MnO_2 system

In Fe^0/MnO_2 system the discoloration efficiency was observed to be 50, 21 and 13 % for MB, Orange II and RR 120 respectively. MnO_2 is reductively dissolved by Fe^{2+} and inhibits dye discoloration in Fe^0/H_2O systems. The corrosion products of Fe^0 are accumulated on the surface of MnO_2 which thereby hinders the iron surface from passivation and induce the generation corrosion products for the dye adsorption and co-precipitation in the long term (Noubactep et al. 2003). Additionally there is formation of new reactive adsorbents MnOOH and FeOOH. Even with the generation of iron corrosion products the efficiency of discoloration is slow due to the delay in-situ formation Fe-oxides (Noubactep et al. 2005). This is caused due to the accumulation of corrosion products on MnO_2 surface. The oxidation capacity for Fe^{II} for MnO_2 has to be exhausted to avail the free corrosion products for greater adsorption and precipitation process of the dyes. The behavior of the identical system was also observed in an experiment performed under shaken conditions for 2 weeks. In the shaken Fe^0/MnO_2 system highest discoloration efficiency is observed that is 98 % and 82 % for MB and Orange II respectively. This shows a vast increment as compared to non-shaken batch experiment. The trend for discoloration is increasing for MB while for Orange II it is the opposite. This can be explained again by the rate of accumulation of in-situ generated corrosion products on the MnO_2 surface which makes more favorable for MB to co-precipitate than the anionic dyes.

5.1.3.3 Fe^0/sand/MnO_2 system

In case of the Fe^0/sand/MnO_2 system, addition of MnO_2 sustains the reactive system. There is occurrence of chemical reactivity in the internal surface of the porous MnO_2 pores instead in the free pores of the whole system. In this manner MnO_2 sustains the systems permeability and retains the efficiency of the free pores (Ghauch et at. 2011). A competition arises between positively charges iron corrosion products and cationic MB to get adsorbed onto the sand but the presence of MnO_2 helps this phenomenon by shielding itself by corrosion products and leases MB dye to get adsorbed onto sand but for Orange II and RR 120 this is unfavorable condition (Btatkeu-K et al. 2014).

In order to compare the discoloration efficiency of the individual reactive materials and mixtures systems, experiments were carried out under different experimental conditions kept in shaker at rate of 75 rpm for 2 weeks and 6 week under non shaken using fixed amount of Fe^0 and various sand and MnO_2 loadings.

5.1.4 Discoloration efficiency of dyes by sand loadings

In the below Fig. 13, discoloration efficiency by different amount of sand loading with fixed amount of Fe^0 is presented under shaken conditions for 2 weeks.

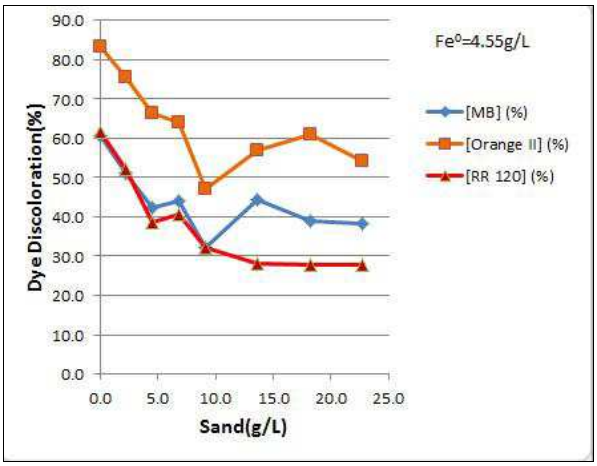

Fig 13: Dye discoloration by Fe^0/sand system under shaken conditions for 2 weeks. Experimental conditions: shaking intensity 75 rpm, temperature 20 ± 3 ^{0}C and initial pH value 8.3. The lines are not fitting functions; they simply connect points to facilitate visualization.

The highest discoloration efficiency for MB is 60 % and for Orange II is 82 %. The discoloration efficiency for both cationic and anionic dyes shows decreasing trend as the sand loading increases. In the initial section of the curves at 0 g L^{-1} sand loading (Fe^0 = 4.55 g L^{-1}) the discoloration efficiency is the highest for all the three dyes. The discoloration efficiency is lowest for MB and Orange II when the sand loading is 9.1 g L^{-1} which is double amount the weight of used Fe^0 which is 4.55 g L^{-1}. The sand works as inhibitor for discoloration of MB and Orange II at approximately 9-13 g L^{-1} and reduces the contact of dye with Fe^0 or iron oxides. The increase in sand loading beyond that shows random increases in discoloration of the dyes due to increase in surface area. But strangely the discoloration efficiency of Orange

II still remain high compared the MB. This result strongly suggests that amount of sand used is not enough to shield the corrosion product instead the corrosion products precipitated on sand and forms a covering in which MB is mildly adsorbed and co-precipitated and Orange II has the higher affinity to get adsorbed on the oxide coated sand. The lowest discoloration of RR 120 is due to its higher molecular weight.

It is extraordinary that the discoloration efficiency in shaken experiments for 2 weeks was lower for the identical sand (22 g L^{-1}) and Fe^0 (4.55 g L^{-1}) mixture system as the 6 weeks non shaken experiment. In the 2 weeks shaken experiment, the discoloration efficiencies are 38, 54 and 28 % for MB, Orange II and RR 120 respectively. This might be due to no attainment of equilibrium state under shaken conditions for 2 weeks compared to long term non- shaken conditions.

This observation justifies that as the amount of sand used with fixed Fe^0 amount has the nature to deal with both cationic and anionic contaminants in a solution. Sand here act as porous admixture dealing with cation and allows the generation of iron oxides to deal with anions in a contaminant solution.

5.1.5 Discoloration Efficiency of dyes by MnO_2 loadings

In the below Fig. 14, discoloration efficiency by different amount of MnO_2 loading with fixed amount of Fe^0 is presented under (a) non-shaken conditions for 6 weeks and (b) shaken conditions for 2 weeks.

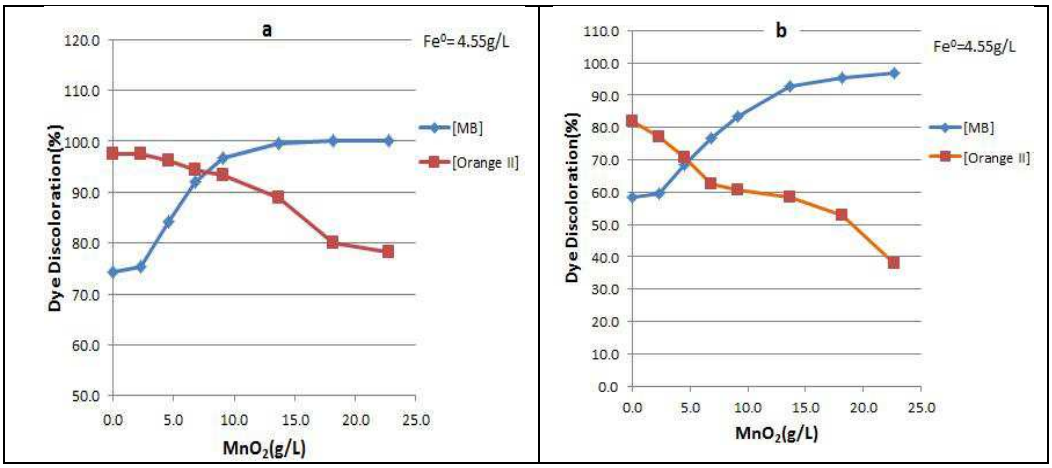

Fig 14: Dye discoloration by Fe^0/MnO_2 system (a) under non shaken conditions for 6 weeks (b) shaken conditions for 2 weeks. The lines are not fitting functions; they simply connect points to facilitate visualization.

It is observed that in both Figs. 14a and 14b the discoloration efficiency for MB increases in the initial part while Orange II shows a gradual decreasing trend. It is observed in Fig. 14a that the highest discoloration efficiency by MB is 100 % and by Orange II is also nearly 100 % while in Fig. 14b. The discoloration efficiency for MB is 98 % and Orange II is 82 %. In

both the figures, discoloration of anionic dyes decreases with increase in MnO_2 loadings and entirely contrasting trend for cationic dye.

The observation of this trend of discoloration proves that cationic dyes have more affinity towards MnO_2 while anionic dyes strongly repel. This can be explained by the in situ generated nascent MnOOH and FeOOH which are adsorbing agents for MB eq. [5.1, 5.2, and 5.3]. The rate of heterogeneous reactions depends on the crystal structure, porosity and chemical composition of MnO_2 including its surface area and composition of the solution (pH value) and the temperatures (Miyajima 2012). The reactions below consume Fe^{2+} and reductive dissolution of MnO_2 by Fe^{2+} either consumes (Eqs. (5.2) and (5.3) - pH increases) or produce H^+ (Eq. (5.1) - pH decreases). Consumption of Fe^{2+} reduces the availability of free corrosion products for MB to co-precipitate and Orange II to get adsorbed (Btatkeu et al. 2014a). Therefore, in this case according to the observation the Eqs. (5.2 and 5.3) seems more favorable due to increase in pH. Increase in pH leads to increment of pzc (point of zero charge) of the system where the surface is negatively charged and hence can attract cation.

$$MnO_2 + 2\,Fe^{2+} + 2\,H^+ \rightarrow MnOOH + 2\,Fe^{3+} \quad [5.1]$$

$$MnO_2 + 2\,Fe^{2+} + 2\,H_2O \rightarrow Mn^{2+} + 2\,FeOOH + 2\,H^+ \quad [5.2]$$

$$MnO_2 + Fe^{2+} + 2\,H_2O \rightarrow MnOOH + FeOOH + 2\,H^+ \quad [5.3]$$

5.1.6 pH values of discolored dyes

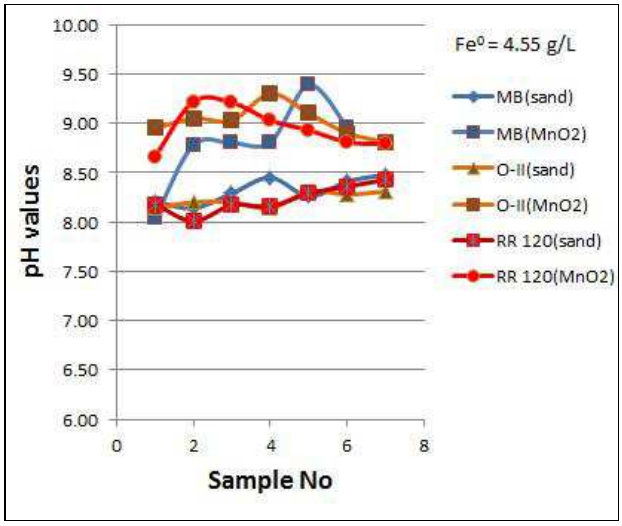

Fig 15: pH values of the discolored dyes by sand and MnO_2 loadings under shaken conditions for 2 weeks. The Fe^0 mass is fixed. The lines are not fitting functions; they simply connect points to facilitate visualization

In Fig. 15, the evolution of pH values of the discolored dyes in the batch experiments performed for 2 weeks under shaken conditions are presented. The pH values are presented for sand and MnO_2 loading with fixed amount of Fe^0 and it is observed that the variation is not significant. But if observed in very detail, the pH values of dyes with MnO_2 loadings are

higher compared to sand loadings. This justifies the reason for affinity of cationic dyes towards higher MnO_2 loadings favoring discoloration than anionic dyes (Eqs. (5.2 and 5.3)).

5.2 Column Experiment

The column experiments were carried out for 93 days in which a total of 10 columns were used with different ratios of the reactive media. The tested systems for each dye are (i) pure sand (0 % Fe^0), (ii) pure Fe^0 (100 % Fe^0) and (iii) Fe^0/sand (50 % Fe^0-vol/vol).

The columns 1, 4, and 7 are the reference systems and contains only sand. Columns 2, 5, and 8 contain 50 % Fe^0 and 50 % sand by volume in the reactive zone whereas columns 3, 6 and 9 contains pure 100 % Fe^0 (100 g) in the reactive zone whereas column 10 also contains 100 % Fe^0 but 200 g weight of Fe^0. In the experimental set up, columns 1, 2, 3 are subjected to Reactive Red 120 dye, columns 4, 5, 6 are subjected to Orange II dyes and columns 7, 8, 9, 10 to MB as shown in the Fig. 16.

5.2.1 Visual observation

Fig. 16 depicts the photograph of the experimental design at day 21 (Fig.16a) and day 93 (Fig. 16b). It is observed that at day 21, column 10 is the sole system that has not experienced dye breakthrough.

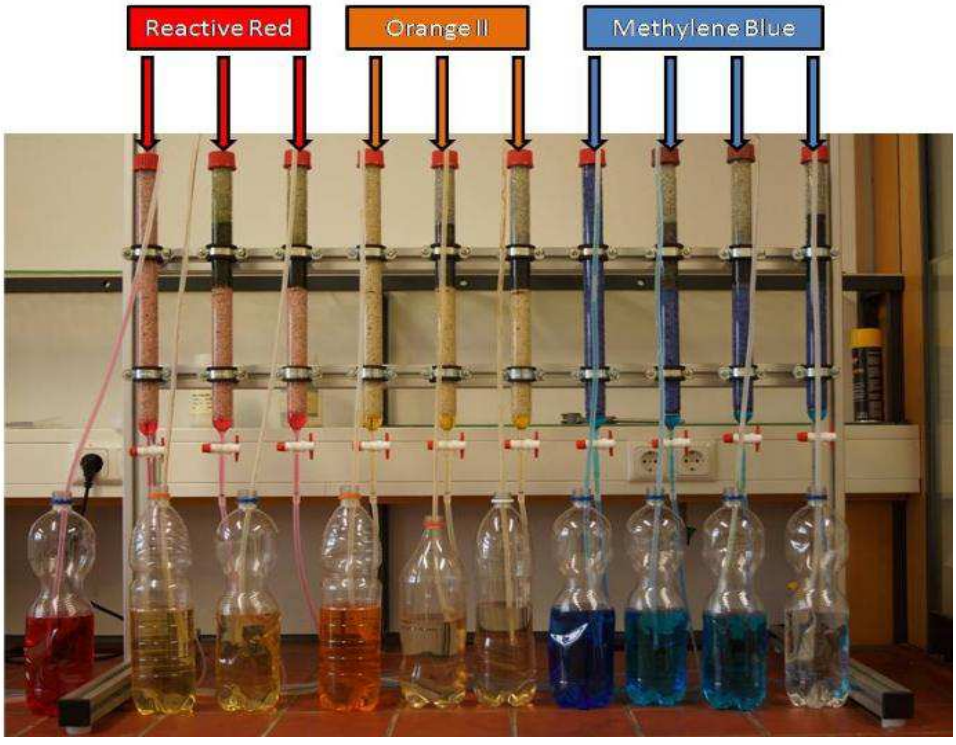

Fig 16a: Photograph of the experimental set–up of Column Experiment on 21st day

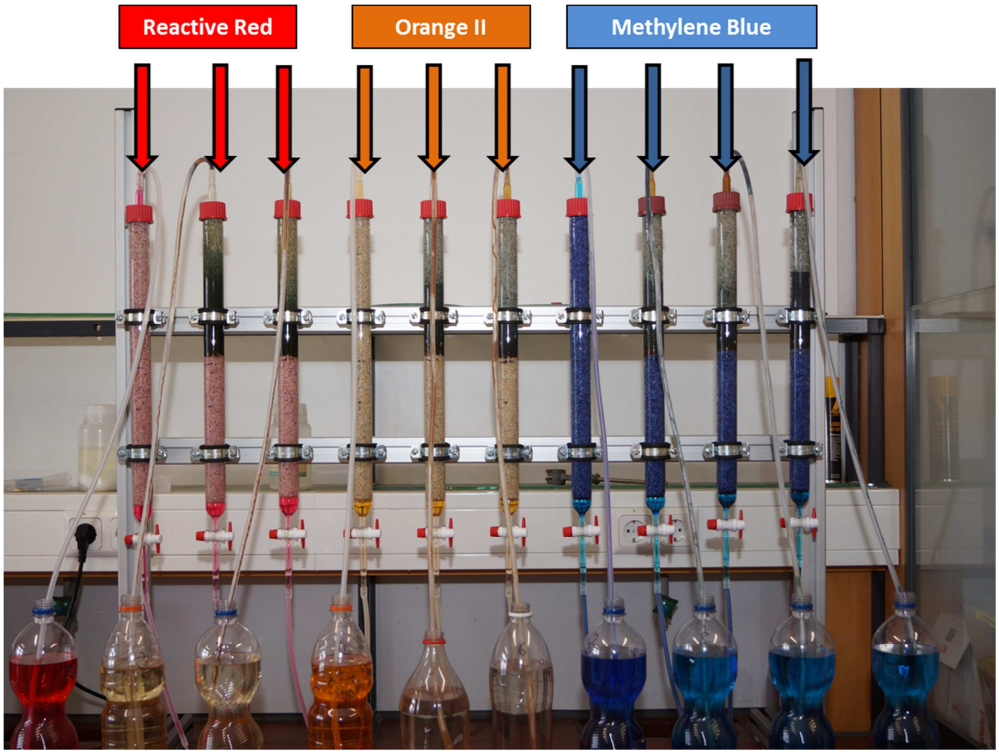

Fig 16b: Photograph of the experimental set–up of Column Experiment on 93rd day.

5.2.2 Pure sand systems

The dye breakthrough has been represented with respect to time for the whole experiment. The breakthrough curves are related to the cummulative volume of solution treated. Fig 17a represents the dye breakthrough curves of the reference systems which contains only sand. In this system the anionic dyes (Orange II and RR 120) shows breakthrough within short duration at the start of the experiment, while for the cationic dye MB breakthrough occurs only after 15 days which was about 2 %. The dye breakthrough for RR 120 and Orange II occurs on 3rd day (approximately 65 hours corresponding to less than 8 pore volumes). The breakthrough was 49 and 55 % for RR 120 and Orange II respectively. These observations can be explained by the negatively charged sand surface and the attractive electrostatic interaction towards positively charged MB which is quantitatively adsorbed on sand. The rapid breakthrough in case of anionic dyes is due to electrostatic repulsions between the negatively charged sand surface and the anionic dyes. In other words, observations have confirmed/proven sand as a non reactive material for Orange II and RR 120 (Phukan et al. 2015).

5.2.3 Fe^0-based systems

Figs. 17b and 17c represents the dye breakthrough curve for Fe^0-based system with 50 % and 100 % Fe^0. It is observed that MB was least discoloured with only 25 % of breakthrough inspite of the delayed breakthrough due to discoloration within H_{sand1} layer. Whereas for Orange the breakthrough was upto 15 % at day 15 and decreases gradually to 4 % (at day 93). This observation has been supported by the fact that Orange II is adsorbed onto iron-oxides

and the these oxides are generated in-situ. In the first few 20 days there was no availibilty of enough iron oxides for the dye removal. The initial quantitative breakthrough corresponds to the time lag between the commencement of the experiment and of quantitative generation of removing agents (iron oxides) (Schreier and Reinhard 1994, Hao et al. 2005, Ghauch et al. 2010, Ghauch et al. 2011, Ghauch 2013). RR 120 dyes shows the similar trend as Orange II. The most important observation is delayed breakthrough in Fe^0-based filters containing 200 g of Fe^0 represented in Fig 17c. The higher amount of Fe^0 in column 10 delays the MB breakthrough and increases the efficeincy with 21 % breakthrough compared to that of 25 % in 100 g of Fe^0-based system over the whole experimental period (93 days). MB breakthrough is observed after 14 days for 100 g of Fe^0 but only after 21 days for the 200 g of Fe^0 system.

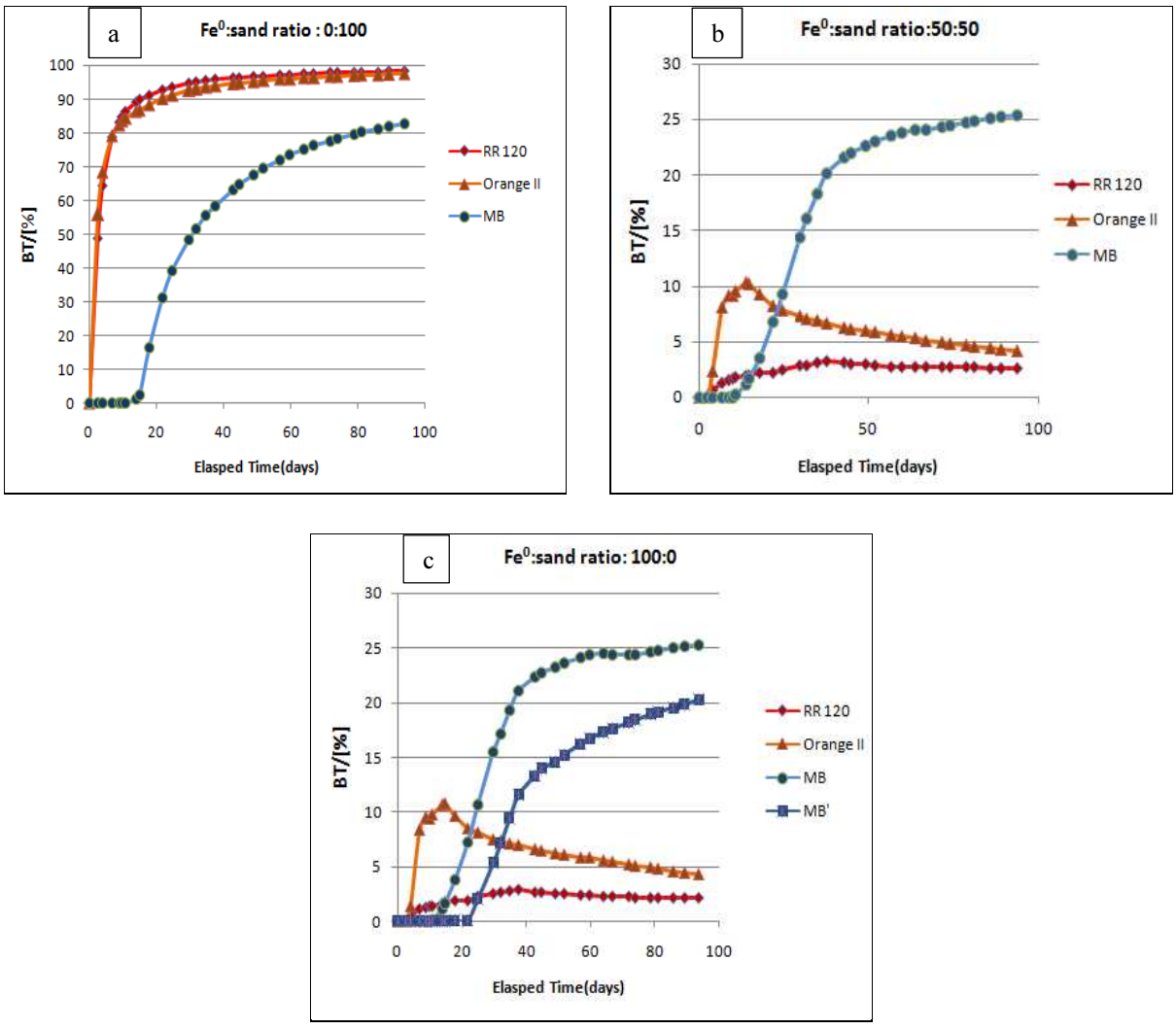

Fig 17: Time dependent evolution of the cummulative dye breakthrough: (a) pure sand system (b) 50 % Fe^0 system (c) pure Fe^0 system. The lines are not fitting functions; they simply connect points to facilitate visualization.

This observation confirms that the process reponsible for MB discoloration in Fe^0-based system is stochastic in nature (Miyajima 2012, Miyajima and Noubactep 2013). In fact, pure reduction is linearly correlated to the mass of the reducing agent. This consequence is also

rationalised by the fact that MB gets adsorbed on sand and co-precipites on the iron oxide coated sand. As the in-situ iron oxides are generated (t > 14) MB breakthrough was observed immedeately after the exhaustion of the adsorption capacity of H_{sand1} (columns 8, 9 and 10). The delayed breakthrough in column 10 is attributed to the larger amount of Fe^0 (200 g).

5.2.4 Evidence of dye retention

In Fig. 18 the time dependency of C/C_0 is discussed for sand and Fe^0-based systems. In Fig. 18a the discoloration is negligible for Orange II and RR 120, while discoloration for MB was quantitative till initial 15 days corresponding to the retention amount of only 5 % and then shows a steep decline following no dye removal process. After 15 days, no dye dye removal was observed. This observation confirms the high stability of azo dyes with regard to biodegradibility as the experimental duration largely exceeded the maturation time of sand filters of 6-8 weeks (Bray and Olanczuk-Neyman 2001, Calvo-Bado et al. 2003).

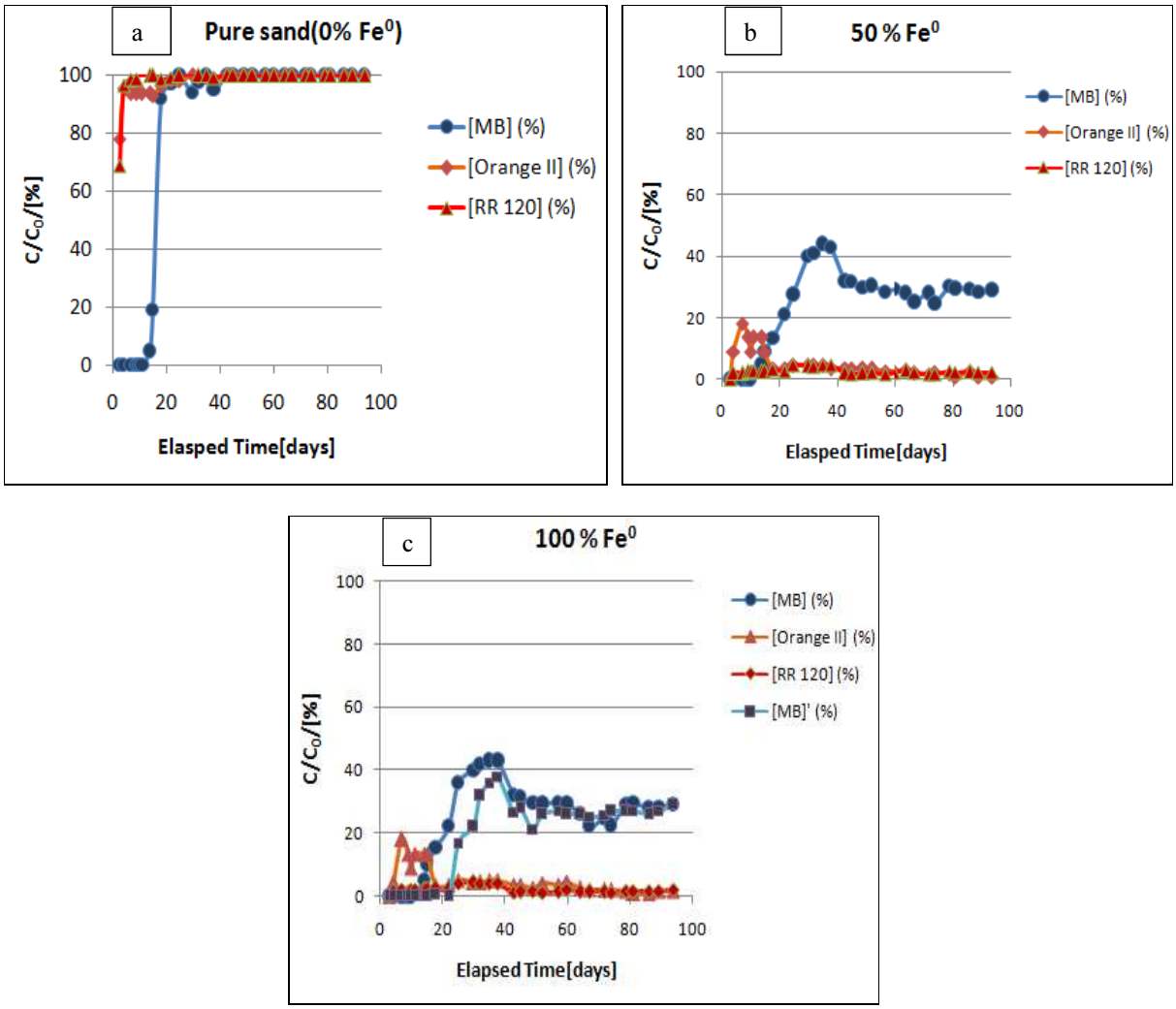

Fig 18: Time evolution of dye breakthrough: (a) pure sand system (b) 50 % Fe^0 system (c) pure Fe^0 system. The lines are not fitting functions; they simply connect points to facilitate visualization.

Therefore, the observation in the pure sand column depicts that the cationic MB gets adsorbed onto the negative sand surface effeciently until the adsorption of sand capacity is exhaused and thereby sand filters can be used in an effective manner for cationic dye removal (Varlikli et al. 2009), whereas sand shows no affinity for adsorption for anionic dyes corresponding to 78 and 68 % retention amount for Orange II and RR 120 respectively and then gradually showing no dye removal.

Similarly the time dependency of C/C_0 shows that there is no significant difference between the sytems with 50 and 100 % Fe^0. As it is observed in Figs. 18b and 18c that for RR 120 dye the discoloration effeciency was quantitative and stable during the whole experimental period (93 d) and the amount of dye retained was less than 4 % throughout. Orange II discoloration was quantitaive after a lag of about 15 d showing gradual increase in the amount of discoloration. This is due to the fact that the adsorbing agents for Orange II dyes or anionic dyes are the iron corrosion products (iron oxides) which are generated in-situ after a substantial amount of time after the commencement of the experiment. The initial quantitative discoloration of MB corresponds to adsorption onto H_{sand1}. However, the extent of breakthrough was leveled to about 25 % after some 45 d and remained constant towards the end of the experiment.

Table 8. Comparison of the extent of dye discoloration in the H_{sand1} layer (180 g of sand) of Fe^0-based systems (§ 4.5). 'm_{dye}' is the mass of discolored dye, 'n_{dye}' is the corresponding number of moles and 'E_s' (μg g^{-1}) derived specific adsorption capacity. The Fe^0-free system (40.0 cm) contained 360 g of sand. It is evident that cationic MB is significantly discoloured by sand.

Dye	M	m_{dye}	n_{dye}	n_{dye}	E_s'
	(g mol^{-1})	(mg)	(mmol)	(μmol)	(μg g^{-1})
MB	319	22.4	0.07	70.2	0.10
Orange II	350	3.8	0.01	10.7	0.01
RR 120	1469	10.9	0.01	7.4	0.01

A substantial difference was observed in the previous experiments in MB discolouration in particular E and Es values (Table 8) with the same experimental design consisting 100 % Fe^0 but varying heights of H_{sand1} and $H_{sand\ 2}$ (Miyajima and Noubactep 2013). The absence of difference might be due to the experimental period (93 d), thereby for long runs the difference in discoloration could be anticipated. This assertion is supported by the differences observed herein for the 100 % Fe^0 system when the used Fe^0 mass were 100 and 200 g respectively. By fixing H_{sand1} herein (20.0 cm), results clearly suggest that future works could be performed without the 100 % Fe^0 system, which is tested as a negative reference (Miyajima and Noubactep 2013, Btatkeu-K et al. 2014a). The values of Es for each Fe^0 based system is important to measure the extent of discoloration of each dye. The Es value for Orange II and RR 120 is about 8 μM g^{-1} which are quantitaive whereas for MB it is only 4.7 μM g^{-1}. However the reported values cannot be assumed to be standard universal data for comparison with other reported values without carefully considering the experimental conditions (Zafarani et al. 2014). The first proof of this statement is the Es value of 200 g Fe^0 system is

2.6 µM g^{-1} which is not even the half of the value with system with 100 g Fe^0. It has already been stated that specific adsorption capacity (Es value) is only valid when Fe^0 is exhausted or with the whole adsorbent is available for contaminant removal. In the case of Fe^0, it is certain that no material exhaustion occurs and that the nature of the adsorbing agent is not known.

Table 9: Summary of the results of the column experiments after 93 days. A total of 26.12 L of each dye solution flowed through the corresponding columns (Tab. 1). "$Fe_{effluent}$" and "$Dye_{effluent}$" are the cumulative mass of Fe and Dye in the effluent. "$Dye_{influent}$" is the total mass of MB which has flowed through the columns. "$Fe_{effluent}$" (%) is the ratio of dissolved Fe which has escaped from the column relative to the used mass of Fe^0. E (%) and E_s (mg g^{-1} and µM g^{-1}) are the MB discoloration efficiencies (see text). For comparison E_s value for MB on sand is 0.1 mg g^{-1} or 0.4 l µM g^{-1}.

Column	**$Fe_{effluent}$**	**$Fe_{effluent}$**	**$Dye_{influent}$**	**$Dye_{effluent}$**	**BT**	**E**	**E_s**	**Es**	**Desorption**
	(mg)	**(%)**	**(mg)**	**(mg)**	**(%)**	**(%)**	**(mg/g)**	**(µM/g)**	**(%)**
1	0.0	_	1248.3	1226.6	98.3	1.7	_	_	23.3
2	11.2	0.01	1248.3	32.7	2.6	97.4	11.9	8.1	0.0
3	17.8	0.02	1248.3	26.5	2.1	97.9	12.0	8.2	0.0
4	0.0	_	297.7	290.3	97.9	2.5	_	_	18.6
5	11.4	0.01	297.7	12.5	4.2	95.8	2.8	7.9	0.0
6	12.5	0.01	297.7	13.0	4.4	95.6	2.8	7.9	0.0
7	0.0	_	261.2	216.4	82.9	17.1	_	_	27.7
8	9.6	0.01	261.2	66.4	25.4	74.6	1.5	4.7	6.3
9	10.6	0.01	261.2	66.0	25.3	74.7	1.5	4.7	5.5
10	9.1	0.01	261.2	52.9	20.3	79.7	0.8	2.6	5.2

*Desorption values are known from Phukan et al(2015).

5.2.5 Evidence of chemical reactions

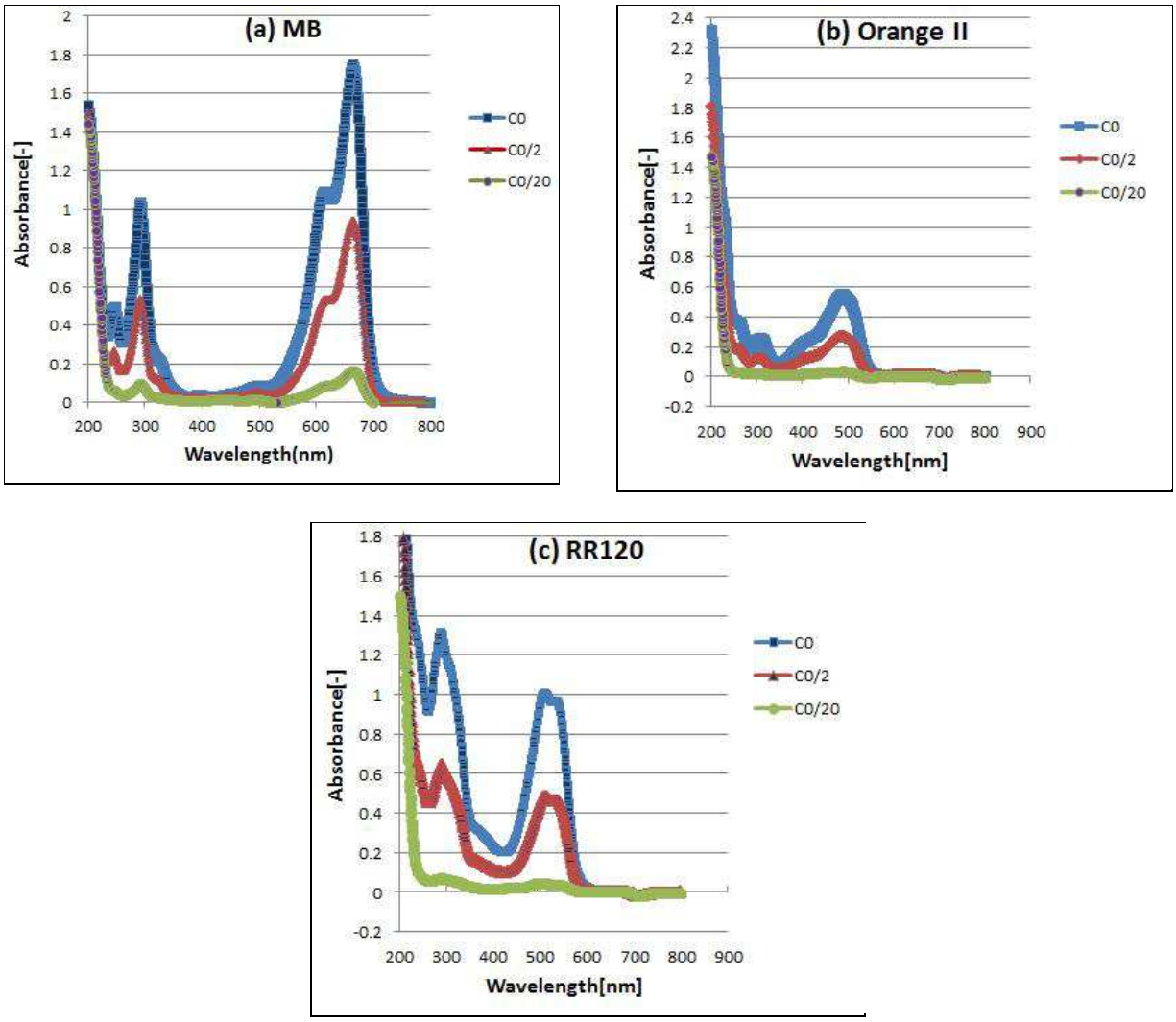

Fig 19: UV-Vis Spectra of (initial) working dye solutions (31 μ M) and their dilution by a factor 2 and 20. It is observed that the maximum are maintained despite dilution.

The working solution of MB, Orange II and RR 120 (31µM) were diluted by a factor 2 and 20 in order to observe the nature of maximum diluted contaminants that could be analysed succesfully. It is observed in Fig. 19 that inspite of dilution upto a factor of 20, the characteristic peaks in the UV-VIS spectrum are observed in all the three dyes within the desired respective wavelengths. On the contrary the UV-Vis spectra of all the three dyes in the reference (0 % Fe^0), 50 % Fe^0 and 100 % Fe^0 systems after 93 d shows different behaviour of the peaks. The spectra for Fe^0-based systems are similar regardless of the Fe^0 ratio, but in Figs. 19b and 19c it is obseved that for Orange II and RR 120, the characteristic peaks dissapears.

.

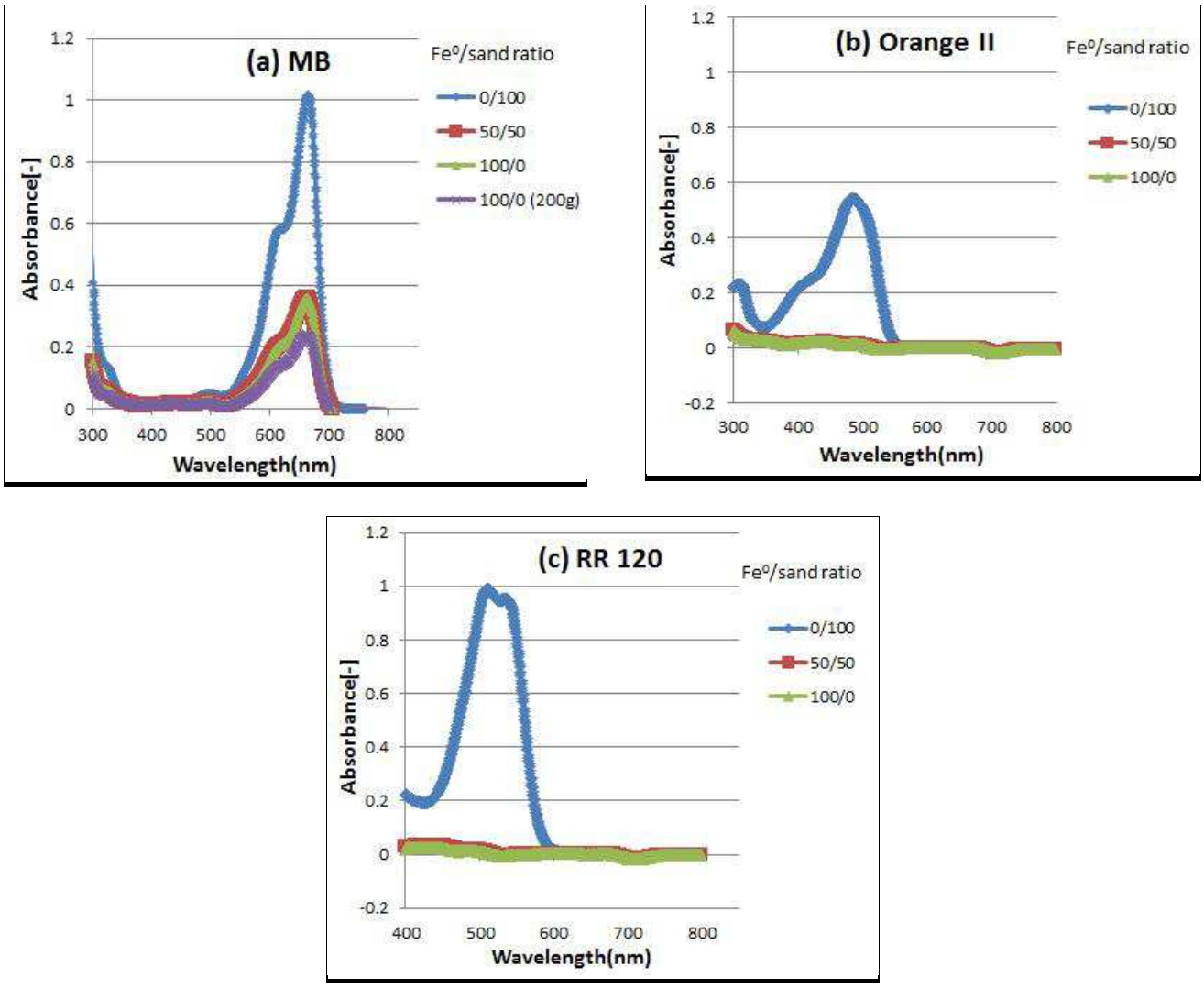

Fig 20: UV-Vis Spectra of dyes after 90 days . For RR 120 and Orange II , the peak of the sand system corresponds to that of the working solution . For MB the peak of lower intensity was obtained due adsorption onto glass vessel.

In Fig. 16b, the discoloration of RR 120 in the Fe^0-based system was quantitaive towards the end of the experiment (93 d) but it yields a weak yellow color in the collecting sample shown from the intial stage and the yellow colour solution exhibits no single adsorption peak within the UV-Vis domain. The treated solution of RR 120 by the Fe^0-based sytem was not clean and potable and could be toxic (Guaratini et al. 2001, Tanaka et al. 2000, Wang et al. 2010). Former research on dye discoloration in Fe^0/H_2O systems have resulted in the formation of various toxic products (Monson et al. 1998, Cao et al. 1999, Nam and Tratnyek 2000, Mielczarski et al. 2005, Bokare et al. 2008, Lin et al. 2008, Fan et al. 2009). Thereby, characterizing the nature of RR 120 reaction products is over the scope of the present work.

Therefore, the results of the spectrum changes can be summarized as follows (i) MB, Orange II and RR 120 are quantitatively discolored in the Fe^0-based system, (ii) MB and Orange II have no visibile generation of new reaction products, (iii) the discoloration of RR 120 is

quantative but the resulting solution is yellow coloured. It is important to mention that the discoloration is related to the parent dye not the effluent solution. Since it is observed that the effluents of RR 120 in the Fig. 20c shows no single characteristic peak of the parent dye, this leads to the conclusion that RR 120 is very reactive in the Fe^0-based system. This behaviour is also reported for the first time and the system could be observed for longer duration (> 93 d) to characterize the system " passivation" or in other words to reduce the chemical reactivity of the sytem by addition of acids. But again yet this is beyond the focus of the thesis work. RR 120 breakthrough (0 % Fe^0 system) is certainly coupled with advanced inhibition of the tested Fe^0 or low intrinsic reactivity. Thereby clearly RR 120 is a candidate for long term characterization of the reactivity of Fe^0 materials in column.

5.2.6 pH values of the column effluent

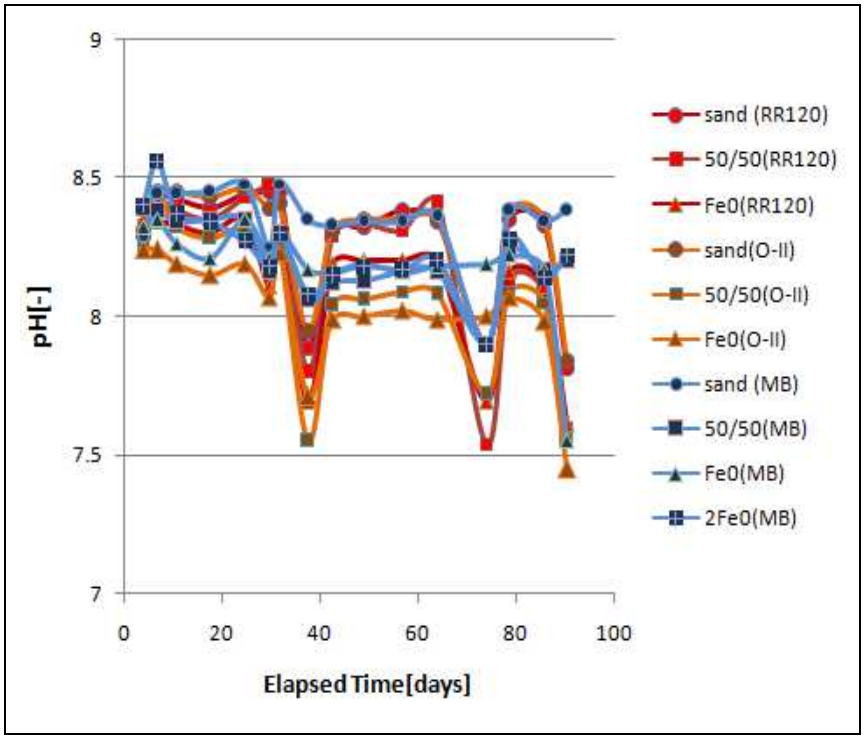

Fig 21: Time dependent evolution of pH of the column experiment. The lines are not fitting functions; they simply connect points to facilitate visualization.

.

The pH values show no significant change (Fig. 21) in all the columns including the reference systems (sand columns). This result is rationalized by the relative low mass of Fe^0 used (100 g) and the low solubility of Fe for the concerned pH range (8.0 – 8.3). The exact values of the pure sand systems is 8.3 while the pH value of the Fe systems ranges from 7.9 to 8.1. However these minor variations of the pH value have practically no impact on the geochemistry of the system. This observation is in tune with geochemistry of iron as the slight pH decreased is attributed to the buffer characteristics of iron hydroxides (Phukan et al., 2015) .

5.2.7 Total iron concentration of the effluent

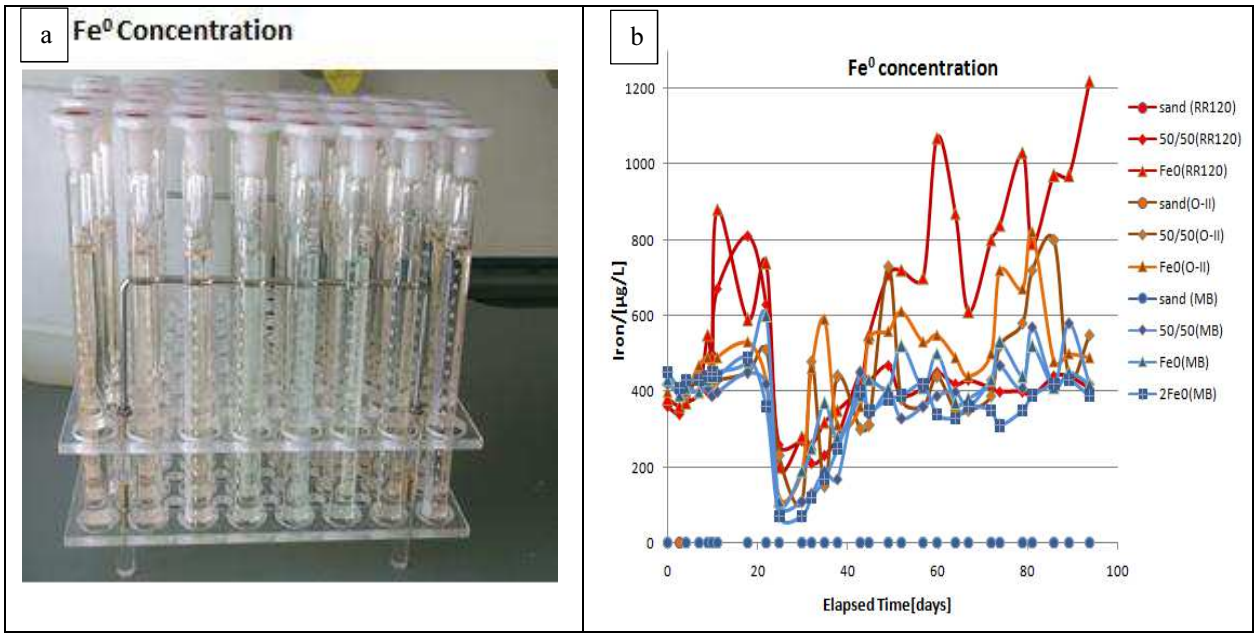

Fig 22: (a) Preparation of samples from the effuent of the columns for measurement of Fe^0 concentration (b) Concentration of dissolved Fe^0 in the effleunt of columns with Fe^0 loading. The lines are not fitting functions; they simply connect points to facilitate visualization.

There is no significant variation of the iron concentration (< 1.0 mg L^{-1}). The mobility of the dissolved iron is low due to low solubilty at pH > 5.0. The dissolved Fe is adsorbed and precipitated on sand particle (in situ coating) and tubing materials is visually observed. A cautious observation of Fig. 22b suggests that the iron concentration of the 100 % Fe^0 column fed with RR 120 was slightly higher. This observation may be rationalized by the fact that RR 120 quantitative discoloration yield reaction products of relatively high affinity for sand. These reaction products lower adsorption of Fe^{II} and Fe^{III} species onto sand and accelerate iron breakthrough. Although the nature of reactions products is not known, their quantitative breakthrough supports their low affinity for iron oxides as well. However, the subject of this thesis is the differential behavior of parent compounds: cationic and anionic dyes.

Another detailed noticeable feature is the variation of the iron concentration from 400 µg L^{-1} to 100 µg L^{-1} for a short time period and back again to constant value of 400 µg L^{-1}. Orange II and RR 120 exhibits an exceptional trend. This observation is acknowledged here in order to conviniently interpret in future only when the the trend is repeated and the reaction products are known. But the analysis of this behaviour is over the scope of this research work.

5.2.8 Hydraulic Conductivity or permeability loss

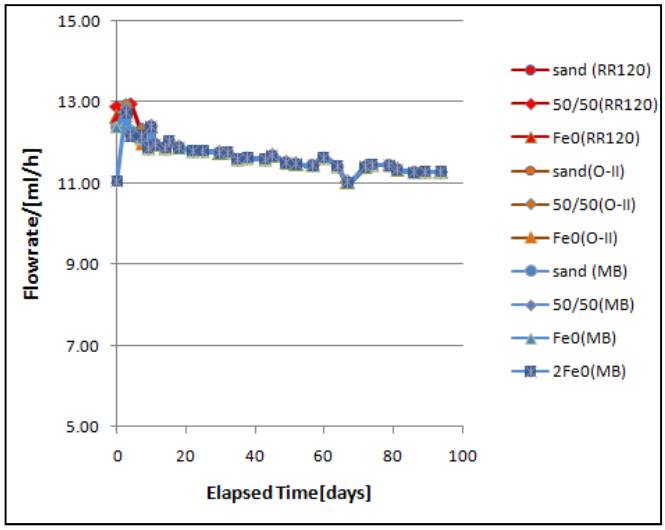

Fig 23: Time dependent evolution of the flow velocity in the 10 test columns. The lines are not fitting functions; they simply connect points to facilitate visualization.

The variation in the hydraulic conductivity of all the 10 columns shows a constant value of 11.5 mL h^{-1} through the entire experimental duration of 93 days (Fig. 23). This indicates the absence of permeability loss which might be misinterpreted as lack of loss in porosity. After dismanteling the columns, material compaction was documented in all Fe^0-based column except the ones flushed with RR 120. Moreover observation of the brown colouration and the measure of the iron concentration certifies oxidative dissolution and precipitation of iron hydroxides. But permeability loss can only be observed when the sum of forces generated in the system (filter resistance) are superior to the pressure supplied by the peristaltic pump (initial driving force) Miyajima and Noubactep (2013). The present work has used the experimental design of Miyajima (2012). Accordingly, the pump rate 0.1 mL min^{-1} was sufficient for transportation generated in-situ iron oxides out of the reactive zone to avoid clogging of the system within the experimental period. The results obtained herein can be further fine-tuned in gravity driven experiments (Btatkeu et al. 2014a).

5.2.9 Cementation of the column materials

A brown coloration was observed in the entrance zone of all columns. This coloration is characteristic for Fe^{III} oxides commonly termed as rust. Usually solid materials (Fe^0 and sand) are cemented to a compact mass. This cementation corresponds to the progressive loss of interconnectivity of the initial inter-particular porosity. In other words, unlike for field experiments, no influent sediment is deposited. Thus, the permeability loss is due to cementation and not to deposition. Given the intrinsic nature of cementation under anoxic conditions (O_2 available), porosity loss is always due to a large extent to iron corrosion, even under anoxic conditions, less voluminous oxides (not brown in color) are formed and contributed to porosity/permeability loss because iron oxides are less dense than metal iron. In other words, iron corrosion is volumetric expansive.

The fact that permeability loss was not observed herein is due to the used pumping rate that was sufficient to transport enough iron oxides away from the reactive zone. In this process, preferential flow patterns are created in the entrance zone and propagated upwards. This preferential flow is the rational for the absence of blue coloration in the $H_{sand,2}$ layer, despite MB breakthrough (columns 8,9 and 10) (Miyajima 2012, Miyajima and Noubactep 2013, Tepong-Tsindé et al. 2015b).
The visual observation of column material revealed a visible brown compacted solid in the lower 2 cm of columns containing only Fe^0 in the reactive zone and up to 4 cm in the pure Fe^0 columns. An exception was observed for the column when flushed with the RR 120 solution. Here, no compaction was observed. Remember that iron release was higher for the RR 120 systems. The rest of the reactive zone was black in color and appeared visually similar to the original Fe^0 material. This corresponds to the observation made in previous works (Mckenzie et al. 1999, Westerhoff and James 2003, Miyajima 2012, Miyajima and Noubactep 2013). The absence of compaction in the RR 120 experiment is rationalized by the large molecular size of RR 120. This suggests that large organic molecules can inhibit particle cementation in Fe^0/H_2O systems. Further research is needed to understand this preliminary observation and possibly exploit it in the design of Fe^0 filters, for example for the treatment of industrial wastewater etc.

5.3 Summary of the results

The results of batch experiment can be summarized as (i) the order of discoloration of the dyes by pure systems $Fe^0 > MnO_2 >$ sand, (ii) the order of dye discoloration by Fe^0 amended systems are Fe^0/sand > $Fe^0/MnO_2 > Fe^0$/sand/MnO_2. The clearest trend was obtained for Orange II discoloration. MnO_2 and sand have confirmed their suitability to optimize the characterization of the ion-selective nature of Fe^0/H_2O systems. In-situ generated corrosion products cover the sand surface and hence favors electrostatic attraction (and thus adsorptive discoloration) of negatively charged Orange II and RR 120 (anions). Even positively charged MB is weakly adsorbed and co-precipitated onto iron oxides generated in-situ and freely precipitating in the bulk solution.

The results of column experiment are summarized in Table 9 and can be read as:

(i) Cationic MB is strongly adsorbed onto negatively charged sand layer, but depicts only weak affinity to the surface of iron oxides. Co-precipitation and adsorptive size exclusion are responsible of MB removal after the sand layer ($H_{sand,1}$). MB is the least discolored dye in Fe^0-based systems with the extent of breakthrough of 25 % after 93 days. In case of 100 % Fe^0-based system with 200 g of iron, the breakthrough was leveled at 20 % for the same period and the initial breakthrough was delayed by 7 days compared to the pure Fe^0 system with 100 g of the reactive material.

(ii) Anionic Orange II shows the highest affinity for adsorption on the positively charged corrosion products. Quantitative discoloration was observed after a lag of 15 days. This period is described as the time needed to generate enough corrosion

products for quantitative discoloration in the system. After this lag period Orange II discoloration was quantitative through the end of the experiment (day 23).

(iii) Anionic RR120 showed quantitative discoloration for whole 93 days, without any lag period. This behavior is attributed to steric effects as RR 120 is significantly larger in size than Orange II. RR 120 has chemically reacted but the reaction products are not identified. The two Fe^0-based columns fed with RR 120 have not experienced any compaction.

(iv) The couple MB/Orange II has unambiguously documented the ion-selective nature of Fe^0/H_2O systems while the couple Orange II/RR 120 has demonstrates the impact of steric effects.

The UV-Vis spectrum change of MB, Orange II and RR 120 showed characteristic peak even after 20-fold dilution of the working solution (31μM) and hence it can be summarized as:

(i) MB, orange II and RR 120 are discolored in Fe^0/H_2O systems,

(ii) MB and Orange II discoloration is not visibly coupled with the appearance of any new species; and

(iii) RR 120 discoloration is quantitative but the resulting solution is yellow colored which is not in the range of the UV-spectrum and might be toxic.

There is no significant change in the pH value in both batch and column experiments. The slight pH decrease is due to the buffer characteristics of the iron hydroxides. RR 120 and Orange II exhibited significant variations of iron concentrations. There was no significant change in the hydraulic conductivity (11.5 mL h^{-1} through the end of the experiments).

6. Concluding Remarks

The present work has characterized the ion-selective nature of Fe^0/H_2O systems for the first time in the remediation research. A commercial Fe^0 is amended with a reactive MnO_2-bearing mineral and commercial sand. The discoloration behavior of three different organic dyes are investigated in the (MnO_2 and sand) amended Fe^0/H_2O systems. While negatively charged sand is an excellent adsorbent for positively charged methylene blue (MB), its adsorptive affinity for negatively charged Orange II and reactive red 120 (RR 120) is less pronounced. MB and Orange II are comparable in size, while RR 120 is significantly larger. Testing two anionic dyes of different molecular size has clearly demonstrated the significance of steric effects on the processes yielding contaminant removal in Fe^0/H_2O systems.

Fe^0 and Fe^0/sand systems were characterized both in batch and column experiments, while Fe^0/MnO_2 and Fe^0/sand/MnO_2 systems were solely characterized in batch experiments. The results of batch experiment were essentially qualitative in nature, while column experiments clearly demonstrated the differential kinetics in the efficiency of pure adsorbent (e.g. sand) and in situ-generated adsorbent which also act as 'local flocculants' for dye co-precipitation. Sand exhibited a typical S-shape breakthrough curve after 15 days, while Fe^0-based systems were more efficient in the long-term (still discoloring at the end of the experiment, 93 days). Additionally, where sand could solely quantitatively discolor MB, Fe^0-based systems could discolor all three dye solutions, with the discoloration being quantitative for the anionic dyes (Orange II and RR 120). Under the experimental conditions tested herein, the effect of sand admixture on the system's sustainability in terms of increase permeability could not be evidenced. In fact the pumping rate was sufficient to avoid the accumulation of iron corrosion products so as to reduce the flow velocity (for the tested experimental duration). However, differential compaction of the Fe^0/sand mixture was observed with no compaction in the columns treating RR 120. This result suggests that large molecules organic species may avoid particle cementation and loss of interconnectivity. However more research is needed as this behavior is documented for the very first time.

The present thesis has confirmed that available discrepancies in the literature are mostly due to the initial premise regarding Fe^0 as a reducing agent. Herein, it is demonstrated that Fe^0 induced sand coating with iron oxides and contaminant co-precipitation with the same. Accordingly all species with high affinity to iron oxides are preferentially removed by adsorption onto iron oxides coating sand surfaces. Such species include arsenic and chromium but as also organics as Orange II. For all other species, removal by co-precipitation and size-exclusion will occur to different extent. This makes Fe^0 a universal material for water treatment. In a treatment chain Fe^0-units should come after units removing cationic species. In a stand-alone treatment plant, proper dimensioning should account for the lower affinity, e.g. through thicker Fe^0 beds.

The other major input of the thesis is that contaminants, to be treated by Fe^0/H_2O systems, should be primordially classified according to their affinity to iron oxides and not to the chemical nature (organic/inorganic) or their origin (e.g natural/anthropogenic, industrial or agricultural effluents, pharmaceutical). The charge and the size should be primordial. It is

certain that the redox properties could play an important role, but the redox reactivity of Fe^0/H_2O systems is not governed by the potential of the couple Fe^{II}/Fe^0 (-0.44 V). It should be kept in mind that Fe^0/H_2O systems for contaminant removal are efficient at pH > 4.5. Such system is necessarily ion selective because the surface of iron oxides are positively charged

The last major feature of the thesis is that it has confirmed the suitability of properly design experiments with small amount of Fe^0 (here 100 g) to achieve reliable results under realistic conditions (no exaggerated acceleration). In column experiment, despite of low affinity for iron corrosion products, MB was removed at a constant rate of 75 % (25 % breakthrough) through the end of the experiment. This reiterates that well-dimensioned Fe^0 filters could even satisfactorily remove species with less affinity to iron oxides. The low affinity of MB in Fe^0/H_2O system makes it a reactive indicator for characterizing the system within reasonable duration. For example, the results reported herein, suggest that conclusive experiments with MB could be performed for 45 days, while 93 days were still insufficient to document changes with both tested anionic dyes. This observation recalls that intelligent tools are required to shorten the experimental duration without any artificial modifications that are not relevant for field situations.

This work provides useful guidance for subsequent laboratory investigations focused on (i) identifying relevant operational factors affecting Fe^0 filter efficiency (e.g. water chemistry, Fe^0 characteristics), and (ii) designing long-term efficient Fe^0 filters. More collaborative research is needed with several groups of contaminants. A way to continue the work initiated herein could consist in (i) seeking the breakthrough for Orange II and RR 120, (ii) seeking the point at which the expected differences between the 50 % and 100 % Fe^0 ratio are observable, (iii) identifying the reaction products of RR 120 and (iv) further characterizing the material compaction in the presence of RR 120. All these aspects would contribute to progress in designing Fe^0-based filters.

7. Epilogue

The presented work corresponds to the original manuscript submitted in January 2015 and available in the Geoscience library of the Georg-August-University of Göttingen (Germany). Minor revisions were performed, mostly limited at actualizing bibliographic references and slightly ameliorating the readability.

This work determines a 20 years-lasting discussion on the relevance of adsorption of organic species as a relevant removal mechanism in Fe^0/H_2O systems. It is still mostly considered that Fe^0/H_2O systems are a reductive one in which adsorption might be important for some inorganic species like arsenic, chromium or selenium while organic species are mostly reductively transformed (Vodyanitskii 2014a, 2014b, Naidu and Birke 2015, Colombo et al. 2015). In using three charged organic species (azo dyes – one cationic and two anionic) and documenting differential quantitative discoloration extents, this study has definitely proven that the chemical affinity of contaminants to iron oxides is the most important factor governing the selectivity of Fe^0/H_2O systems. Accordingly, redox processes (if applicable) are of secondary relevance. In particular for water treatment even reduced species must be removed from the aqueous phase. For environmental remediation, it might be enough that reduced species are better biodegradable.

In essence the 'establishment' of the ion-selective nature of Fe^0/H_2O systems is by no means a discovery as Kyzas et al. (2013) reported on initial knowledge on dye adsorption by metal oxides (for wastewater treatment) gained during 1951–1970. The ion-selective nature of metal oxides for dyes was established during these years. A particular work was performed by Mitchell et al. (1955) and published in *Nature*. These authors clearly showed that methylene blue (MB) adsorbed differently onto natural sand samples and that in each case, coating sand by iron oxides considerably lessened the adsorption capacity for MB. The findings of Mitchell et al. (1955) were already exploited to elucidate the importance of admixing non-expansive materials to Fe^0 to warrant systems's sustainability (Miyajima 2012, Btatkeu-K et al. 2014a, 2014b, Tepong-Tsindé et al. 2015b). The present study has purposefully tested anionic dyes in the same systems to confirm results available from the 1950s, but not yet properly considered within the 'Fe^0 remediation' research community.

Properly considering the affinity of aqueous species to iron oxides within Fe^0/H_2O systems is crucial for further research for at least two reasons (Noubactep 2015c):

(i) contaminants should be mainly classified due to their affinity to iron oxides (at relevant pH values), whether they are organic or inorganic in nature;
(ii) Beside the affinity to iron oxides, the steric hindrance (molecular size) should be considered.

Parallel experiments with organic and inorganic species having various affinities to Fe oxides and molecular sized are necessary to gain overview information capable at facilitating a non-site specific system design. Clearly, a scientific discussion (Noubactep 2015a, 2015b) and ground level research with multi-contaminant systems is needed (Tepong-Tsindé et al. 2015a) before some rules of thumb for the design of Fe^0-based filtration systems can be formulated.

REFERENCES

Abramian L., El-Rassy H. Adsorption of kinetics and thermodynamics of azo-dye Orange II onto highly porous titania aerogel. Chemical Engineering Journal 150 (2009) 403–410.

Allred B J., Trost B.C., Laboratory comparison of four iron-based filter materials for water treatment of trace element contaminants, Water Environment Research 86 (2014) 852-62.

Ali I., New generation of adsorbents for water treatment. Chemical Reviews. 112 (2012) 5073-5091.

Ali I. Water treatment by adsorption columns: Evaluation at ground level. Separation & Purification Reviews 43 (2014) 175–205.

Aviles M., Garrido S.E., Esteller M.V., De la Paz J.S., Najera C., Cortés J. Removal of groundwater arsenic using a household filter with iron spikes and stainless steel. Journal of Environmental Management 131 (2013) 103–109.

Bhaumik M., Noubactep C., Gupta V.K., McCrindle R.I., Maity A. Polyaniline/Fe^0 composite nanofibers: An excellent adsorbent for the removal of arsenic from aqueous solutions. Chemical Engineering Journal 271 (2015) 135–146.

Bilardi S., Calabrò P.S., Caré S., Moraci N., Noubactep C. Improving the sustainability of granular iron/pumice systems for water treatment. Journal of Environmental Management 121 (2013) 133–141.

Bojic A., Purenovic M., Kocic B., Perovic J., Ursic-Jankovic J., Bojic D. The inactivation of Escherichia coli by microalloyed aluminium based composite Facta Universitatis. 2 (2001) 115–124.

Bojic A.L., Purenovic M., Bojic D. Removal of chromium(VI) from water by micro-alloyed aluminium composite (MAlC) under flow conditions. Water SA 30 (2004) 353–359.

Bokare A.D., Chikate R.C., Rode C.V., Paknikar K.M. Iron-nickel bimetallic nanoparticles for reductive degradation of azo dye Orange G in aqueous solution. Applied Catalysis B: Environmental 79 (2008) 270–278.

Bray R., Olanczuk-Neyman K. The influence of changes in groundwater composition on the efficiency of manganese and ammonia nitrogen removal on mature quartz sand filtering beds. Water Science and Technology Water Supply 1 (2001) 91–98.

Btatkeu-K. B.D., Miyajima K., Noubactep C., Caré S. Testing the suitability of metallic iron for environmental remediation: Discoloration of methylene blue in column studies. Chemical Engineering Journal 215–216 (2013) 959–968.

Btatkeu-K. B.D., Olvera-Vargas H., Tchatchueng J.B., Noubactep C., Caré S. Determining the optimum Fe^0 ratio for sustainable granular Fe^0/sand water filters. Chemical Engineering Journal 247 (2014a) 265–274.

Btatkeu-K. B.D., Olvera-Vargas H., Tchatchueng J.B., Noubactep C., Caré S. Characterizing the impact of MnO_2 on the efficiency of Fe^0-based filtration systems. Chemical Engineering Journal 250 (2014b) 416–422.

Calvo-Bado L.A., Pettitt T.R., Parsons N., Petch G.M., Morgan J.A.W., Whipps J.M. Spatial and temporal analysis of the microbial community in slow sand filters used for treating horticultural irrigation water. Applied and Environmental Microbiology 69 (2003) 2116–2125.

Cao J., Wei L., Huang Q., Wang L., Han S. Reducing degradation of azo dye by zero-valent iron in aqueous solution. Chemosphere 38 (1999) 565–571.

Caré S., Crane R., Calabro P.S., Ghauch A., Temgoua E., Noubactep C. Modelling the permeability loss of metallic iron water filtration systems. Clean - Soil, Air, Water 41 (2013) 275–282.

Chiu, P.C. Applications of zero-valent iron (ZVI) and nanoscale ZVI to municipal and decentralized drinking water systems–a review. Novel solutions to water pollution. ACS Symposium Series (2013) Vol. 1123.

Clement J., Hayes M., Sarin P., Kriven W.M., Bebee J., Jim K., Becket M., Snoeyink V.L., Kirmeyer G.J., Pierson G. Development of Red Water Control Strategies. Denver, Colo.: AwwaRF and AWWA USACERL Technical Report (2002) 99/39.

Cohen M.H., Turnbull D. Molecular transport in liquids and glasses. The Journal of Chemical Physics 31 (1959) 1164–1169.

Colombo A., Dragonetti C., Magni M., Roberto D., Degradation of toxic halogenated organic compounds by iron-containing mono-, bi- and tri-metallic particles in water. Inorganica Chimica Acta 431 (2015) 48–60.

Comba S., Di Molfetta A., Sethi R. A comparison between field applications of nano-, micro-, and millimetric zero-valent iron for the remediation of contaminated aquifers. Water, Air, & Soil Pollution 215 (2011) 595–607.

Crane R., Noubactep C. Elemental metals for environmental remediation: learning from hydrometallurgy. Fresenius Environmental Bulletin 21 (2012) 1192–1196.

Crawford R.J., Harding I.H., Mainwaring D.E. Adsorption and co-precipitation of single heavy metal ions onto the hydrated oxides of iron and chromium. Langmuir 9 (1993) 3050–3056.

Dafale N., Rao N.N., Meshram S.U., Wate S.R. Decolorization of azo dyes and simulated dye bath wastewater using acclimatized microbial consortium–biostimulation and halo tolerance." Bioresource Technology 99 (2008) 2552–2558.

Domga R., Togue-Kamga F., Noubactep C., Tchatchueng J.B., Discussing porosity loss of Fe^0 packed water filters at ground level. Chemical Engineering Journal 263 (2015) 127–134

Fan J., Guo Y., Wang J., Fan M., Rapid decolorization of azo dye methyl orange in aqueous solution by nanoscale zerovalent iron particles. Journal of Hazardous Materials 166 (2009) 904–910.

Gatcha-Bandjun N., Noubactep C. Metallic iron for environmental remediation: Missing the 'valley of death'. Fresenius Environmental Bulletin 22 (2013) 2632– 2639.

Gatcha-Bandjun N., Noubactep C., Loura Mbenguela B. Water treatment with Fe^0/H_2O systems: Learning from internal electrolysis. Fresenius Environmental Bulletin 23 (2014) 2663–2669.

Ghauch A. Iron-based metallic systems: An excellent choice for sustainable water treatment. Habilitation Thesis (2013), University of Grenoble, France

Ghauch A., Abou Assi H., Tuqan A., Investigating the mechanism of Chlofibric acid removal in Fe^0/H_2O systems. Journal of Hazardous Materials 176 (2010) 48–55.

Ghauch A., Abou Assi H., Baydoun H., Tuqan A., Bejjani A., Fe^0-based trimetallic systems for the removal of aqueous diclofenac, Mechanism and kinetics. Chemical Engineering Journal 172 (2011) 1033–1044.

Gheju M., Hexavalent chromium reduction with zero-valent iron (ZVI) in aquatic systems. Water, Air, & Soil Pollution 222 (2011) 103–148.

Gheju M., Balcu I., Removal of chromium from Cr(VI) polluted wastewaters by reduction with scrap iron and subsequent precipitation of resulted cations. Journal of hazardous materials 196 (2011) 131–138.

Ghosemi J., Asadpour S., Thermodynamics studies of the adsorption process of methylene blue on activated carbon at different ionic strengths. Journal of Chemical Thermodynamics 39 (2007) 967–971.

Guan X., Sun Y., Qin H., Li J., Lo I.M.C., He D., Dong H. The limitations of applying zero-valent iron technology in contaminants sequestration and the corresponding

countermeasures: The development in zero-valent iron technology in the last two decades (1994–2014). Water Research 75 (2015) 224–248.

Guaratinia C.C.I., Fogg A.G., Zanoni M.V.B. Assessment of the application of cathodic stripping voltammetry to the analysis of diazo reactive dyes and their hydrolysis products. Dyes Pigments 50 (2001) 211–221.

Gunawardana B., Singhal N., Swedlund P., Degradation of chlorinated phenols by zero valent iron and bimetals of iron: A review. Environmental Engineering Research 16 (2011) 187–203.

Hao Z., Xu X., Jin J., He P., Liu Y., Wang D. Simultaneous removal of nitrate and heavy metals by iron metal. Journal of Zhejiang University Science 6B (2005) 353–356.

Henderson A.D., Demond A.H. Long-term performance of zero-valent iron permeable reactive barriers: a critical review. Environmental Engineering Science 24 (2007) 401–423.

Herro H.M., Port R.D. The Nalco guide to cooling water system failure analysis, McGraw-Hill (1993) New York.

Honrath R.E. Environmental Engineering Fundamentals: Part I, Physical Processes (1995) Michigan Technological University.

Hussam A., Munir A.K.M. A simple and effective arsenic filter based on composite iron matrix: Development and deployment studies for groundwater of Bangladesh. Journal of Environmental Science and Health Part A 42 (2007) 1869–1878.

Imamura K., Ikeda E., Nagayasu T., Sakiyama T., Nakanishi K. Adsorption behavior of Methylene Blue and its congeners on a stainless steel surface. Journal of Colloid and Interface Science 245 (2002) 50–57

Jhimli P., Rawat K.P., Sarma K.S.S., Sabharwal S. Decoloration and degradation of Reactive Red-120 dye by electron beam irradiation in aqueous solution. Applied Radiation and Isotopes 69 (2011) 982–987.

Jiao L., Zhang L., Wang X., Diankov G., Dai H. Narrow graphene nanoribbons from carbon nanotubes. Nature 458 (2009) 877–880.

Kaplan D.I. Influence of surface charge of an Fe-oxide and an organic matter dominated soil on iodide and pertechnetate sorption. Radiochimica Acta 91 (2003) 173–178.

Karmanova L.P., Kutchin A.V., Korolyova A.A., Hurshkainen T.V., Kutchin V.A ,Base water solution extraction as the basis of new technology of production of fungicide and plant growth stimulation. Chem. and Computational Simulation, Butherov Communication (2002).

Keeney-Kennicutt, Wendy L., Morse J.W. The redox chemistry of Pu (V) O_2^+ interaction with common mineral surfaces in dilute solutions and seawater. Geochimica et Cosmochimica Acta 49 (1985) 2577–2588.

Kipling J.J., Wilson R.B., Adsorption of methylene blue in the determination of surface areas. Journal of Applied Chemistry 10 (1960) 109–113.

Kobbe-Dama N., Noubactep C., Tchatchueng J.B. Metallic iron for water treatment: Prevailing paradigm hinders progress. Fresenius Environmental Bulletin 22 (2013) 2953–2957.

Koch D.F.A. Kinetics of the reaction between manganese dioxide and ferrous iron. Australian Journal of Chemistry 10 (1957) 150–159

Kosmulski M. Compilation of PZC and IEP of sparingly soluble metal oxides and hydroxides from literature. Advances in Colloid and Interface Science 152 (2009) 14–25.

Kyzas G.Z., Fu J., Matis K.A., The change from past to future for adsorbent materials in treatment of dyeing wastewaters. Materials 6 (2013) 5131–5158.

Kowalski K.P., Søgaard E.G. Implementation of zero-valent iron (ZVI) into drinking water supply – Role of the ZVI and biological processes. Chemosphere 117 (2014) 108–114.

Kurth A.M., Discoloration of methylene blue by elemental iron: Influence of the shaking intensity. Bachelor Dissertation, University of Goettingen (2008) 40 pp.

Larson T.E., Skold R.V. Corrosion and tuberculation of cast iron. Journal - American Water Works Association 9 (1957) 1294–1302.

Lin J., Zhao X., Liu D., Yu Z., Zhang Y., Xu H. The decoloration and mineralization of azo dye C.I. Acid Red 14 by sonochemical process: rate improvement via Fenton's reactions, Journal of Hazardous Materials 157 (2008) 541–546.

Liu X., Millero F.J. The solubility of iron hydroxide in sodium chloride solutions. Geochimica et Cosmochimica Acta 63 (1999) 3487–3497.

Mackenzie P.D., Horney D.P., Sivavec T.M. Mineral precipitation and porosity losses in granular iron columns. Journal of Hazardous Materials 68 (1999) 1–17.

Matheson L.J., Tratnyek P.G. Reductive dehalogenation of chlorinated methanes by iron metal. Environmental Science & Technology 28 (1994) 2045–2053.

Mielczarski J.A., Atenas G.M., Mielczarski E. Role of iron surface oxidation layers in decomposition of azo-dye water pollutants in weak acidic solutions. Applied Catalysis B: Environmental 56 (2005) 289–303.

Mitchell G., Poole P., Segrove H.D. Adsorption of methylene blue by high-silica sands. Nature 176 (1955) 1025–1026.

Miyajima K. Optimizing the design of metallic iron filters for water treatment. Freiberg Online Geoscience 32 (2012) 60 pp.

Miyajima K., Noubactep C. Impact of Fe^0 amendment on methylene blue discoloration by sand columns. Chemical Engineering Journal 217 (2013) 310–319.

Miyajima K., Noubactep C. Characterizing the impact of sand addition on the efficiency of granular iron for contaminant removal in batch systems. Chemical Engineering Journal 262 (2015) 891–896.

Monson S.J., Ma L., Cassada D.A., Spalding R.F. Confirmation and method development for dechlorinated atrazine from reductive dehalogenation of atrazine with Fe^0. Analytica Chimica Acta 373 (1998) 153–160.

Nam S., Tratnyek P.G., Reduction of azo dyes with zero-valent iron. Water Research 34 (2000) 1837–1845.

Naidu R., Birke V., Permeable Reactive Barrier: Sustainable Groundwater Remediation (2015). CRC Press, ISBN: 978-1-4822-2447-4., 333 pp

Nesic S. Key issues related to modeling of internal corrosion of oil and gas pipelines - A review: Corrosion Science 49 (2007) 4308–4338.

Ngai T.K.K., Shrestha R.R., Dangol B., Maharjan M., Murcott S.E. Design for sustainable development – Household drinking water filter for arsenic and pathogen treatment in Nepal. J. Environ. Sci. Health A 42 (2007) 1879–1888.

Nitzsche K.S., Lan V.M., Kim Trang P.T., Viet P.H., Berg M., Voegelin A., Planer-Friedrich B., Zahoransky J., Müller S.-K., Byrne J.M., Schröder C., Behrens S., Kappler A. Arsenic removal from drinking water by a household sand filter in Vietnam — Effect of filter usage practices on arsenic removal efficiency and microbiological water quality. Science of The Total Environment 502 (2015) 526–536

Nordsveen N., Nesic S., Nyborg R., Stangeland A. A mechanistic model for carbon dioxide corrosion of mild steel in the presence of protective iron carbonate films. Part 1: Theory and verification. Corrosion 59 (2003) 443–456.

Noubactep C., Meinrath G., Dietrich P., Merkel B. Mitigating uranium in ground water: prospects and limitations. Environmental Science & Technology 37 (2003) 4304–4308.

Noubactep C., Meinrath G., Dietrich P., Sauter M., Merkel B. Testing the suitability of zerovalent iron materials for reactive walls. Environmental Chemistry 2 (2005) 71–76.

Noubactep C. Processes of contaminant removal in "Fe^0–H_2O" systems revisited: The importance of co-precipitation. Open Environmental Journal 1 (2007) 9–13.

Noubactep C. A critical review on the mechanism of contaminant removal in Fe^0–H_2O systems. Environmental Technology 29 (2008a) 909–920.

Noubactep C. Comments on "Sorption of triazoles to soil and iron minerals" by Y. Jia et al. Chemosphere 67 (2007) 250-258]. Chemosphere 71 (2008b) 802–806.

Noubactep C., An analysis of the evolution of reactive species in Fe^0/H_2O systems. Journal of Hazardous Materials 168 (2009a) 1626–1631.

Noubactep C. Characterizing the discoloration of methylene blue in Fe^0/H_2O systems. Journal of Hazardous Materials 166 (2009b) 79–87.

Noubactep C., Schöner A., Woafo P. Metallic iron filters for universal access to safe drinking water. Clean – Soil, Air, and Water 37 (2009a) 930–937.

Noubactep C., Licha T., Scott T.B., Fall M., Sauter M. Exploring the influence of operational parameters on the reactivity of elemental iron materials. Journal of Hazardous Materials 172 (2009b) 943–951.

Noubactep C., Kurth A.-M.F., Sauter M. Evaluation of the effects of shaking intensity on the process of methylene blue discoloration by metallic iron. Journal of Hazardous Materials 169 (2009c), 1005–1011.

Noubactep C. Metallic iron for safe drinking water worldwide. Chemical Engineering Journal 165 (2010a) 740–749.

Noubactep C. Characterizing the reactivity of metallic iron in Fe^0/EDTA/H_2O systems with column experiments. Chemical Engineering Journal 162 (2010b) 656–661.

Noubactep C. The suitability of metallic iron for environmental remediation: Environmental Progress & Sustainable Energy 29 (2010c) 286–291.

Noubactep C. The fundamental mechanism of aqueous contaminant removal by metallic iron. Water SA 36 (2010d) 663–670.

Noubactep C. Metallic iron for safe drinking water production. Freiberg Online Geology, vol. 27(2011) 38 pp, ISSN 1434-7512. (www.geo.tu-freiberg.de/fog)

Noubactep C. Aqueous contaminant removal by metallic iron: Is the paradigm shifting? Water SA 37 (2011a) 419–426.

Noubactep C. Metallic iron for safe drinking water production. Freiberg Online Geoscience, 27 (2011b) 38 pp.

Noubactep C. Metallic iron for water treatment: A knowledge system challenges mainstream science. Fresenius Environmental Bulletin 20 (2011) 2632–2637.

Noubactep C., Btatkeu K.B.D., Tchatchueng J.B. Impact of MnO_2 on the efficiency of metallic iron for the removal of dissolved Cr^{VI}, Cu^{II}, Mo^{VI}, Sb^{V}, U^{VI} and Zn^{II}. Chemical Engineering Journal 178 (2011) 78–84.

Noubactep C., Caré S. Designing laboratory metallic iron columns for better result comparability. Journal of Hazardous Materials 189 (2011) 809–813.

Noubactep C. Investigating the processes of contaminant removal in Fe^0/H_2O systems. Korean Journal of Chemical Engineering 29 (2012a) 1050–1056.

Noubactep C. Characterizing the reactivity of metallic iron in Fe^0/As-rock/H_2O systems by long-term column experiments. Water SA. 38 (2012b) 511–517.

Noubactep C., Caré S., Btatkeu K.B.D., Nanseu-Njiki C.P. Enhancing the sustainability of household Fe^0/sand filters by using bimetallics and MnO_2. Clean Soil, Air, Water 40 (2012a) 100–109.

Noubactep C., Caré S., Crane R.A. Nanoscale metallic iron for environmental remediation: prospects and limitations. Water Air Soil Pollut. 223 (2012b) 1363–1382.

Noubactep C., Temgoua E., Rahman M.A. Designing iron-amended biosand filters for decentralized safe drinking water provision. Clean: Soil, Air, Water 40 (2012c) 798–807.

Noubactep C. Metallic iron for environmental remediation: the long walk to evidence. Corrosion Review 31 (2013a) 51–59.

Noubactep C. Metallic iron for water treatment: A critical review. Clean - Soil, Air, Water 41 (2013b) 702–710.

Noubactep C. Relevant reducing agents in remediation Fe^0/H_2O systems. Clean: Soil, Air, Water 41 (2013c) 493–502.

Noubactep C. On the suitability of admixing sand to metallic iron for water treatment. International Journal of Environmental Pollution 1 (2013d) 22–36.

Noubactep C. Water remediation by metallic iron: Much ado about nothing - As profitless as water in a sieve? CLEAN - Soil, Air, Water 42 (2014a) 1177–1178.

Noubactep C. Flaws in the design of Fe^0-based filtration systems? Chemosphere 117 (2014b) 104–107.

Noubactep C. Designing metallic iron packed-beds for water treatment: A critical review. Clean - Soil, Air, Water (2015a) doi:10.1002/clen.201400304.

Noubactep C., No scientific debate in the zero-valent iron literature. CLEAN - Soil, Air, Water (2015b) doi: 10.1002/clen.201400780.

Noubactep C., Metallic iron for environmental remediation: A review of reviews. Water Research (2015c) doi: 10.1016/j.watres.2015.08.023.

O'Hannesin S.F., Gillham R.W. Long–term performance of an in situ"iron wall" for remediation of VOCs. Ground Water 36 (1988) 164–170.

Phukan M., Noubactep C., Licha T. Characterizing the ion-selective nature of Fe^0-based filters using azo dyes. Chemical Engineering Journal 259 (2015) 481–491.

Pilling N.B., Bedworth R.E. Oxidation of copper-nickel alloys at high temperatures. Industrial & Engineering Chemistry 17 (1923) 372–376.

Rahman M.A., Karmakar S., Salama H., Gactha-Bandjun N., Btatkeu K. B.D., Noubactep C. Optimising the design of Fe^0-based filtration systems for water treatment: The suitability of porous iron composites. Journal of Applied Solution Chemistry and Modeling 2 (2013) 165–177.

Richards M.D., Pope C.G. Adsorption of methylene blue from aqueous solutions by amorphous alumosilicate gels and Zeolite X. Journal of the Chemical Society, Faraday Transactions 92 (1996) 317–323.

Roberts A.L., Totten L.A., Arnold W.A., Burris D.R., Campbell T.J. Reductive elimination of chlorinated ethylenes by zero-valent metals. Environmental Science & Technology 30 (1996) 2654–2659.

Sarin P., Snoeyink V.L., Bebee J., Jim K.K., Beckett M.A., Kriven W.M., Clement J.A. Iron release from corroded iron pipes in drinking water distribution systems: effect of dissolved oxygen. Water Research 38 (2004b) 1259–1269.

Sarin P., Snoeyink V.L., Bebee J., Kriven W.M., Clement J.A. Physico-chemical characteristics of corrosion scales in old iron pipes. Water Research 35 (2001) 2961–2969.

Sarin P., Snoeyink V.L., Lytle D.A., Kriven W.M. Iron corrosion scales: Model for scale growth, iron release, and colored water formation. Journal of Environmental Engineering 130 (2004a) 364–373.

Sato N. Surface oxides affecting metallic corrosion. Corrosion Reviews. 19 (2001) 253–272.

Sato Y., Young D.J. High-Temperature corrosion of iron at 900 °C in atmospheres containing HCl and H_2O. Oxidation of Metals 55 (2001) 243–260.

Schreier C.G., Reinhard M., Transformation of chlorinated organic compounds by iron and manganese powders in buffered water and in landfill leachate. Chemosphere 29 (1994) 1743–1753.

Scott T.B., Popescu I.C., Crane R.A., Noubactep C. Nano-scale metallic iron for the treatment of solutions containing multiple inorganic contaminants. Journal of Hazardous Materials 186 (2011) 280–287.

Shannon M.A., Bohn P.W., Elimelech M., Georgiadis J.G., Marinas B.J., Mayes A.M. Science and technology for water purification in the coming decades Nature 452 (2008) 301–310.

Smith P.G., Coackley P. A method for determining specific surface area of activated sludge by dye adsorption. Water Research 5 (1983), 595–598.

Stratmann M., Müller J. The mechanism of the oxygen reduction on rust covered metal substrates. Corrosion Science 36 (1994) 327–359.

Tanaka K., Padermpole K., Hisanaga T. Photocatalytic degradation of commercial azo dyes. Water Research 34 (2000) 327–333.

Tepong-Tsindé R., Crane R., Noubactep C., Nassi A., Ruppert H. Testing metallic iron filtration systems for decentralized water treatment at pilot scale. Water 7 (2015a) 868–897.

Tepong-Tsindé R., Phukan M., Nassi A., Noubactep C., Ruppert H. Validating the efficiency of the MB discoloration method for the characterization of Fe^0/H_2O systems using accelerated corrosion by chloride ions. Chemical Engineering Journal 279 (2015b) 353-362

Togue-Kamga F., Btatkeu B.D., Noubactep C., Woafo P. Metallic iron for environmental remediation: Back to textbooks. Fresenius Environmental Bulletin 21 (2012) 1992–1997.

Trost B.M., Scanlan T.S. Synthesis of allyl sulfides via a palladium mediated allylation. Tetrahedron letters 27 (1986) 4141–4144.

Van Der Kamp G., Van Stempvoort D.R., Wassenaar L.I. The radial diffusion method 1: Using intact cores to determine isotopic composition, chemistry and effective porosities for groundwater in aquitards. Water Resources Research 32 (1996) 1815–1822.

Varlikli C., Bekiari V., Kus M., Boduroglu n., Oner I., Lianos P., Lyberatos G., Icli S. Adsorption of dyes on Sahara desert sand. Journal of Hazardous Materials 170 (2009) 27–34.

Vidic R.D., Suidan M.T. Role of dissolved oxygen on the adsorptive capacity of activated carbon for synthetic and natural organic matter. Environmental Science & Technology 25 (1991) 1612–1618.

Vodyanitskii Yu.N., Effect of reduced iron on the degradation of chlorinated hydrocarbons in contaminated soil and ground water: A review of publications. Eurasian Soil Science 47 (2014) 119–133.

Vodyanitskii Yu.N., Artificial permeable redox barriers for purification of soil and ground water: A review of publications. Eurasian Soil Science 47 (2014) 1058–1068.

Wang K.-S., Lin C.-L., Wei M.-C., Liang H.-H., Li H.-C., Chang C.-H., Fang Y.-T., Chang S.-H. Effects of dissolved oxygen on dye removal by zero-valent iron. Journal of Hazardous Materials 182 (2010) 886–895.

Weber E.J. Iron-mediated reductive transformations: investigation of reaction mechanism. Environmental Science & Technology 30 (1996) 716–719.

Wenk C.B., Kaegi R., Hug S.J., Factors affecting arsenic and uranium removal with zero-valent iron: laboratory tests with Kanchan-type iron nail filter columns with different groundwaters. Environmental Chemistry 11 (2014) 547–557.

Westerhoff P., James J. Nitrate removal in zero-valent iron packed columns. Water Research 37 (2003) 1818–1830.

WHO/UNICEFF 2014. Progress on drinking water and sanitation 2014 update.

You Y., Han J., Chiu P.C., Jin. Y. Removal and inactivation of waterborne viruses using zerovalent iron. Environmental Science & Technology 39 (2005) 9263–9269.

Zafarani H.R., Gactha-Bandjun N., Tsamo C., Bahrololoom M.E., Noubactep C., Tashkhourian J. Evaluating the suitability of the testing procedures for alternative adsorbing materials for wastewater treatment. Fresenius Environmental Bulletin 26 (2014) 1433–1437.

Appendix

This segment presents experimental data which includes

The weight of each reactive system in batch and column experiments,

The measured concentration of each dye in the individual test-tubes or each column experiment,

Mean dye concentration with statistical data.

Appendix 1: Chemicals and Experimental Devices used

Chemicals

Dyes- Methylene Blue (MB), Orange II, Reactive Red (RR 120)
Ascorbic Acid to remove adsorbed dyes and to reduce Fe^{3+} species to more stable Fe^{2+} species in all the test-tubes and columns containing Fe^{0}.
HCl solutions were used for washing in order to remove persistent species on the test tubes in batch experiment.

Experimental devices

Sartorius digital weighing machine (0.001)
Dispenser
Test tubes with 20 mL graduated capacity
Racks for test tubes
Precision pipettes with volumes either 10-1000 μL.
Shaker HS 501D by "Janke and Kunkel", DCM Laborservice, with shaking intensity 75 rpm
UV-VIS Spectrophotometer Cary 50 by Varian
Peristaltic Pump (Ismatec , ICP 24)
10 columns (H = 40cm, B = 2.6 cm inner diameter)
Tygon tubes connecting inlet reservoir, pump, column and outlet.
Samples bottles with 1 L capacity

APPENDIX 1: Batch Experiment

Experiment 1: Performed experiment for pure sand, ZVI, and MnO_2 and mixtures under 6 weeks non shaken condition for **MB**

Table A1.1a: Experimental Condition

	Sand				MnO_2				ZVI			
Sample no	Initial wt.(g)	Actual measured wt.(g)	Mean Std	Deviation	Initial wt(g)	Actual measured wt.(g)	Mean Std	Deviation	Initial wt(g)	Actual measured wt.(g)	Mean Std	Deviation
1	0.0	0.0			0.0	0.0			0.0	0.0		
2	0.0	0.0	0.0	0.0	0.0	0.0	0.0	0.0	0.0	0.0	0.0	0.0
3	0.0	0			0.0	0.0			0.0	0.0		
4	0.5	0.55			0.0	0.0			0.0	0.0		
5	0.5	0.51	0.5	0.02	0.0	0.0	0.0	0.0	0.0	0.0	0	0.0
6	0.5	0.50			0.0	0.0			0.0	0.0		
7	0.0	0.0			0.5	0.53			0.0	0.0		
8	0.0	0.0	0.0	0.0	0.5	0.51	0.5	0.03	0.0	0.0	0	0.0
9	0.0	0.0			0.5	0.56			0.0	0.0		
10	0.0	0.0			0.0	0.0			0.1	0.10		
11	0.0	0.0	0.0	0.0	0.0	0.0	0.0	0.0	0.1	0.11	0.1	0.01
12	0.0	0.0			0.0	0.0			0.1	0.13		
13	0.0	0.0			0.0	0.0			0.1	0.10		
14	0.0	0.0	0.0	0.0	0.0	0.0	0.0	0.0	0.1	0.10	0.1	0.0
15	0.0	0.0			0.0	0.0			0.1	0.10		
16	0.5	0.50			0.0	0.0			0.1	0.13		
17	0.5	0.52	0.5	0.01	0.0	0.0	0.0	0.0	0.1	0.11	0.1	0.02
18	0.5	0.53			0.0	0.0			0.1	0.13		
19	0.5	0.50			0.0	0.0			0.1	0.11		
20	0.5	0.54	0.5	0.03	0.0	0.0	0.0	0.0	0.1	0.10	0.1	0.0
21	0.5	0.56			0.0	0.0			0.1	0.10		
22	0.0				0.5	0.50			0.1	0.13		
23	0.0		0.0	0.0	0.5	0.52	0.5	0.01	0.1	0.16	0.1	0.02
24	0.0				0.5	0.53			0.1	0.12		
25	0.0				0.5	0.50			0.1	0.10		
26	0.0		0.0	0.0	0.5	0.50	0.5	0.0	0.1	0.11	0.1	0.02
27	0.0				0.5	0.50			0.1	0.14		
28	0.5	0.51			0.5	0.50			0.1	0.13		
29	0.5	0.50	0.5	0.0	0.5	0.51	0.5	0.0	0.1	0.13	0.1	0.02
30	0.5	0.51			0.5	0.50			0.1	0.11		

Experiment 1: Performed experiment for pure sand, ZVI, and MnO_2 and mixtures under 6 weeks non shaken condition for **Orange II**

Table A1.1b: Experimental Condition

	Sand				**MnO_2**				**ZVI**			
Sample no	Initial wt.(g)	Actual measured wt.(g)	Mean Std	Deviation	Initial wt(g)	Actual measured wt.(g)	Mean Std	Deviation	Initial wt(g)	Actual measured wt.(g)	Mean Std	Deviation
1	**0.0**	**0.0**			**0.0**	**0.0**			**0.0**	**0.0**		
2	**0.0**	**0.0**	**0.0**	**0.0**	**0.0**	**0.0**	**0.0**	**0.0**	**0.0**	**0.0**	**0.0**	**0.0**
3	**0.0**	**0.0**			**0.0**	**0.0**			**0.0**	**0.0**		
4	**0.5**	**0.50**			**0.0**	**0.0**			**0.0**	**0.0**		
5	**0.5**	**0.50**	**0.5**	**0.02**	**0.0**	**0.0**	**0.0**	**0.0**	**0.0**	**0.0**	**0.0**	**0.0**
6	**0.5**	**0.54**			**0.0**	**0.0**			**0.0**	**0.0**		
7	**0.0**	**0.0**			**0.5**	**0.52**			**0.0**	**0.0**		
8	**0.0**	**0.0**	**0.0**	**0.0**	**0.5**	**0.54**	**0.5**	**0.03**	**0.0**	**0.0**	**0.0**	**0.0**
9	**0.0**	**0.0**			**0.5**	**0.50**			**0.0**	**0.0**		
10	**0.0**	**0.0**			**0.0**	**0.0**			**0.1**	**0.12**		
11	**0.0**	**0.0**	**0.0**	**0.0**	**0.0**	**0.0**	**0.0**	**0.0**	**0.1**	**0.13**	**0.1**	**0.01**
12	**0.0**	**0.0**			**0.0**	**0.0**			**0.1**	**0.10**		
13	**0.0**	**0.0**			**0.0**	**0.0**			**0.1**	**0.10**		
14	**0.0**	**0.0**	**0.0**	**0.0**	**0.0**	**0.0**	**0.0**	**0.0**	**0.1**	**0.10**	**0.1**	**0.0**
15	**0.0**	**0.0**			**0.0**	**0.0**			**0.1**	**0.12**		
16	**0.5**	**0.51**			**0.0**	**0.0**			**0.1**	**0.13**		
17	**0.5**	**0.52**	**0.5**	**0.01**	**0.0**	**0.0**	**0.0**	**0.0**	**0.1**	**0.11**	**0.1**	**0.02**
18	**0.5**	**0.50**			**0.0**	**0.0**			**0.1**	**0.10**		
19	**0.5**	**0.54**			**0.0**	**0.0**			**0.1**	**0.10**		
20	**0.5**	**0.50**	**0.5**	**0.03**	**0.0**	**0.0**	**0.0**	**0.0**	**0.1**	**0.13**	**0.1**	**0.0**
21	**0.5**	**0.50**			**0.0**	**0.0**			**0.1**	**0.11**		
22	**0.0**				**0.5**	**0.50**			**0.1**	**0.11**		
23	**0.0**		**0.0**	**0.0**	**0.5**	**0.50**	**0.5**	**0.0**	**0.1**	**0.14**	**0.1**	**0.01**
24	**0.0**				**0.5**	**0.51**			**0.1**	**0.10**		
25	**0.0**				**0.5**	**0.52**			**0.1**	**0.13**		
26	**0.0**		**0.0**	**0.0**	**0.5**	**0.50**	**0.5**	**0.01**	**0.1**	**0.10**	**0.1**	**0.01**
27	**0.0**				**0.5**	**0.50**			**0.1**	**0.12**		
28	**0.5**	**0.51**			**0.5**	**0.52**			**0.1**	**0.11**		
29	**0.5**	**0.51**	**0.5**	**0.01**	**0.5**	**0.50**	**0.5**	**0.01**	**0.1**	**0.13**	**0.1**	**0.01**
30	**0.5**	**0.50**			**0.5**	**0.52**			**0.1**	**0.10**		

Experiment 1: Performed experiment for pure sand, ZVI, and MnO_2 and mixtures under 6 weeks non shaken condition for **RR 120**

Table A1.1c: Experimental Condition

	Sand				**MnO_2**				**ZVI**			
Sample no	Initial wt.(g)	Actual measured wt.(g)	Mean Std	Deviation	Initial wt(g)	Actual measured wt.(g)	Mean Std	Deviation	Initial wt(g)	Actual measured wt.(g)	Mean Std	Deviation
1	**0.0**	**0.0**			**0.0**	**0.0**			**0.0**	**0.0**		
2	**0.0**	**0.0**	**0.0**	**0.0**	**0.0**	**0.0**	**0.0**	**0.0**	**0.0**	**0.0**	**0.0**	**0.0**
3	**0.0**	**0.0**			**0.0**	**0.0**			**0.0**	**0.0**		
4	**0.5**	**0.52**			**0.0**	**0.0**			**0.0**	**0.0**		
5	**0.5**	**0.50**	**0.5**	**0.01**	**0.0**	**0.0**	**0.0**	**0.0**	**0.0**	**0.0**	**0.0**	**0.0**
6	**0.5**	**0.50**			**0.0**	**0.0**			**0.0**	**0.0**		
7	**0.0**	**0.0**			**0.5**	**0.50**			**0.0**	**0.0**		
8	**0.0**	**0.0**	**0.0**	**0.0**	**0.5**	**0.53**	**0.5**	**0.03**	**0.0**	**0.0**	**0.0**	**0.0**
9	**0.0**	**0.0**			**0.5**	**0.51**			**0.0**	**0.0**		
10	**0.0**	**0.0**			**0.0**	**0.0**			**0.1**	**0.10**		
11	**0.0**	**0.0**	**0.0**	**0.0**	**0.0**	**0.0**	**0.0**	**0.0**	**0.1**	**0.12**	**0.1**	**0.01**
12	**0.0**	**0.0**			**0.0**	**0.0**			**0.1**	**0.10**		
13	**0.0**	**0.0**			**0.0**	**0.0**			**0.1**	**0.14**		
14	**0.0**	**0.0**	**0.0**	**0.0**	**0.0**	**0.0**	**0.0**	**0.0**	**0.1**	**0.10**	**0.0**	**0.02**
15	**0.0**	**0.0**			**0.0**	**0.0**			**0.1**	**0.11**		
16	**0.5**	**0.51**			**0.0**	**0.0**			**0.1**	**0.11**		
17	**0.5**	**0.50**	**0.5**	**0.00**	**0.0**	**0.0**	**0.0**	**0.0**	**0.1**	**0.10**	**0.1**	**0.0**
18	**0.5**	**0.50**			**0.0**	**0.0**			**0.1**	**0.10**		
19	**0.5**	**0.52**			**0.0**	**0.0**			**0.1**	**0.10**		
20	**0.5**	**0.50**	**0.5**	**0.01**	**0.0**	**0.0**	**0.0**	**0.0**	**0.1**	**0.10**	**0.1**	**0.0**
21	**0.5**	**0.52**			**0.0**	**0.0**			**0.1**	**0.10**		
22	**0.0**				**0.5**	**0.51**			**0.1**	**0.10**		
23	**0.0**		**0.0**	**0.0**	**0.5**	**0.51**	**0.5**	**0.01**	**0.1**	**0.14**	**0.1**	**0.02**
24	**0.0**				**0.5**	**0.53**			**0.1**	**0.10**		
25	**0.0**				**0.5**	**0.54**			**0.1**	**0.10**		
26	**0.0**		**0.0**	**0.0**	**0.5**	**0.51**	**0.5**	**0.02**	**0.1**	**0.10**	**0.1**	**0.01**
27	**0.0**				**0.5**	**0.50**			**0.1**	**0.13**		
28	**0.5**	**0.51**			**0.5**	**0.54**			**0.1**	**0.10**		
29	**0.5**	**0.51**	**0.5**	**0.01**	**0.5**	**0.50**	**0.5**	**0.02**	**0.1**	**0.13**	**0.1**	**0.02**
30	**0.5**	**0.52**			**0.5**	**0.50**			**0.1**	**0.11**		

Experiment 1: Performed experiment for pure sand, ZVI, and MnO_2 and mixtures under 6 weeks non shaken condition for **MB, Orange II and RR 120**

Table A1.1d: Results for MB, Orange II and RR 120.

$[MB]_1$	$[MB]_2$	$[MB]_3$	**[MB]mean**	$\lambda_{[MB]}$	D1	D2	D3	**D mean**	**σ D**
(mg/L)	(mg/L)	(mg/L)	**(mg/L)**	**(mg/L)**	(%)	(%)	(%)	**(%)**	**(%)**
9.5	9.6	9.6	**9.6**	**0.1**	1.0	0.0	0.0	**0.3**	**0.6**
7.6	7.2	7.2	**7.3**	**0.2**	20.8	25.0	25,0	**23.6**	**2.4**
3.7	3.7	3.9	**3.8**	**0.1**	61.5	61.5	59.4	**60.8**	**1.2**
4.4	4.6	5.1	**4.7**	**0.4**	54.2	52.1	46.9	**51.0**	**3.8**
5.2	5.4	6.0	**5.5**	**0.4**	45.8	43.8	37.5	**42.4**	**4.3**
5.9	5.2	5.0	**5.4**	**0.5**	38.5	45.8	47.9	**44.1**	**4.9**
6.2	6.7	6.6	**6.5**	**0.3**	35.4	30.2	31.3	**32.3**	**2.8**
5.1	5.1	5.8	**5.3**	**0.4**	46.9	46.9	39.6	**44.4**	**4.2**
6.1	6.2	5.3	**5.9**	**0.5**	36.5	35.4	44,8	**38.9**	**5.1**
5.7	6.6	5.5	**5.9**	**0.6**	40.6	31.3	42.7	**38.2**	**6.1**
$[Orange\ II]_1$	$[Orange\ II]_2$	$[Orange\ II]_3$	**$[Orange\ II]_{mean}$**	**$\lambda_{[Orange\ II]}$**	D1	D2	D3	**D_{mean}**	**σ D**
(mg/L)	(mg/L)	(mg/L)	**(mg/L)**	**(mg/L)**	(%)	(%)	(%)	**(%)**	**(%)**
11.3	11.3	11.3	**11.3**	**0.0**	0.0	0.0	0,0	**0.0**	**0.0**
11.1	11.1	11.2	**11.1**	**0.1**	0.0	0.0	-0,9	**-0.3**	**0.5**
9.7	10.0	9.8	**9.8**	**0.2**	14.2	11.5	13,3	**13.0**	**1.4**
0.4	0.4	0.5	**0.4**	**0.1**	96.5	96.5	95,6	**96.2**	**0.5**
1.5	1.7	1.3	**1.5**	**0.2**	86.7	85.0	88,5	**86.7**	**1.8**
1.6	4.0	2.9	**2.8**	**1.2**	85.8	64.6	74,3	**74.9**	**10.6**
3.8	7.2	5.8	**5.6**	**1.7**	66.4	36.3	48,7	**50.4**	**15.1**
9.1	7.8	9.9	**8.9**	**1.1**	19.5	31.0	12,4	**20.9**	**9.4**
10.0	9.5	10.0	**9.8**	**0.3**	11.5	15.9	11,5	**13.0**	**2.6**
9.2	8.8	9.2	**9.1**	**0.2**	18.6	22.1	18,6	**19.8**	**2.0**
$[RR\ 120]_1$	$[RR\ 120]_2$	$[RR\ 120]_3$	**$[RR\ 120]_{mean}$**	**$\lambda_{[RR120]}$**	D1	D2	D3	**D_{mean}**	**σ D**
(mg/L)	(mg/L)	(mg/L)	**(mg/L)**	**(mg/L)**	(%)	(%)	(%)	**(%)**	**(%)**
47.4	47.7	47.8	**47.6**	**0.2**	0.42	-0.21	-0,42	**0.0**	**0.4**
47.5	47.6	47.5	**47.5**	**0.1**	0.21	0.00	0,21	**0.1**	**0.1**
45.1	45.1	45.4	**45.2**	**0.2**	5.25	5.25	4,62	**5.0**	**0.4**
8.5	8.0	9.2	**8.6**	**0.6**	82.14	83.19	80,67	**82.0**	**1.3**

14.3	19.3	18.1	**17.2**	**2.6**	69.96	59.45	61,97	**63.8**	**5.5**
26.9	26.5	27.7	**27.0**	**0.6**	43.49	44.33	41,81	**43.2**	**1.3**
27.0	33.7	33.3	**31.3**	**3.8**	43.28	29.20	30,04	**34.2**	**7.9**
42.2	40.7	40.7	**41.2**	**0.9**	11.34	14.50	14,50	**13.4**	**1.8**
42.2	41.1	41.6	**41.6**	**0.6**	11.34	13.66	12,61	**12.5**	**1.2**
39.2	41.3	41.4	**40.6**	**1.2**	17.65	13.24	13,03	**14.6**	**2.6**

Experiment 2: Performed experiment for pure ZVI/sand mixtures under 2weeks shaken condition for **MB.**

Table A1.2a: Experimental Conditions

	Sand				**ZVI**			
Sample no	Initial wt.(g)	Actual measured wt.(g)	Mean Std	Deviation	Initial wt.(g)	Actual measured wt.(g)	Mean Std	Deviation
1	**0.00**	**0.00**			**0.00**	**0.00**		
2	**0.00**	**0.00**	**0.00**	**0.00**	**0.00**	**0.00**	**0.00**	**0.00**
3	**0.00**	**0.00**			**0.00**	**0.00**		
4	**0.50**	**0.50**			**0.00**	**0.00**		
5	**0.50**	**0.50**	**0.50**	**0.00**	**0.00**	**0.00**	**0.00**	**0.00**
6	**0.50**	**0.50**			**0.00**	**0.00**		
7	**0.00**	**0.00**			**0.10**	**0.10**		
8	**0.00**	**0.00**	**0.00**	**0.00**	**0.10**	**0.10**	**0.10**	**0.00**
9	**0.00**	**0.00**			**0.10**	**0.11**		
10	**0.05**	**0.05**			**0.10**	**0.11**		
11	**0.05**	**0.05**	**0.05**	**0.00**	**0.10**	**0.11**	**0.11**	**0.01**
12	**0.05**	**0.05**			**0.10**	**0.10**		
13	**0.10**	**0.10**			**0.10**	**0.10**		
14	**0.10**	**0.10**	**0.10**	**0.00**	**0.10**	**0.10**	**0.10**	**0.00**
15	**0.10**	**0.10**			**0.10**	**0.11**		
16	**0.15**	**0.15**			**0.10**	**0.10**		
17	**0.15**	**0.15**	**0.15**	**0.00**	**0.10**	**0.11**	**0.11**	**0.01**
18	**0.15**	**0.15**			**0.10**	**0.11**		
19	**0.20**	**0.21**			**0.10**	**0.10**		
20	**0.20**	**0.20**	**0.20**	**0.00**	**0.10**	**0.11**	**0.11**	**0.01**
21	**0.20**	**0.20**			**0.10**	**0.11**		
22	**0.30**	**0.30**			**0.10**	**0.11**		
23	**0.30**	**0.30**	**0.31**	**0.01**	**0.10**	**0.10**	**0.10**	**0.00**
24	**0.30**	**0.32**			**0.10**	**0.10**		
25	**0.40**	**0.41**			**0.10**	**0.10**		
26	**0.40**	**0.40**	**0.40**	**0.00**	**0.10**	**0.10**	**0.11**	**0.01**
27	**0.40**	**0.40**			**0.10**	**0.12**		
28	**0.50**	**0.50**			**0.10**	**0.11**		
29	**0.50**	**0.50**	**0.50**	**0.00**	**0.10**	**0.10**	**0.10**	**0.00**

30	**0.50**	**0.51**			**0.10**	**0.10**		

Experiment 2: Performed experiment for pure ZVI/sand mixtures under 2weeks shaken condition for **Orange II.**

Table A1.2b: Experimental Conditions

	Sand				**ZVI**			
Sample no	Initial wt.(g)	Actual measured wt.(g)	Mean Std	Deviation	Initial wt.(g)	Actual measured wt.(g)	Mean Std	Deviation
1	**0.00**	**0.00**			**0.00**	**0.00**		
2	**0.00**	**0.00**	**0.00**	**0.00**	**0.00**	**0.00**	**0.00**	**0.00**
3	**0.00**	**0.00**			**0.00**	**0.00**		
4	**0.50**	**0.51**			**0.00**	**0.00**		
5	**0.50**	**0.50**	**0.50**	**0.00**	**0.00**	**0.00**	**0.00**	**0.00**
6	**0.50**	**0.50**			**0.00**	**0.00**		
7	**0.00**	**0.00**			**0.10**	**0.11**		
8	**0.00**	**0.00**	**0.00**	**0.00**	**0.10**	**0.10**	**0.10**	**0.00**
9	**0.00**	**0.00**			**0.10**	**0.10**		
10	**0.05**	**0.05**			**0.10**	**0.10**		
11	**0.05**	**0.05**	**0.05**	**0.00**	**0.10**	**0.11**	**0.11**	**0.01**
12	**0.05**	**0.05**			**0.10**	**0.12**		
13	**0.10**	**0.10**			**0.10**	**0.12**		
14	**0.10**	**0.10**	**0.10**	**0.00**	**0.10**	**0.10**	**0.11**	**0.01**
15	**0.10**	**0.10**			**0.10**	**0.10**		
16	**0.15**	**0.15**			**0.10**	**0.11**		
17	**0.15**	**0.15**	**0.15**	**0.00**	**0.10**	**0.11**	**0.11**	**0.01**
18	**0.15**	**0.15**			**0.10**	**0.11**		
19	**0.20**	**0.20**			**0.10**	**0.11**		
20	**0.20**	**0.20**	**0.20**	**0.00**	**0.10**	**0.12**	**0.11**	**0.01**
21	**0.20**	**0.20**			**0.10**	**0.11**		
22	**0.30**	**0.32**			**0.10**	**0.10**		
23	**0.30**	**0.30**	**0.32**	**0.02**	**0.10**	**0.12**	**0.12**	**0.02**
24	**0.30**	**0.32**			**0.10**	**0.10**		
25	**0.40**	**0.40**			**0.10**	**0.10**		
26	**0.40**	**0.40**	**0.40**	**0.00**	**0.10**	**0.13**	**0.12**	**0.02**
27	**0.40**	**0.41**			**0.10**	**0.12**		
28	**0.50**	**0.51**			**0.10**	**0.10**		
29	**0.50**	**0.50**	**0.51**	**0.01**	**0.10**	**0.13**	**0.12**	**0.02**

30	**0.50**	**0.51**			**0.10**	**0.11**		

Experiment 2: Performed experiment for pure ZVI/sand mixtures under 2weeks shaken condition for **RR 120.**

Table A1.2c: Experimental Conditions

	Sand				**ZVI**			
Sample no	Initial wt.(g)	Actual measured wt.(g)	Mean Std	Deviation	Initial wt.(g)	Actual measured wt.(g)	Mean Std	Deviation
1	**0.00**	**0.00**			**0.00**	**0.00**		
2	**0.00**	**0.00**	**0.00**	**0.00**	**0.00**	**0.00**	**0.00**	**0.00**
3	**0.00**	**0.00**			**0.00**	**0.00**		
4	**0.50**	**0.50**			**0.00**	**0.00**		
5	**0.50**	**0.50**	**0.50**	**0.00**	**0.00**	**0.00**	**0.00**	**0.00**
6	**0.50**	**0.50**			**0.00**	**0.00**		
7	**0.00**	**0.00**			**0.10**	**0.10**		
8	**0.00**	**0.00**	**0.00**	**0.00**	**0.10**	**0.10**	**0.11**	**0.01**
9	**0.00**	**0.00**			**0.10**	**0.12**		
10	**0.05**	**0.05**			**0.10**	**0.11**		
11	**0.05**	**0.05**	**0.05**	**0.00**	**0.10**	**0.10**	**0.11**	**0.01**
12	**0.05**	**0.05**			**0.10**	**0.11**		
13	**0.10**	**0.13**			**0.10**	**0.11**		
14	**0.10**	**0.10**	**0.11**	**0.01**	**0.10**	**0.11**	**0.11**	**0.01**
15	**0.10**	**0.10**			**0.10**	**0.12**		
16	**0.15**	**0.15**			**0.10**	**0.13**		
17	**0.15**	**0.15**	**0.15**	**0.00**	**0.10**	**0.11**	**0.11**	**0.01**
18	**0.15**	**0.15**			**0.10**	**0.11**		
19	**0.20**	**0.21**			**0.10**	**0.11**		
20	**0.20**	**0.20**	**0.20**	**0.00**	**0.10**	**0.11**	**0.11**	**0.01**
21	**0.20**	**0.20**			**0.10**	**0.10**		
22	**0.30**	**0.30**			**0.10**	**0.11**		
23	**0.30**	**0.30**	**0.30**	**0.02**	**0.10**	**0.11**	**0.11**	**0.01**
24	**0.30**	**0.31**			**0.10**	**0.10**		
25	**0.40**	**0.40**			**0.10**	**0.10**		
26	**0.40**	**0.43**	**0.42**	**0.02**	**0.10**	**0.10**	**0.10**	**0.00**
27	**0.40**	**0.41**			**0.10**	**0.10**		
28	**0.50**	**0.50**			**0.10**	**0.10**		
29	**0.50**	**0.50**	**0.50**	**0.00**	**0.10**	**0.10**	**0.10**	**0.00**

30	**0.50**	**0.50**			**0.10**	**0.10**		

Experiment 2: Performed experiment for pure ZVI/Sand mixtures under 2weeks shaken condition for **MB, Orange II and RR120.**

Table A1.2d: Results for MB, Orange II and RR120

$[MB]_1$	$[MB]_2$	$[MB]_3$	$\mathbf{[MB]_{mean}}$	$\square_{\square MB]}$	D1	D2	D3	$\mathbf{D_{mean}}$	**σ D**
(mg/L)	(mg/L)	(mg/L)	**(mg/L)**	**(mg/L)**	(%)	(%)	(%)	**(%)**	**(%)**
9.5	9.6	9.6	**9.6**	**0.1**	1.0	0.0	0.0	**0.3**	**0.6**
7.6	7.2	7.2	**7.3**	**0.2**	20.8	25.0	25.0	**23.6**	**2.4**
3.7	3.7	3.9	**3.8**	**0.1**	61.5	61.5	59.4	**60.8**	**1.2**
4.4	4.6	5.1	**4.7**	**0.4**	54.2	52.1	46.9	**51.0**	**3.8**
5.2	5.4	6.0	**5.5**	**0.4**	45.8	43.8	37.5	**42.4**	**4.3**
5.9	5.2	5.0	**5.4**	**0.5**	38.5	45.8	47.9	**44.1**	**4.9**
6.2	6.7	6.6	**6.5**	**0.3**	35.4	30.2	31.3	**32.3**	**2.8**
5.1	5.1	5.8	**5.3**	**0.4**	46.9	46.9	39.6	**44.4**	**4.2**
6.1	6.2	5.3	**5.9**	**0.5**	36.5	35.4	44.8	**38.9**	**5.1**
5.7	6.6	5.5	**5.9**	**0.6**	40.6	31.3	42.7	**38.2**	**6.1**
$[Orange\ II]_1$	$[Orange\ II]_2$	$[Orange\ II]_3$	$\mathbf{[Orange\ II]_{mean}}$	$\mathbf{s_{[Orange\ II]}}$	D1	D2	D3	$\mathbf{D_{mean}}$	**σ D**
(mg/L)	(mg/L)	(mg/L)	**(mg/L)**	**(mg/L)**	(%)	(%)	(%)	**(%)**	**(%)**
11.3	11.3	11.3	**11.3**	**0.0**	0.0	0.0	0.0	**0.0**	**0.0**
11.3	11.4	11.4	**11.4**	**0.1**	0.9	0.0	0.0	**0.3**	**0.5**
1.5	2.0	2.2	**1.9**	**0.4**	86.8	82.5	80.7	**83.3**	**3.2**
3.4	2.6	2.4	**2.8**	**0.5**	70.2	77.2	78.9	**75.4**	**4.6**
2.9	4.6	4.0	**3.8**	**0.9**	74.6	59.6	64.9	**66.4**	**7.6**
3.7	3.9	4.7	**4.1**	**0.5**	67.5	65.8	58.8	**64.0**	**4.6**
7.3	5.9	4.9	**6.0**	**1.2**	36.0	48.2	57.0	**47.1**	**10.6**
6.0	3.8	4.9	**4.9**	**1.1**	47.4	66.7	57.0	**57.0**	**9.6**
5.0	4.1	4.2	**4.4**	**0.5**	56.1	64.0	63.2	**61.1**	**4.3**
6.3	4.9	4.5	**5.2**	**0.9**	44.7	57.0	60.5	**54.1**	**8.3**
$[RR\ 120]_1$	$[RR\ 120]_2$	$[RR\ 120]_3$	$\mathbf{[RR\ 120]_{mean}}$	$\mathbf{s_{[RR\ 120]}}$	D1	D2	D3	$\mathbf{D_{mean}}$	**σ D**
(mg/L)	(mg/L)	(mg/L)	**(mg/L)**	**(mg/L)**	(%)	(%)	(%)	**(%)**	**(%)**
47.3	47.3	47.3	**47.3**	**0.0**	0.0	0.0	0.0	**0.0**	**0.0**
47.2	47.3	47.3	**47.3**	**0.1**	0.2	0.0	0.0	**0.1**	**0.1**
20.0	18.9	15.7	**18.2**	**2.2**	57.7	60.0	66.8	**61.5**	**4.7**
21.4	21.6	25.0	**22.7**	**2.0**	54.8	54.3	47.1	**52.1**	**4.3**

33.0	29.1	25.2	**29.1**	**3.9**	30.2	38.5	46.7	**38.5**	**8.2**
29.6	27.9	26.7	**28.1**	**1.5**	37.4	41.0	43.6	**40.7**	**3.1**
32.5	27.2	36.4	**32.0**	**4.6**	31.3	42.5	23.0	**32.3**	**9.8**
34.4	30.2	37.3	**34.0**	**3.6**	27.3	36.2	21.1	**28.2**	**7.5**
33.4	34.8	34.2	**34.1**	**0.7**	29.4	26.4	27.7	**27.8**	**1.5**
31.6	36.8	33.9	**34.1**	**2.6**	33.2	22.2	28.3	**27.9**	**5.5**

Experiment 3: Performed experiment for pure ZVI/MnO_2 mixtures under 2weeks shaken condition for **MB.**

Table A1.3a: Experimental Conditions

	MnO_2				**ZVI**			
Sample no	Initial wt.(g)	Actual measured wt.(g)	Mean Std	Deviation	Initial wt.(g)	Actual measured wt.(g)	Mean Std	Deviation
1	**0.00**	**0.00**			**0.00**	**0.00**		
2	**0.00**	**0.00**	**0.00**	**0.00**	**0.00**	**0.00**	**0.00**	**0.00**
3	**0.00**	**0.00**			**0.00**	**0.00**		
4	**0.50**	**0.50**			**0.00**	**0.00**		
5	**0.50**	**0.57**	**0.52**	**0.02**	**0.00**	**0.00**	**0.00**	**0.00**
6	**0.50**	**0.51**			**0.00**	**0.00**		
7	**0.00**	**0.00**			**0.10**	**0.12**		
8	**0.00**	**0.00**	**0.00**	**0.00**	**0.10**	**0.10**	**0.12**	**0.02**
9	**0.00**	**0.00**			**0.10**	**0.12**		
10	**0.05**	**0.05**			**0.10**	**0.10**		
11	**0.05**	**0.05**	**0.05**	**0.00**	**0.10**	**0.11**	**0.11**	**0.01**
12	**0.05**	**0.05**			**0.10**	**0.11**		
13	**0.10**	**0.10**			**0.10**	**0.12**		
14	**0.10**	**0.10**	**0.10**	**0.00**	**0.10**	**0.11**	**0.11**	**0.01**
15	**0.10**	**0.10**			**0.10**	**0.11**		
16	**0.15**	**0.15**			**0.10**	**0.12**		
17	**0.15**	**0.15**	**0.15**	**0.00**	**0.10**	**0.11**	**0.11**	**0.01**
18	**0.15**	**0.15**			**0.10**	**0.11**		
19	**0.20**	**0.20**			**0.10**	**0.12**		
20	**0.20**	**0.22**	**0.21**	**0.01**	**0.10**	**0.10**	**0.12**	**0.02**
21	**0.20**	**0.20**			**0.10**	**0.14**		
22	**0.30**	**0.30**			**0.10**	**0.11**		
23	**0.30**	**0.30**	**0.31**	**0.01**	**0.10**	**0.12**	**0.12**	**0.02**
24	**0.30**	**0.32**			**0.10**	**0.13**		
25	**0.40**	**0.41**			**0.10**	**0.13**		
26	**0.40**	**0.44**	**0.42**	**0.02**	**0.10**	**0.16**	**0.13**	**0.03**
27	**0.40**	**0.40**			**0.10**	**0.10**		
28	**0.50**	**0.50**			**0.10**	**0.10**		
29	**0.50**	**0.51**	**0.50**	**0.00**	**0.10**	**0.11**	**0.10**	**0.00**

30	**0.50**	**0.50**			**0.10**	**0.10**		

Experiment 3: Performed experiment for pure ZVI/MnO_2 mixtures under 2weeks shaken condition for **Orange II.**

Table A1.3b: Experimental Conditions

	MnO_2				**ZVI**			
Sample no	Initial wt.(g)	Actual measured wt.(g)	Mean Std	Deviation	Initial wt.(g)	Actual measured wt.(g)	Mean Std	Deviation
1	**0.00**	**0.00**			**0.00**	**0.00**		
2	**0.00**	**0.00**	**0.00**	**0.00**	**0.00**	**0.00**	**0.00**	**0.00**
3	**0.00**	**0.00**			**0.00**	**0.00**		
4	**0.50**	**0.50**			**0.00**	**0.00**		
5	**0.50**	**0.51**	**0.50**	**0.00**	**0.00**	**0.00**	**0.00**	**0.00**
6	**0.50**	**0.50**			**0.00**	**0.00**		
7	**0.00**	**0.00**			**0.10**	**0.10**		
8	**0.00**	**0.00**	**0.00**	**0.00**	**0.10**	**0.10**	**0.12**	**0.02**
9	**0.00**	**0.00**			**0.10**	**0.10**		
10	**0.05**	**0.05**			**0.10**	**0.12**		
11	**0.05**	**0.05**	**0.05**	**0.00**	**0.10**	**0.10**	**0.12**	**0.02**
12	**0.05**	**0.05**			**0.10**	**0.12**		
13	**0.10**	**0.10**			**0.10**	**0.12**		
14	**0.10**	**0.13**	**0.11**	**0.01**	**0.10**	**0.12**	**0.12**	**0.02**
15	**0.10**	**0.10**			**0.10**	**0.10**		
16	**0.15**	**0.15**			**0.10**	**0.12**		
17	**0.15**	**0.15**	**0.15**	**0.00**	**0.10**	**0.10**	**0.11**	**0.01**
18	**0.15**	**0.15**			**0.10**	**0.11**		
19	**0.20**	**0.20**			**0.10**	**0.11**		
20	**0.20**	**0.25**	**0.22**	**0.02**	**0.10**	**0.11**	**0.11**	**0.01**
21	**0.20**	**0.21**			**0.10**	**0.12**		
22	**0.30**	**0.31**			**0.10**	**0.12**		
23	**0.30**	**0.30**	**0.32**	**0.02**	**0.10**	**0.12**	**0.12**	**0.02**
24	**0.30**	**0.35**			**0.10**	**0.13**		
25	**0.40**	**0.41**			**0.10**	**0.13**		
26	**0.40**	**0.40**	**0.41**	**0.01**	**0.10**	**0.11**	**0.12**	**0.02**
27	**0.40**	**0.42**			**0.10**	**0.13**		
28	**0.50**	**0.52**			**0.10**	**0.10**		
29	**0.50**	**0.53**	**0.52**	**0.02**	**0.10**	**0.10**	**0.10**	**0.00**

30	**0.50**	**0.51**			**0.10**	**0.11**		

Experiment 3: Performed experiment for pure ZVI/MnO_2 mixtures under 2weeks shaken condition for **RR 120.**

Table A1.3c: Experimental Conditions

	MnO_2				**ZVI**			
Sample no	Initial wt.(g)	Actual measured wt.(g)	Mean Std	Deviation	Initial wt.(g)	Actual measured wt.(g)	Mean Std	Deviation
1	**0.00**	**0.00**			**0.00**	**0.00**		
2	**0.00**	**0.00**	**0.00**	**0.00**	**0.00**	**0.00**	**0.00**	**0.00**
3	**0.00**	**0.00**			**0.00**	**0.00**		
4	**0.50**	**0.51**			**0.00**	**0.00**		
5	**0.50**	**0.51**	**0.51**	**0.01**	**0.00**	**0.00**	**0.00**	**0.00**
6	**0.50**	**0.52**			**0.00**	**0.00**		
7	**0.00**	**0.00**			**0.10**	**0.10**		
8	**0.00**	**0.00**	**0.00**	**0.00**	**0.10**	**0.10**	**0.11**	**0.01**
9	**0.00**	**0.00**			**0.10**	**0.12**		
10	**0.05**	**0.05**			**0.10**	**0.11**		
11	**0.05**	**0.05**	**0.05**	**0.00**	**0.10**	**0.10**	**0.11**	**0.01**
12	**0.05**	**0.05**			**0.10**	**0.11**		
13	**0.10**	**0.13**			**0.10**	**0.13**		
14	**0.10**	**0.13**	**0.13**	**0.03**	**0.10**	**0.14**	**0.12**	**0.02**
15	**0.10**	**0.14**			**0.10**	**0.11**		
16	**0.15**	**0.15**			**0.10**	**0.15**		
17	**0.15**	**0.15**	**0.15**	**0.00**	**0.10**	**0.13**	**0.13**	**0.03**
18	**0.15**	**0.15**			**0.10**	**0.11**		
19	**0.20**	**0.20**			**0.10**	**0.10**		
20	**0.20**	**0.24**	**0.22**	**0.02**	**0.10**	**0.10**	**0.10**	**0.00**
21	**0.20**	**0.20**			**0.10**	**0.11**		
22	**0.30**	**0.30**			**0.10**	**0.12**		
23	**0.30**	**0.32**	**0.31**	**0.01**	**0.10**	**0.11**	**0.11**	**0.01**
24	**0.30**	**0.30**			**0.10**	**0.10**		
25	**0.40**	**0.41**			**0.10**	**0.10**		
26	**0.40**	**0.40**	**0.40**	**0.00**	**0.10**	**0.10**	**0.10**	**0.00**
27	**0.40**	**0.40**			**0.10**	**0.10**		
28	**0.50**	**0.53**			**0.10**	**0.10**		
29	**0.50**	**0.53**	**0.52**	**0.02**	**0.10**	**0.10**	**0.10**	**0.00**
30	**0.50**	**0.51**			**0.10**	**0.10**		

Experiment 3: Performed experiment for pure ZVI/MnO_2 mixtures under 2weeks shaken condition for **MB, Orange II and RR 120.**

Table A1.3d: Results for MB, Orange II and RR120

$[MB]_1$	$[MB]_2$	$[MB]_3$	**$[MB]_{mean}$**	**$\Delta_{[MB]}$**	D1	D2	D3	**D_{mean}**	**σ D**
(mg/L)	(mg/L)	(mg/L)	**(mg/L)**	**(mg/L)**	(%)	(%)	(%)	**(%)**	**(%)**
10.1	10.2	10.1	**10.1**	**0.1**	0.0	-1.0	0.0	**-0.3**	**0.6**
0.5	0.3	0.4	**0.4**	**0.1**	95.0	97.0	96.0	**96.0**	**1.0**
3.9	4.6	4.1	**4.2**	**0.4**	61.4	54.5	59.4	**58.4**	**3.6**
4.3	4.3	3.7	**4.1**	**0.3**	57.4	57.4	63.4	**59.4**	**3.4**
3	3.5	3	**3.2**	**0.3**	70.3	65.3	70.3	**68.6**	**2.9**
2.3	2.4	2.3	**2.3**	**0.1**	77.2	76.2	77.2	**76.9**	**0.6**
1.9	1.2	1.9	**1.7**	**0.4**	81.2	88.1	81.2	**83.5**	**4.0**
1	0.6	0.6	**0.7**	**0.2**	90.1	94.1	94.1	**92.7**	**2.3**
0.4	0.5	0.5	**0.5**	**0.1**	96.0	95.0	95.0	**95.4**	**0.6**
0.3	0.4	0.3	**0.3**	**0.1**	97.0	96.0	97.0	**96.7**	**0.6**
[Orange II]$_1$	[Orange II]$_2$	[Orange II]$_3$	**[Orange II]$_{mean}$**	**$\Delta_{[Orange\ II]}$**	D1	D2	D3	**D_{mean}**	**σ D**
(mg/L)	(mg/L)	(mg/L)	**(mg/L)**	**(mg/L)**	(%)	(%)	(%)	**(%)**	**(%)**
11.6	11.7	11.7	**11.7**	**0.1**	0.9	0.0	0.0	**0.3**	**0.5**
11.5	11.4	10.7	**11.2**	**0.4**	1.7	2.6	8.5	**4.3**	**3.7**
2.1	2.3	2.0	**2.1**	**0.2**	82.1	80.3	82.9	**81.8**	**1.3**
2.6	2.9	2.6	**2.7**	**0.2**	77.8	75.0	78.2	**77.0**	**1.7**
3.5	3.3	3.4	**3.4**	**0.1**	69.9	71.4	71.3	**70.9**	**0.8**
4.4	5.2	3.6	**4.4**	**0.8**	62.2	56.0	69.6	**62.6**	**6.8**
4.6	4.9	4.4	**4.6**	**0.2**	60.9	58.4	62.3	**60.5**	**2.0**
3.9	5.3	5.3	**4.9**	**0.8**	66.4	54.4	54.7	**58.5**	**6.8**
7.1	5.6	3.8	**5.5**	**1.6**	39.3	51.7	67.3	**52.8**	**14.0**
7.2	6.6	8.0	**7.3**	**0.7**	38.5	43.6	31.6	**37.9**	**6.0**
[RR 120]$_1$	[RR 120]$_2$	[RR 120]$_3$	**[RR 120]$_{mean}$**	**$\Delta_{RR\ 120]}$**	D1	D2	D3	**D_{mean}**	**σ D**
(mg/L)	(mg/L)	(mg/L)	**(mg/L)**	**(mg/L)**	(%)	(%)	(%)	**(%)**	**(%)**
45.3	45.7	45.6	**45.5**	**0.2**	0.4	-0.4	-0.2	**-0.1**	**0.5**
40.5	40.4	40.3	**40.4**	**0.1**	11.0	11.2	11.4	**11.2**	**0.2**
19.7	21.2	18.4	**19.8**	**1.4**	56.7	53.4	59.6	**56.6**	**3.1**
22.4	20.9	22.1	**21.8**	**0.8**	50.8	54.1	51.4	**52.1**	**1.7**

24	24.8	26.7	**25.2**	**1.4**	47.3	45.5	41.3	**44.7**	**3.0**
20.2	21.5	26.2	**22.6**	**3.2**	55.6	52.7	42.4	**50.3**	**6.9**
26.6	30.7	28.6	**28.6**	**2.1**	41.5	32.5	37.1	**37.1**	**4.5**
28.1	29	33.2	**30.1**	**2.7**	38.2	36.3	27.0	**33.8**	**6.0**
34.4	32.3	31.8	**32.8**	**1.4**	24.4	29.0	30.1	**27.8**	**3.0**
33	31.4	33.2	**32.5**	**1.0**	27.5	31.0	27.0	**28.5**	**2.2**

Experiment 4: Performed experiment for pure ZVI/MnO_2 mixtures under 6 weeks non- shaken condition for **MB.**

Table A1.4a: Experimental Conditions

	MnO_2				**ZVI**			
Sample no	Initial wt.(g)	Actual measured wt.(g)	Mean Std	Deviation	Initial wt.(g)	Actual measured wt.(g)	Mean Std	Deviation
1	**0.00**	**0.00**			**0.00**	**0.00**		
2	**0.00**	**0.00**	**0.00**	**0.00**	**0.00**	**0.00**	**0.00**	**0.00**
3	**0.00**	**0.00**			**0.00**	**0.00**		
4	**0.50**	**0.56**			**0.00**	**0.00**		
5	**0.50**	**0.50**	**0.52**	**0.02**	**0.00**	**0.00**	**0.00**	**0.00**
6	**0.50**	**0.50**			**0.00**	**0.00**		
7	**0.00**	**0.00**			**0.10**	**0.10**		
8	**0.00**	**0.00**	**0.00**	**0.00**	**0.10**	**0.10**	**0.10**	**0.00**
9	**0.00**	**0.00**			**0.10**	**0.10**		
10	**0.05**	**0.05**			**0.10**	**0.11**		
11	**0.05**	**0.05**	**0.05**	**0.00**	**0.10**	**0.11**	**0.11**	**0.01**
12	**0.05**	**0.05**			**0.10**	**0.12**		
13	**0.10**	**0.13**			**0.10**	**0.10**		
14	**0.10**	**0.13**	**0.12**	**0.02**	**0.10**	**0.11**	**0.10**	**0.00**
15	**0.10**	**0.14**			**0.10**	**0.10**		
16	**0.15**	**0.15**			**0.10**	**0.10**		
17	**0.15**	**0.15**	**0.15**	**0.00**	**0.10**	**0.10**	**0.10**	**0.00**
18	**0.15**	**0.15**			**0.10**	**0.10**		
19	**0.20**	**0.21**			**0.10**	**0.11**		
20	**0.20**	**0.21**	**0.21**	**0.01**	**0.10**	**0.10**	**0.10**	**0.00**
21	**0.20**	**0.22**			**0.10**	**0.10**		
22	**0.30**	**0.30**			**0.10**	**0.10**		
23	**0.30**	**0.30**	**0.30**	**0.00**	**0.10**	**0.11**	**0.11**	**0.01**
24	**0.30**	**0.30**			**0.10**	**0.11**		
25	**0.40**	**0.42**			**0.10**	**0.10**		
26	**0.40**	**0.40**	**0.40**	**0.00**	**0.10**	**0.10**	**0.10**	**0.00**
27	**0.40**	**0.40**			**0.10**	**0.11**		
28	**0.50**	**0.50**			**0.10**	**0.11**		
29	**0.50**	**0.50**	**0.50**	**0.00**	**0.10**	**0.11**	**0.11**	**0.01**

30	**0.50**	**0.50**			**0.10**	**0.10**		

Experiment 4: Performed experiment for pure ZVI/MnO_2 mixtures under 6 weeks non- shaken condition for **Orange II.**

Table A1.4b: Experimental Conditions

	MnO_2				**ZVI**			
Sample no	Initial wt.(g)	Actual measured wt.(g)	Mean Std	Deviation	Initial wt.(g)	Actual measured wt.(g)	Mean Std	Deviation
1	**0.00**	**0.00**			**0.00**	**0.00**		
2	**0.00**	**0.00**	**0.00**	**0.00**	**0.00**	**0.00**	**0.00**	**0.00**
3	**0.00**	**0.00**			**0.00**	**0.00**		
4	**0.50**	**0.51**			**0.00**	**0.00**		
5	**0.50**	**0.50**	**0.50**	**0.00**	**0.00**	**0.00**	**0.00**	**0.00**
6	**0.50**	**0.50**			**0.00**	**0.00**		
7	**0.00**	**0.00**			**0.10**	**0.10**		
8	**0.00**	**0.00**	**0.00**	**0.00**	**0.10**	**0.10**	**0.10**	**0.00**
9	**0.00**	**0.00**			**0.10**	**0.11**		
10	**0.05**	**0.05**			**0.10**	**0.11**		
11	**0.05**	**0.05**	**0.05**	**0.00**	**0.10**	**0.10**	**0.10**	**0.00**
12	**0.05**	**0.05**			**0.10**	**0.10**		
13	**0.10**	**0.10**			**0.10**	**0.10**		
14	**0.10**	**0.11**	**0.11**	**0.01**	**0.10**	**0.10**	**0.10**	**0.00**
15	**0.10**	**0.11**			**0.10**	**0.10**		
16	**0.15**	**0.15**			**0.10**	**0.10**		
17	**0.15**	**0.15**	**0.15**	**0.00**	**0.10**	**0.10**	**0.10**	**0.00**
18	**0.15**	**0.15**			**0.10**	**0.10**		
19	**0.20**	**0.24**			**0.10**	**0.10**		
20	**0.20**	**0.22**	**0.22**	**0.02**	**0.10**	**0.11**	**0.10**	**0.00**
21	**0.20**	**0.20**			**0.10**	**0.10**		
22	**0.30**	**0.33**			**0.10**	**0.10**		
23	**0.30**	**0.30**	**0.31**	**0.01**	**0.10**	**0.11**	**0.10**	**0.00**
24	**0.30**	**0.30**			**0.10**	**0.10**		
25	**0.40**	**0.40**			**0.10**	**0.10**		
26	**0.40**	**0.40**	**0.40**	**0.00**	**0.10**	**0.10**	**0.10**	**0.00**
27	**0.40**	**0.41**			**0.10**	**0.10**		
28	**0.50**	**0.51**			**0.10**	**0.10**		
29	**0.50**	**0.50**	**0.50**	**0.00**	**0.10**	**0.10**	**0.10**	**0.00**

30	**0.50**	**0.50**			**0.10**	**0.10**		

Experiment 4: Performed experiment for pure ZVI/MnO_2 mixtures under 6 weeks non- shaken condition for **RR 120**

Table A1.4c: Experimental Conditions

	MnO_2				**ZVI**			
Sample no	Initial wt.(g)	Actual measured wt.(g)	Mean Std	Deviation	Initial wt.(g)	Actual measured wt.(g)	Mean Std	Deviation
1	**0.00**	**0.00**			**0.00**	**0.00**		
2	**0.00**	**0.00**	**0.00**	**0.00**	**0.00**	**0.00**	**0.00**	**0.00**
3	**0.00**	**0.00**			**0.00**	**0.00**		
4	**0.50**	**0.50**			**0.00**	**0.00**		
5	**0.50**	**0.51**	**0.51**	**0.01**	**0.00**	**0.00**	**0.00**	**0.00**
6	**0.50**	**0.52**			**0.00**	**0.00**		
7	**0.00**	**0.00**			**0.10**	**0.10**		
8	**0.00**	**0.00**	**0.00**	**0.00**	**0.10**	**0.12**	**0.10**	**0.00**
9	**0.00**	**0.00**			**0.10**	**0.10**		
10	**0.05**	**0.05**			**0.10**	**0.10**		
11	**0.05**	**0.05**	**0.05**	**0.00**	**0.10**	**0.10**	**0.10**	**0.00**
12	**0.05**	**0.05**			**0.10**	**0.10**		
13	**0.10**	**0.10**			**0.10**	**0.11**		
14	**0.10**	**0.10**	**0.10**	**0.00**	**0.10**	**0.10**	**0.10**	**0.00**
15	**0.10**	**0.10**			**0.10**	**0.10**		
16	**0.15**	**0.15**			**0.10**	**0.10**		
17	**0.15**	**0.15**	**0.15**	**0.00**	**0.10**	**0.10**	**0.10**	**0.00**
18	**0.15**	**0.15**			**0.10**	**0.11**		
19	**0.20**	**0.20**			**0.10**	**0.10**		
20	**0.20**	**0.21**	**0.20**	**0.00**	**0.10**	**0.10**	**0.10**	**0.00**
21	**0.20**	**0.20**			**0.10**	**0.11**		
22	**0.30**	**0.30**			**0.10**	**0.10**		
23	**0.30**	**0.30**	**0.30**	**0.00**	**0.10**	**0.10**	**0.10**	**0.00**
24	**0.30**	**0.30**			**0.10**	**0.11**		
25	**0.40**	**0.40**			**0.10**	**0.10**		
26	**0.40**	**0.40**	**0.40**	**0.00**	**0.10**	**0.12**	**0.10**	**0.00**
27	**0.40**	**0.40**			**0.10**	**0.10**		
28	**0.50**	**0.51**			**0.10**	**0.10**		
29	**0.50**	**0.51**	**0.51**	**0.01**	**0.10**	**0.11**	**0.10**	**0.00**

30	**0.50**	**0.51**			**0.10**	**0.10**		

Experiment 4: Performed experiment for pure ZVI/MnO_2 mixtures under 6 weeks non- shaken condition for **MB, Orange II and RR 120**

Table A.4d: Results for MB, Orange II and RR120.

$[MB]_1$	$[MB]_2$	$[MB]_3$	**$[MB]_{mean}$**	**$\Delta_{[MB]}$**	D1	D2	D3	**D_{mean}**	**σ D**
(mg/L)	(mg/L)	(mg/L)	**(mg/L)**	**(mg/L)**	(%)	(%)	(%)	**(%)**	**(%)**
10	9.9	10	**10.0**	**0.1**	0.0	1.0	0.0	**0.3**	**0.6**
0.2	0.1	0.1	**0.1**	**0.1**	98.0	99.0	99.0	**98.7**	**0.6**
2.5	2.6	2.6	**2.6**	**0.1**	75.0	74.0	74.0	**74.3**	**0.6**
2.5	2.5	2.4	**2.5**	**0.1**	75.0	75.0	76.0	**75.3**	**0.6**
1.7	1.5	1.5	**1.6**	**0.1**	83.0	85.0	85.0	**84.3**	**1.2**
0.8	0.9	0.7	**0.8**	**0.1**	92.0	91.0	93.0	**92.0**	**1.0**
0.5	0.4	0.1	**0.3**	**0.2**	95.0	96.0	99.0	**96.7**	**2.1**
0.1	0	0	**0.0**	**0.1**	99.0	100.0	100.0	**99.7**	**0.6**
0	0	0	**0.0**	**0.0**	100.0	100.0	100.0	**100.0**	**0.0**
0	0	0	**0.0**	**0.0**	100.0	100.0	100.0	**100.0**	**0.0**
[Orange II]$_1$	[Orange II]$_2$	[Orange II]$_3$	**[Orange II]$_{mean}$**	**$\Delta_{[Orange\ II]}$**	D1	D2	D3	**D_{mean}**	**σ D**
(mg/L)	(mg/L)	(mg/L)	**(mg/L)**	**(mg/L)**	(%)	(%)	(%)	**(%)**	**(%)**
11.9	12	11.9	**11.9**	**0.1**	0.0	-0.8	0.0	**-0.3**	**0.5**
11.4	11.4	11.4	**11.4**	**0.0**	4.2	4.2	4.2	**4.2**	**0.0**
0.3	0.4	0.2	**0.3**	**0.1**	97.5	96.6	98.3	**97.5**	**0.8**
0.4	0.2	0.3	**0.3**	**0.1**	96.6	98.3	97.5	**97.5**	**0.8**
0.5	0.3	0.6	**0.5**	**0.2**	95.8	97.5	95.0	**96.1**	**1.3**
0.6	0.4	1	**0.7**	**0.3**	95.0	96.6	91.6	**94.4**	**2.6**
0.6	0.7	1.1	**0.8**	**0.3**	95.0	94.1	90.8	**93.3**	**2.2**
1.4	1.5	1.1	**1.3**	**0.2**	88.2	87.4	90.8	**88.8**	**1.7**
2.9	1.8	2.4	**2.4**	**0.6**	75.6	84.9	79.8	**80.1**	**4.6**
1.6	2.9	3.3	**2.6**	**0.9**	86.6	75.6	72.3	**78.2**	**7.5**
[RR 120]$_1$	[RR 120]$_2$	[RR 120]$_3$	**[RR 120]$_{mean}$**	**Δ [RR 120]**	D1	D2	D3	**D_{mean}**	**σ D**
(mg/L)	(mg/L)	(mg/L)	**(mg/L)**	**(mg/L)**	(%)	(%)	(%)	**(%)**	**(%)**
47.9	48.3	48	**48.1**	**0.2**	0.4	-0.4	0.2	**0.1**	**0.4**
41.9	41.5	41.8	**41.7**	**0.2**	12.9	13.7	13.1	**13.2**	**0.4**
6.5	4.5	6	**5.7**	**1.0**	86.5	90.6	87.5	**88.2**	**2.2**

10.3	7.5	7.3	**8.4**	**1.7**	78.6	84.4	84.8	**82.6**	**3.5**
8.2	7.8	9.3	**8.4**	**0.8**	83.0	83.8	80.7	**82.5**	**1.6**
8.1	12.3	9.4	**9.9**	**2.2**	**83.2**	**74.4**	**80.5**	**79.3**	**4.5**
15.4	8	7.3	**10.2**	**4.5**	**68.0**	**83.4**	**84.8**	**78.7**	**9.3**
17.1	16.4	10.8	**14.8**	**3.5**	**64.4**	**65.9**	**77.5**	**69.3**	**7.2**
20.5	18.4	20.5	**19.8**	**1.2**	**57.4**	**61.7**	**57.4**	**58.8**	**2.5**
23.2	17.3	16.7	**19.1**	**3.6**	**51.8**	**64.0**	**65.3**	**60.4**	**7.5**

Experiment 5: Performed experiment for pure MnO_2 under 2weeks shaken condition for **MB** and **Orange II**.

Table A1.5a: Experimental Conditions

	MB				**Orange II**				**ZVI**	
	MnO_2				**MnO_2**					
Sample no	Initial wt.(g)	Actual measured wt.(g)	Mean Std	Deviation	Initial wt.(g)	Actual measured wt.(g)	Mean Std	Deviation	Initial wt.(g)	Actual measured wt.(g)
1	**0.00**	**0.00**			**0.00**	**0.00**			**0.00**	**0.00**
2	**0.00**	**0.00**	**0.00**	**0.00**	**0.00**	**0.00**	**0.00**	**0.00**	**0.00**	**0.00**
3	**0.00**	**0.00**			**0.00**	**0.00**			**0.00**	**0.00**
4	**0.025**	**0.02**			**0.025**	**0.02**			**0.00**	**0.00**
5	**0.025**	**0.02**	**0.20**	**0.00**	**0.025**	**0.02**	**0.20**	**0.00**	**0.00**	**0.00**
6	**0.025**	**0.02**			**0.025**	**0.02**			**0.00**	**0.00**
7	**0.05**	**0.05**			**0.05**	**0.05**			**0.00**	**0.00**
8	**0.05**	**0.05**	**0.05**	**0.00**	**0.05**	**0.05**	**0.05**	**0.00**	**0.00**	**0.00**
9	**0.05**	**0.05**			**0.05**	**0.05**			**0.00**	**0.00**
10	**0.075**	**0.07**			**0.075**	**0.07**			**0.00**	**0.00**
11	**0.075**	**0.07**	**0.07**	**0.00**	**0.075**	**0.07**	**0.07**	**0.00**	**0.00**	**0.00**
12	**0.075**	**0.07**			**0.075**	**0.07**			**0.00**	**0.00**
13	**0.10**	**0.12**			**0.10**	**0.11**			**0.00**	**0.00**
14	**0.10**	**0.10**	**0.11**	**0.01**	**0.10**	**0.10**	**0.10**	**0.00**	**0.00**	**0.00**
15	**0.10**	**0.11**			**0.10**	**0.10**			**0.00**	**0.00**
16	**0.15**	**0.15**			**0.15**	**0.15**			**0.00**	**0.00**
17	**0.15**	**0.15**	**0.15**	**0.00**	**0.15**	**0.15**	**0.15**	**0.00**	**0.00**	**0.00**
18	**0.15**	**0.15**			**0.15**	**0.15**			**0.00**	**0.00**
19	**0.20**	**0.20**			**0.20**	**0.20**			**0.00**	**0.00**
20	**0.20**	**0.21**	**0.20**	**0.00**	**0.20**	**0.22**	**0.21**	**0.01**	**0.00**	**0.00**
21	**0.20**	**0.20**			**0.20**	**0.22**			**0.00**	**0.00**
22	**0.30**	**0.30**			**0.30**	**0.32**			**0.00**	**0.00**
23	**0.30**	**0.30**	**0.31**	**0.01**	**0.30**	**0.33**	**0.31**	**0.01**	**0.00**	**0.00**
24	**0.30**	**0.34**			**0.30**	**0.30**			**0.00**	**0.00**
25	**0.40**	**0.40**			**0.40**	**0.41**			**0.00**	**0.00**
26	**0.40**	**0.40**	**0.40**	**0.00**	**0.40**	**0.40**	**0.40**	**0.00**	**0.00**	**0.00**
27	**0.40**	**0.41**			**0.40**	**0.40**			**0.00**	**0.00**

28	**0.50**	**0.50**			**0.50**	**0.50**			**0.00**	**0.00**
29	**0.50**	**0.53**	**0.51**	**0.01**	**0.50**	**0.50**	**0.50**	**0.00**	**0.00**	**0.00**
30	**0.50**	**0.51**			**0.50**	**0.50**			**0.00**	**0.00**

Experiment 5: Performed experiment for pure MnO_2 under 2weeks shaken condition for **MB** and **Orange II**.

Table A1.5b: Results

[MB]1	[MB]2	[MB]3	**$[MB]_{mean}$**	**λ**	D1	D2	D3	**D_{mean}**	**σ D**
(mg/L)	(mg/L)	(mg/L)	**(mg/L)**	**(mg/L)**	(%)	(%)	(%)	**(%)**	**(%)**
10.2	10.2	10.3	**10.2**	**0.1**	0.0	0.0	-1.0	**-0.3**	**0.6**
7.3	7.2	7.7	**7.4**	**0.3**	28.4	29.4	24.5	**27.5**	**2.6**
4.9	4.9	5.0	**4.9**	**0.1**	52.0	52.0	51.0	**51.6**	**0.6**
3.5	3.2	3.4	**3.4**	**0.2**	65.7	68.6	66.7	**67.0**	**1.5**
2.4	3.1	2.8	**2.8**	**0.4**	76.5	69.6	72.5	**72.9**	**3.4**
2.4	2.0	2.1	**2.2**	**0.2**	76.5	80.4	79.4	**78.8**	**2.0**
1.6	1.3	1.1	**1.3**	**0.3**	84.3	87.3	89.2	**86.9**	**2.5**
0.6	0.8	0.8	**0.7**	**0.1**	94.1	92.2	92.2	**92.8**	**1.1**
0.5	0.6	0.4	**0.5**	**0.1**	95.1	94.1	96.1	**95.1**	**1.0**
0.5	0.4	0.4	**0.4**	**0.1**	95.1	96.1	96.1	**95.8**	**0.6**
$[orange\ II]_1$	$[orange\ II]_2$	$[orange\ II]_3$	**$[orange\ II]_{mean}$**	**λ**	D1	D2	D3	**D_{mean}**	**σ D**
(mg/L)	(mg/L)	(mg/L)	**(mg/L)**	**(mg/L)**	(%)	(%)	(%)	**(%)**	**(%)**
11.2	11.3	11.3	**11.27**	**0.06**	0.88	0.00	0.00	**0.29**	**0.51**
11.3	11.3	11.1	**11.23**	**0.12**	0.00	0.00	1.77	**0.59**	**1.02**
11.3	11.2	11.3	**11.27**	**0.06**	0.00	0.88	0.00	**0.29**	**0.51**
11.3	11.2	11.3	**11.27**	**0.06**	0.00	0.88	0.00	**0.29**	**0.51**
11.2	11.3	11.3	**11.27**	**0.06**	0.88	0.00	0.00	**0.29**	**0.51**
11.3	11.2	11.3	**11.27**	**0.06**	0.00	0.88	0.00	**0.29**	**0.51**
11.3	11.1	11.2	**11.20**	**0.10**	0.00	1.77	0.88	**0.88**	**0.88**
11.3	11.3	11.2	**11.27**	**0.06**	0.00	0.00	0.88	**0.29**	**0.51**
11.2	11.3	11.3	**11.27**	**0.06**	0.88	0.00	0.00	**0.29**	**0.51**
11.2	11.2	11.1	**11.17**	**0.06**	0.88	0.88	1.77	**1.18**	**0.51**

APPENDIX 2: Column Experiment

Table A2.I Height of individual reactive materials in each column

Column	Dye	Fe^0	Fe^0	$H_{sand,1}$	Hrz	$H_{sand,2}$
		(g)	(%v/v)	(cm)	(cm)	(cm)
1	RR 120	0.0	0.0	40.0	0.0	0.0
2	RR 120	50.0	50.0	20.0	14.0	6.0
3	RR 120	100.0	100.0	20.0	6.0	14.0
4	Orange II	0.0	0.0	40.0	0.0	0.0
5	Orange II	50.0	50.0	20.0	14.0	6.0
6	Orange II	100.0	100.0	20.0	6.0	14.0
7	MB	0.0	0.0	40.0	0.0	0.0
8	MB	50.0	50.0	20.0	14.0	6.0
9	MB	100.0	100.0	20.0	6.0	14.0
10	MB	200.0	100.0	20.0	10.0	10.0

Table A2.II Conductivity of NaCl solution

Serial No.	V	∑V	LF
	[mL]	[mL]	[µS/cm]
1	5.0	5.0	278.0
2	8.0	13.0	276.0
3	6.0	19.0	283.0
4	6.0	25.0	281.0
5	5.2	30.2	285.0
6	6.0	36.2	282.0
7	5.0	41.2	282.0
8	7.2	48.4	283.0

9	6.0	54.4	287.0
10	6.0	60.4	288.0
11	6.0	66.4	289.0
12	6.4	72.8	294.0
13	7.0	79.8	336.0
14	7.0	86.8	469.0
15	7.0	93.8	597.0
16	7.4	101.2	697.0
17	6.0	107.2	673.0
18	7.0	114.2	758.0
19	7.0	121.2	776.0
20	7.2	128.4	796.0

Table A2.1: Experimental condition for Column 1

Overview of the total input volume of RR 120 solution (V) time (t), pH and dissolved iron concentration (Fe)

Date	Time	Δt	t	V	[RR 120]	pH	[Fe]
		(h)	(days)	(mL)	(mg/L)	(-)	(mg/L)
3/10/2014	16:00	0		0	-		
3/11/2014	11:00	19	0.00	235	-		0.0
3/13/2014	8:30	45.5	2.69	570	32.9		0.0
3/14/2014	15:45	31.25	3.99	385	46.3	8.31	0.0
3/17/2014	14:00	70.25	6.92	850	47.3	8.43	0.0
3/19/2014	14:00	48	8.92	570	47.3		0.0
3/20/2014	13:00	23	9.88	285	47.9		0.0
3/21/2014	15:20	26.37	10.97	315	47.9	8.42	0.0
3/24/2014	15:00	71.67	13.96	850	47.8		0.0
3/25/2014	14:15	23.25	14.93	280	47.8		0.0
3/28/2014	10:00	67.75	17.75	805	47.2	8.39	0.0
4/1/2014	11:30	97.50	21.81	1150.00	47.5		0.0
4/4/2014	11:30	72.00	24.81	850	47.8	8.44	0.0
4/9/2014	11:30	120.00	29.81	1410	48.2	8.45	0.0
4/11/2014	14:30	51.00	31.94	600	47.8	8.45	0.0
4/14/2014	11:30	69.00	34.81	800	47.8		0.0
4/17/2014	8:45	69.25	37.70	805	47.4	7.89	0.0
4/22/2014	9:30	120.75	42.73	1400	47.8	8.31	0.0
4/24/2014	10:20	48.83	44.77	570	47.8		0.0
4/28/2014	14:20	100	48.93	1150	47.8	8.32	0.0
5/1/2014	14:40	72.33	51.95	830	47.8		0.0
5/6/5014	11:20	116.67	56.81	1335	47.8	8.38	0.0

5/9/2014	**12:00**	**71.33**	**59.78**	**830**	**47.8**		**0.0**
5/13/2014	**13:40**	**97.67**	**63.85**	**1115**	**47.8**	**8.34**	**0.0**
5/16/2014	**12:15**	**72.58**	**66.87**	**800**	**47.8**		**0.0**
5/21/2014	**9:45**	**117.5**	**71.77**	**1340**	**47.8**		**0.0**
5/23/2014	**11:30**	**49.75**	**73.84**	**570**	**47.8**	**7.9**	**0.0**
5/28/2014	**10:20**	**118.83**	**78.79**	**1360**	**47.8**	**8.35**	**0.0**
5/30/2014	**15:25**	**52.92**	**81.00**	**600**	**47.8**		**0.0**
6/4/2014	**12:55**	**117.5**	**85.89**	**1325**	**47.8**	**8.33**	**0.0**
6/7/2014	**18:00**	**77.08**	**85.93**	**870**	**47.8**		**0.0**
6/12/2014	**9:35**	**111.58**	**90.57**	**1260**	**47.8**	**7.81**	**0.0**

Table A2.2: Experimental condition for Column 2

Overview of the total input volume of RR 120 solution (V) time (t), pH and dissolved iron concentration (Fe)

Date	**Time**	**Δt**	**t**	**V**	**[MB]**	**pH**	**[Fe]**
		(h)	**(days)**	**(mL)**	**(mg/L)**	**(-)**	**(mg/L)**
3/10/2014	**16:00**	**0**		**0**	**-**		
3/11/2014	**11:00**	**19**	**0.00**	**245**	**-**		**0.36**
3/13/2014	**8:30**	**45.5**	**2.69**	**580**	**0**		**0.34**
3/14/2014	**15:45**	**31.25**	**3.99**	**405**	**1.0**	**8.32**	**0.38**
3/17/2014	**14:00**	**70.25**	**6.92**	**860**	**1.0**	**8.41**	**0.44**
3/19/2014	**14:00**	**48**	**8.92**	**570**	**1.2**		**0.40**
3/20/2014	**13:00**	**23**	**9.88**	**285**	**1.3**		**0.50**
3/21/2014	**15:20**	**26.37**	**10.97**	**315**	**1.3**	**8.38**	**0.67**
3/24/2014	**15:00**	**71.67**	**13.96**	**850**	**1.2**		
3/25/2014	**14:15**	**23.25**	**14.93**	**280**	**1.2**		
3/28/2014	**10:00**	**67.75**	**17.75**	**805**	**1.5**	**8.35**	**0.81**
4/1/2014	**11:30**	**97.50**	**21.81**	**1150.00**	**1.3**		**0.63**
4/4/2014	**11:30**	**72.00**	**24.81**	**850**	**2.2**	**8.43**	**0.26**
4/9/2014	**11:30**	**120.00**	**29.81**	**1410**	**2.1**	**8.47**	**0.27**
4/11/2014	**14:30**	**51.00**	**31.94**	**600**	**2.0**	**8.41**	**0.21**
4/14/2014	**11:30**	**69.00**	**34.81**	**800**	**2.2**		**0.23**
4/17/2014	**8:45**	**69.25**	**37.70**	**805**	**2.3**	**7.8**	**0.28**
4/22/2014	**9:30**	**120.75**	**42.73**	**1400**	**1.0**	**8.29**	**0.45**
4/24/2014	**10:20**	**48.83**	**44.77**	**570**	**0.9**		**0.43**
4/28/2014	**14:20**	**100**	**48.93**	**1150**	**1.0**	**8.33**	**0.47**
5/1/2014	**14:40**	**72.33**	**51.95**	**830**	**1.0**		**0.39**
5/6/5014	**11:20**	**116.67**	**56.81**	**1335**	**0.8**	**8.31**	**0.41**

5/9/2014	**12:00**	**71.33**	**59.78**	**830**	**1.1**		**0.45**
5/13/2014	**13:40**	**97.67**	**63.85**	**1115**	**1.4**	**8.41**	**0.42**
5/16/2014	**12:15**	**72.58**	**66.87**	**800**	**1.1**		**0.43**
5/21/2014	**9:45**	**117.5**	**71.77**	**1340**	**0.9**		**0.41**
5/23/2014	**11:30**	**49.75**	**73.84**	**570**	**0.8**	**7.54**	**0.40**
5/28/2014	**10:20**	**118.83**	**78.79**	**1360**	**1.3**	**8.13**	**0.40**
5/30/2014	**15:25**	**52.92**	**81.00**	**600**	**1.1**		**0.39**
6/4/2014	**12:55**	**117.5**	**85.89**	**1325**	**1.2**	**8.09**	**0.44**
6/7/2014	**18:00**	**77.08**	**89.11**	**870**	**1.1**		**0.44**
6/12/2014	**9:35**	**111.58**	**93.76**	**1260**	**1.1**	**7.6**	**0.41**

Table A2.3: Experimental condition for Column 3

Overview of the total input volume of RR 120 solution (V) time (t), pH and dissolved iron concentration (Fe)

Date	**Time**	**Δt**	**t**	**V**	**[MB]**	**pH**	**[Fe]**
		(h)	**(days)**	**(mL)**	**(mg/L)**	**(-)**	**(mg/L)**
3/10/2014	**16:00**	**0**		**0**	**-**		
3/11/2014	**11:00**	**19**	**0.00**	**240**	**-**		**0.38**
3/13/2014	**8:30**	**45.5**	**2.69**	**580**	**0**		**0.36**
3/14/2014	**15:45**	**31.25**	**3.99**	**385**	**0.7**	**8.35**	**0.37**
3/17/2014	**14:00**	**70.25**	**6.92**	**850**	**1.0**	**8.34**	**0.40**
3/19/2014	**14:00**	**48**	**8.92**	**570**	**0.9**		**0.55**
3/20/2014	**13:00**	**23**	**9.88**	**285**	**1.0**		**0.49**
3/21/2014	**15:20**	**26.37**	**10.97**	**315**	**1.1**	**8.33**	**0.88**
3/24/2014	**15:00**	**71.67**	**13.96**	**850**	**1.2**		
3/25/2014	14:15	23.25	**14.93**	**280**	**1.2**		
3/28/2014	10:00	67.75	**17.75**	**805**	**1.2**	**8.3**	**0.59**
4/1/2014	**11:30**	**97.50**	**21.81**	**1150.00**	**1.2**		**0.74**
4/4/2014	**11:30**	**72.00**	**24.81**	**850**	**2.0**	**8.35**	**0.20**
4/9/2014	**11:30**	**120.00**	**29.81**	**1410**	**2.1**	**8.11**	**0.28**
4/11/2014	**14:30**	**51.00**	**31.94**	**600**	**2.0**	**8.27**	**0.26**
4/14/2014	**11:30**	**69.00**	**34.81**	**800**	**2.0**		**0.32**
4/17/2014	**8:45**	**69.25**	**37.70**	**805**	**2.0**	**7.69**	**0.35**
4/22/2014	**9:30**	**120.75**	**42.73**	**1400**	**0.6**	**8.19**	**0.42**
4/24/2014	**10:20**	**48.83**	**44.77**	**570**	**0.7**		**0.55**
4/28/2014	**14:20**	**100**	**48.93**	**1150**	**0.8**	**8.2**	**0.71**
5/1/2014	**14:40**	**72.33**	**51.95**	**830**	**0.6**		**0.72**
5/6/5014	**11:20**	**116.67**	**56.81**	**1335**	**0.7**	**8.2**	**0.70**

5/9/2014	**12:00**	**71.33**	**59.78**	**830**	**1.0**		**1.07**
5/13/2014	**13:40**	**97.67**	**63.85**	**1115**	**0.7**	**8.2**	**0.87**
5/16/2014	**12:15**	**72.58**	**66.87**	**800**	**0.7**		**0.61**
5/21/2014	**9:45**	**117.5**	**71.77**	**1340**	**0.7**		**0.80**
5/23/2014	**11:30**	**49.75**	**73.84**	**570**	**0.5**	**7.69**	**0.84**
5/28/2014	**10:20**	**118.83**	**78.79**	**1360**	**0.9**	**8.16**	**1.03**
5/30/2014	**15:25**	**52.92**	**81.00**	**600**	**0.8**		**0.79**
6/4/2014	**12:55**	**117.5**	**85.89**	**1325**	**0.8**	**8.11**	**0.97**
6/7/2014	**18:00**	**77.08**	**89.11**	**870**	**0.9**		**0.97**
6/12/2014	**9:35**	**111.58**	**93.76**	**1260**	**1.0**	**7.61**	**1.22**

Table A2.4: Experimental condition for Column 4

Overview of the total input volume of Orange II solution (V) time (t), pH and dissolved iron concentration (Fe)

Date	**Time**	**Δt**	**t**	**V**	**[MB]**	**pH**	**[Fe]**
		(h)	**(days)**	**(mL)**	**(mg/L)**	**(-)**	**(mg/L)**
3/10/2014	**16:00**	**0**		**0**	**-**		
3/11/2014	**11:00**	**19**	**0.00**	**235**	**-**		**0.0**
3/13/2014	**8:30**	**45.5**	**2.69**	**590**	**8.9**		**0.0**
3/14/2014	**15:45**	**31.25**	**3.99**	**385**	**10.9**	**8.29**	**0.0**
3/17/2014	**14:00**	**70.25**	**6.92**	**870**	**10.7**	**8.45**	**0.0**
3/19/2014	**14:00**	**48**	**8.92**	**570**	**10.7**		**0.0**
3/20/2014	**13:00**	**23**	**9.88**	**285**	**10.8**		**0.0**
3/21/2014	**15:20**	**26.37**	**10.97**	**315**	**10.7**	**8.45**	**0.0**
3/24/2014	**15:00**	**71.67**	**13.96**	**850**	**10.7**		**0.0**
3/25/2014	**14:15**	**23.25**	**14.93**	**280**	**10.6**		**0.0**
3/28/2014	**10:00**	**67.75**	**17.75**	**805**	**11.0**	**8.43**	**0.0**
4/1/2014	**11:30**	**97.50**	**21.81**	**1150.00**	**11.2**		**0.0**
4/4/2014	**11:30**	**72.00**	**24.81**	**850**	**11.2**	**8.46**	**0.0**
4/9/2014	**11:30**	**120.00**	**29.81**	**1410**	**11.4**	**8.39**	**0.0**
4/11/2014	**14:30**	**51.00**	**31.94**	**600**	**11.3**	**8.41**	**0.0**
4/14/2014	**11:30**	**69.00**	**34.81**	**800**	**11.3**		**0.0**
4/17/2014	**8:45**	**69.25**	**37.70**	**805**	**11.3**	**7.95**	**0.0**
4/22/2014	**9:30**	**120.75**	**42.73**	**1400**	**11.4**	**8.31**	**0.0**
4/24/2014	**10:20**	**48.83**	**44.77**	**570**	**11.4**		**0.0**
4/28/2014	**14:20**	**100**	**48.93**	**1150**	**11.4**	**8.35**	**0.0**
5/1/2014	**14:40**	**72.33**	**51.95**	**830**	**11.4**		**0.0**
5/6/5014	**11:20**	**116.67**	**56.81**	**1335**	**11.4**	**8.35**	**0.0**

5/9/2014	**12:00**	**71.33**	**59.78**	**830**	**11.4**		**0.0**
5/13/2014	**13:40**	**97.67**	**63.85**	**1115**	**11.4**	**8.35**	**0.0**
5/16/2014	**12:15**	**72.58**	**66.87**	**800**	**11.4**		**0.0**
5/21/2014	**9:45**	**117.5**	**71.77**	**1340**	**11.4**		**0.0**
5/23/2014	**11:30**	**49.75**	**73.84**	**570**	**11.4**	**7.9**	**0.0**
5/28/2014	**10:20**	**118.83**	**78.79**	**1360**	**11.4**	**8.38**	**0.0**
5/30/2014	**15:25**	**52.92**	**81.00**	**600**	**11.4**		**0.0**
6/4/2014	**12:55**	**117.5**	**85.89**	**1325**	**11.4**	**8.35**	**0.0**
6/7/2014	**18:00**	**77.08**	**89.11**	**870**	**11.4**		**0.0**
6/12/2014	**9:35**	**111.58**	**93.76**	**1260**	**11.4**	**7.84**	**0.0**

Table A2.5: Experimental condition for Column 5

Overview of the total input volume of Orange II solution (V) time (t), pH and dissolved iron concentration (Fe)

Date	**Time**	**Δt**	**t**	**V**	**[MB]**	**pH**	**[Fe]**
		(h)	**(days)**	**(mL)**	**(mg/L)**	**(-)**	**(mg/L)**
3/10/2014	**16:00**	**0**		**0**	**-**		
3/11/2014	**11:00**	**19**	**0.00**	**540**	**-**		**0.42**
3/13/2014	**8:30**	**45.5**	**2.69**	**590**	**0**		
3/14/2014	**15:45**	**31.25**	**3.99**	**385**	**1.03**	**8.25**	**0.39**
3/17/2014	**14:00**	**70.25**	**6.92**	**865**	**2.06**	**8.44**	**0.44**
3/19/2014	**14:00**	**48**	**8.92**	**570**	**1.54**		**0.44**
3/20/2014	**13:00**	**23**	**9.88**	**285**	**1.03**		**0.42**
3/21/2014	**15:20**	**26.37**	**10.97**	**315**	**1.54**	**8.32**	**0.43**
3/24/2014	**15:00**	**71.67**	**13.96**	**850**	**1.54**		
3/25/2014	**14:15**	**23.25**	**14.93**	**280**	**1.03**		
3/28/2014	**10:00**	**67.75**	**17.75**	**805**	**0.4**	**8.28**	**0.45**
4/1/2014	**11:30**	**97.50**	**21.81**	**1150.00**	**0.4**		**0.51**
4/4/2014	**11:30**	**72.00**	**24.81**	**850**	**0.5**	**8.32**	**0.23**
4/9/2014	**11:30**	**120.00**	**29.81**	**1410**	**0.5**	**8.22**	**0.11**
4/11/2014	**14:30**	**51.00**	**31.94**	**600**	**0.5**	**8.25**	**0.48**
4/14/2014	**11:30**	**69.00**	**34.81**	**800**	**0.5**		**0.15**
4/17/2014	**8:45**	**69.25**	**37.70**	**805**	**0.4**	**7.55**	**0.44**
4/22/2014	**9:30**	**120.75**	**42.73**	**1400**	**0.4**	**8.04**	**0.30**
4/24/2014	**10:20**	**48.83**	**44.77**	**570**	**0.4**		**0.31**
4/28/2014	**14:20**	**100**	**48.93**	**1150**	**0.4**	**8.06**	**0.73**
5/1/2014	**14:40**	**72.33**	**51.95**	**830**	**0.4**		**0.38**
5/6/5014	**11:20**	**116.67**	**56.81**	**1335**	**0.3**	**8.09**	**0.36**

5/9/2014	**12:00**	**71.33**	**59.78**	**830**	**0.3**		**0.44**
5/13/2014	**13:40**	**97.67**	**63.85**	**1115**	**0.4**	**8.08**	**0.35**
5/16/2014	**12:15**	**72.58**	**66.87**	**800**	**0.2**		**0.35**
5/21/2014	**9:45**	**117.5**	**71.77**	**1340**	**0.2**		**0.39**
5/23/2014	**11:30**	**49.75**	**73.84**	**570**	**0.2**	**7.72**	**0.52**
5/28/2014	**10:20**	**118.83**	**78.79**	**1360**	**0.20**	**8.09**	**0.58**
5/30/2014	**15:25**	**52.92**	**81.00**	**600**	**0.10**		**0.72**
6/4/2014	**12:55**	**117.5**	**85.89**	**1325**	**0.31**	**8.05**	**0.80**
6/7/2014	**18:00**	**77.08**	**89.11**	**870**	**0.10**		**0.44**
6/12/2014	**9:35**	**111.58**	**93.76**	**1260**	**0.10**	**7.55**	**0.55**

Table A2.6: Experimental condition for Column 6

Overview of the total input volume of Orange II solution (V) time (t), pH and dissolved iron concentration (Fe)

Date	**Time**	**Δt**	**t**	**V**	**[MB]**	**pH**	**[Fe]**
		(h)	**(days)**	**(mL)**	**(mg/L)**	**(-)**	**(mg/L)**
3/10/2014	**16:00**	**0**		**0**	**-**		
3/11/2014	**11:00**	**19**	**0.00**	**235**	**-**		**0.40**
3/13/2014	**8:30**	**45.5**	**2.69**	**575**	**0**		
3/14/2014	**15:45**	**31.25**	**3.99**	**380**	**0.51**	**8.24**	**0.40**
3/17/2014	**14:00**	**70.25**	**6.92**	**840**	**2.06**	**8.24**	**0.47**
3/19/2014	**14:00**	**48**	**8.92**	**570**	**1.54**		**0.49**
3/20/2014	**13:00**	**23**	**9.88**	**285**	**1.03**		**0.43**
3/21/2014	**15:20**	**26.37**	**10.97**	**315**	**1.54**	**8.19**	**0.49**
3/24/2014	**15:00**	**71.67**	**13.96**	**850**	**1.54**		
3/25/2014	**14:15**	**23.25**	**14.93**	**280**	**1.54**		
3/28/2014	**10:00**	**67.75**	**17.75**	**805**	**0.4**	**8.15**	**0.53**
4/1/2014	**11:30**	**97.50**	**21.81**	**1150.00**	**0.4**		**0.43**
4/4/2014	**11:30**	**72.00**	**24.81**	**850**	**0.6**	**8.19**	**0.12**
4/9/2014	**11:30**	**120.00**	**29.81**	**1410**	**0.5**	**8.07**	**0.19**
4/11/2014	**14:30**	**51.00**	**31.94**	**600**	**0.5**	**8.23**	**0.46**
4/14/2014	**11:30**	**69.00**	**34.81**	**800**	**0.6**		**0.59**
4/17/2014	**8:45**	**69.25**	**37.70**	**805**	**0.6**	**7.71**	**0.31**
4/22/2014	**9:30**	**120.75**	**42.73**	**1400**	**0.4**	**7.99**	**0.36**
4/24/2014	**10:20**	**48.83**	**44.77**	**570**	**0.4**		**0.54**
4/28/2014	**14:20**	**100**	**48.93**	**1150**	**0.3**	**8.00**	**0.56**
5/1/2014	**14:40**	**72.33**	**51.95**	**830**	**0.5**		**0.61**
5/6/5014	**11:20**	**116.67**	**56.81**	**1335**	**0.4**	**8.02**	**0.53**

5/9/2014	**12:00**	**71.33**	**59.78**	**830**	**0.5**		**0.55**
5/13/2014	**13:40**	**97.67**	**63.85**	**1115**	**0.3**	**7.99**	**0.49**
5/16/2014	**12:15**	**72.58**	**66.87**	**800**	**0.3**		**0.44**
5/21/2014	**9:45**	**117.5**	**71.77**	**1340**	**0.2**		**0.50**
5/23/2014	**11:30**	**49.75**	**73.84**	**570**	**0.2**	**8**	**0.72**
5/28/2014	**10:20**	**118.83**	**78.79**	**1360**	**0.20**	**8.07**	**0.67**
5/30/2014	**15:25**	**52.92**	**81.00**	**600**	**0.10**		**0.82**
6/4/2014	**12:55**	**117.5**	**85.89**	**1325**	**0.10**	**7.98**	**0.48**
6/7/2014	**18:00**	**77.08**	**89.11**	**870**	**0.21**		**0.50**
6/12/2014	**9:35**	**111.58**	**93.76**	**1260**	**0.21**	**7.45**	**0.49**

Table A2.7: Experimental condition for Column 7

Overview of the total input volume of MB solution (V) time (t), pH and dissolved iron concentration (Fe)

Date	**Time**	**Δt**	**t**	**V**	**[MB]**	**[Fe]**	**pH**
		(h)	**(days)**	**(mL)**	**(L)**	**(mg/L)**	**(-)**
3/10/2014	**16:00**	**0**		**0**		**-**	
3/11/2014	**11:00**	**19**	**0.00**	**235**	**0.24**	**-**	
3/13/2014	**8:30**	**45.5**	**2.69**	**580**	**0.58**	**0**	
3/14/2014	**15:45**	**31.25**	**3.99**	**385**	**0.39**	**0.0**	**8.29**
3/17/2014	**14:00**	**70.25**	**6.92**	**850**	**0.85**	**0.0**	**8.44**
3/19/2014	**14:00**	**48**	**8.92**	**570**	**0.57**	**0.0**	
3/20/2014	**13:00**	**23**	**9.88**	**285**	**0.29**	**0.0**	
3/21/2014	**15:20**	**26.37**	**10.97**	**315**	**0.32**	**0.0**	**8.44**
3/24/2014	**15:00**	**71.67**	**13.96**	**850**	**0.85**	**0.5**	
3/25/2014	**14:15**	**23.25**	**14.93**	**280**	**0.28**	**1.9**	
3/28/2014	**10:00**	**67.75**	**17.75**	**805**	**0.81**	**9.22**	**8.45**
4/1/2014	**11:30**	**97.50**	**21.81**	**1150.00**	**1.15**	**9.75**	
4/4/2014	**11:30**	**72.00**	**24.81**	**850**	**0.85**	**10.00**	**8.48**
4/9/2014	**11:30**	**120.00**	**29.81**	**1410**	**1.41**	**9.4**	**8.25**
4/11/2014	**14:30**	**51.00**	**31.94**	**600**	**0.60**	**9.8**	**8.48**
4/14/2014	**11:30**	**69.00**	**34.81**	**800**	**0.80**	**10.0**	
4/17/2014	**8:45**	**69.25**	**37.70**	**805**	**0.81**	**9.5**	**8.35**
4/22/2014	**9:30**	**120.75**	**42.73**	**1400**	**1.40**	**10.0**	**8.33**
4/24/2014	**10:20**	**48.83**	**44.77**	**570**	**0.57**	**10.0**	
4/28/2014	**14:20**	**100**	**48.93**	**1150**	**1.15**	**10.0**	**8.34**
5/1/2014	**14:40**	**72.33**	**51.95**	**830**	**0.83**	**10.0**	
5/6/5014	**11:20**	**116.67**	**56.81**	**1335**	**1.34**	**10.0**	**8.34**

5/9/2014	**12:00**	**71.33**	**59.78**	**830**	**0.83**	**10.0**	
5/13/2014	**13:40**	**97.67**	**63.85**	**1115**	**1.12**	**10.00**	**8.36**
5/16/2014	**12:15**	**72.58**	**66.87**	**800**	**0.80**	**10.00**	
5/21/2014	**9:45**	**117.5**	**71.77**	**1340**	**1.34**	**10.00**	
5/23/2014	**11:30**	**49.75**	**73.84**	**570**	**0.57**	**10.00**	**7.9**
5/28/2014	**10:20**	**118.83**	**78.79**	**1360**	**1.36**	**10**	**8.38**
5/30/2014	**15:25**	**52.92**	**81.00**	**600**	**0.60**	**10**	
6/4/2014	**12:55**	**117.5**	**85.89**	**1325**	**1.33**	**10**	**8.34**
6/7/2014	**18:00**	**77.08**	**89.11**	**870**	**0.87**	**10**	
6/12/2014	**9:35**	**111.58**	**93.76**	**1260**	**1.26**	**10**	**8.38**

Table A2.8: Experimental condition for Column 8

Overview of the total input volume of MB solution (V) time (t), pH and dissolved iron concentration (Fe)

Date	**Time**	**Δt**	**t**	**V**	**[MB]**	**[Fe]**	**pH**
		(h)	(days)	(mL)	(mg/L)	(mg/L)	(-)
3/10/2014	16:00	0		0	-		
3/11/2014	11:00	19	0.00	235	-	0.42	
3/13/2014	8:30	45.5	2.69	585	0	0.40	
3/14/2014	15:45	31.25	3.99	380	0.0	0.40	8.39
3/17/2014	14:00	70.25	6.92	845	0.0	0.40	8.38
3/19/2014	14:00	48	8.92	570	0.0	0.41	
3/20/2014	13:00	23	9.88	285	0.0	0.39	
3/21/2014	15:20	26.37	10.97	315	0.2	0.40	8.34
3/24/2014	15:00	71.67	13.96	850	0.5		
3/25/2014	14:15	23.25	14.93	280	0.9		
3/28/2014	10:00	67.75	17.75	805	1.35	0.45	8.35
4/1/2014	11:30	97.50	21.81	1150.00	2.12	0.42	
4/4/2014	11:30	72.00	24.81	850	2.76	0.10	8.35
4/9/2014	11:30	120.00	29.81	1410	4.0	0.11	8.16
4/11/2014	14:30	51.00	31.94	600	4.1	0.13	8.3
4/14/2014	11:30	69.00	34.81	800	4.4	0.19	
4/17/2014	8:45	69.25	37.70	805	4.3	0.17	8.06
4/22/2014	9:30	120.75	42.73	1400	3.2	0.45	8.12
4/24/2014	10:20	48.83	44.77	570	3.2	0.34	
4/28/2014	14:20	100	48.93	1150	3.0	0.40	8.13
5/1/2014	14:40	72.33	51.95	830	3.1	0.33	
5/6/5014	11:20	116.67	56.81	1335	2.8	0.36	8.16

5/9/2014	12:00	71.33	59.78	830	2.9	0.39	
5/13/2014	13:40	97.67	63.85	1115	2.81	0.40	8.16
5/16/2014	12:15	72.58	66.87	800	2.53	0.36	
5/21/2014	9:45	117.5	71.77	1340	2.81	0.43	
5/23/2014	11:30	49.75	73.84	570	2.47	0.47	7.9
5/28/2014	10:20	118.83	78.79	1360	3.03	0.41	8.24
5/30/2014	15:25	52.92	81.00	600	2.95	0.57	
6/4/2014	12:55	117.5	85.89	1325	2.93	0.42	8.17
6/7/2014	18:00	77.08	89.11	870	2.83	0.58	
6/12/2014	9:35	111.58	93.76	1260	2.90	0.42	8.2

Table A2.9: Experimental condition for Column 9

Overview of the total input volume of MB solution (V) time (t), pH and dissolved iron concentration (Fe)

Date	**Time**	**Δt**	**t**	**V**	**[MB]**	**pH**	**[Fe]**
		(h)	**(days)**	**(mL)**	**(mg/L)**	**(-)**	**(mg/L)**
3/10/2014	**16:00**	**0**		**0**	**-**		
3/11/2014	**11:00**	**19**	**0.00**	**235**	**-**		**0.43**
3/13/2014	**8:30**	**45.5**	**2.69**	**570**	**0.0**		**0.39**
3/14/2014	**15:45**	**31.25**	**3.99**	**380**	**0.0**	**8.32**	**0.41**
3/17/2014	**14:00**	**70.25**	**6.92**	**850**	**0.0**	**8.35**	**0.40**
3/19/2014	**14:00**	**48**	**8.92**	**570**	**0.0**		**0.43**
3/20/2014	**13:00**	**23**	**9.88**	**285**	**0.0**		**0.44**
3/21/2014	**15:20**	**26.37**	**10.97**	**315**	**0.1**	**8.26**	**0.45**
3/24/2014	**15:00**	**71.67**	**13.96**	**850**	**0.5**		
3/25/2014	**14:15**	**23.25**	**14.93**	**280**	**1.0**		
3/28/2014	**10:00**	**67.75**	**17.75**	**805**	**1.53**	**8.21**	**0.48**
4/1/2014	**11:30**	**97.50**	**21.81**	**1150.00**	**2.21**		**0.60**
4/4/2014	**11:30**	**72.00**	**24.81**	**850**	**3.6**	**8.35**	**0.11**
4/9/2014	**11:30**	**120.00**	**29.81**	**1410**	**4.0**	**8.21**	**0.19**
4/11/2014	**14:30**	**51.00**	**31.94**	**600**	**4.2**	**8.31**	**0.25**
4/14/2014	**11:30**	**69.00**	**34.81**	**800**	**4.3**		**0.37**
4/17/2014	**8:45**	**69.25**	**37.70**	**805**	**4.3**	**8.17**	**0.28**
4/22/2014	**9:30**	**120.75**	**42.73**	**1400**	**3.2**	**8.16**	**0.39**
4/24/2014	**10:20**	**48.83**	**44.77**	**570**	**3.2**		**0.43**
4/28/2014	**14:20**	**100**	**48.93**	**1150**	**3.0**	**8.19**	**0.41**
5/1/2014	**14:40**	**72.33**	**51.95**	**830**	**2.9**		**0.52**
5/6/5014	**11:20**	**116.67**	**56.81**	**1335**	**3.0**	**8.16**	**0.41**

5/9/2014	**12:00**	**71.33**	**59.78**	**830**	**2.9**		**0.50**
5/13/2014	**13:40**	**97.67**	**63.85**	**1115**	**2.60**	**8.18**	**0.37**
5/16/2014	**12:15**	**72.58**	**66.87**	**800**	**2.21**		**0.38**
5/21/2014	**9:45**	**117.5**	**71.77**	**1340**	**2.47**		**0.43**
5/23/2014	**11:30**	**49.75**	**73.84**	**570**	**2.25**	**8.19**	**0.53**
5/28/2014	**10:20**	**118.83**	**78.79**	**1360**	**2.92**	**8.22**	**0.44**
5/30/2014	**15:25**	**52.92**	**81.00**	**600**	**2.95**		**0.52**
6/4/2014	**12:55**	**117.5**	**85.89**	**1325**	**2.83**	**8.17**	**0.41**
6/7/2014	**18:00**	**77.08**	**89.11**	**870**	**2.83**		**0.45**
6/12/2014	**9:35**	**111.58**	**93.76**	**1260**	**2.90**	**7.55**	**0.42**

Table A2.10: Experimental condition for Column 10

Overview of the total input volume of MB solution (V) time (t), pH and dissolved iron concentration (Fe)

Date	**Time**	**Δt**	**t**	**V**	**[MB]**	**pH**	**[Fe]**
		(h)	(days)	(mL)	(mg/L)	(-)	(mg/L)
3/10/2014	16:00	0.00		0	-		
3/11/2014	11:00	19.00	0.00	210	0.0		0.45
3/13/2014	8:30	45.50	2.69	580	0.0		0.41
3/14/2014	15:45	31.25	3.99	380	0.0	8.40	0.43
3/17/2014	14:00	70.25	6.92	855	0.0	8.56	0.43
3/19/2014	14:00	48.00	8.92	570	0.0		0.44
3/20/2014	13:00	23.00	9.88	285	0.0		0.45
3/21/2014	15:20	26.37	10.97	315	0.0	8.37	0.44
3/24/2014	15:00	71.67	13.96	850	0.0		
3/25/2014	14:15	23.25	14.93	280	0.0		
3/28/2014	10:00	67.75	17.75	805	0.04	8.34	0.49
4/1/2014	11:30	97.50	21.81	1150	0.00		0.36
4/4/2014	11:30	72.00	24.81	850	1.7	8.27	0.07
4/9/2014	11:30	120.00	29.81	1410	2.2	8.18	0.07
4/11/2014	14:30	51.00	31.94	600	3.2	8.30	0.12
4/14/2014	11:30	69.00	34.81	800	3.6		0.17
4/17/2014	8:45	69.25	37.70	805	3.8	8.08	0.25
4/22/2014	9:30	120.75	42.73	1400	2.7	8.15	0.40
4/24/2014	10:20	48.83	44.77	570	2.8		0.35
4/28/2014	14:20	100	48.93	1150	2.1	8.18	0.38
5/1/2014	14:40	72.33	51.95	830	2.6		0.39
5/6/2014	11:20	116.67	56.81	1335	2.7	8.17	0.42

5/9/2014	12:00	71.33	59.78	830	2.6		0.34
5/13/2014	13:40	97.67	63.85	1115	2.60	8.20	0.33
5/16/2014	12:15	72.58	66.87	800	2.53		0.36
5/21/2014	9:45	117.5	71.77	1340	2.58		0.35
5/23/2014	11:30	49.75	73.84	570	2.70	7.90	0.31
5/28/2014	10:20	118.83	78.79	1360	2.70	8.28	0.35
5/30/2014	15:25	52.92	81.00	600	2.73		0.39
6/4/2014	12:55	117.5	85.89	1325	2.61	8.14	0.42
6/7/2014	18:00	77.08	89.11	870	2.72		0.43
6/12/2014	9:35	111.58	93.76	1260	2.90	8.22	0.39